Journal of Computational Mathematics
Vol.xx, No.x, 2025, 1–42.
http://www.global-sci.org/jcm
doi:10.4208/jcm.2502-m2024-0134

ERROR ESTIMATES OF A CLASS OF SERENDIPITY VIRTUAL ELEMENT METHODS FOR SEMILINEAR PARABOLIC INTEGRO-DIFFERENTIAL EQUATIONS ON CURVED DOMAINS*

Yang Xu, Zhenguo Zhou and Jingjun Zhao[1)]
School of Mathematics, Harbin Institute of Technology, Harbin 150001, China
Email: hit_zjj@hit.edu.cn

Abstract

The rigorous error analysis of a class of serendipity virtual element methods applied to numerically solve semilinear parabolic integro-differential equations on curved domains is the focus of this study. Different from the standard virtual element method, the serendipity virtual element method eliminates all the internal-moment degrees of freedom only under certain conditions of the mesh and the degree of approximation. Consequently, if the interpolation operators are utilized to approximate the nonlinear terms, the implementation of Newton's iteration algorithm can be simplified. Nonhomogeneous Dirichlet boundary conditions are considered in this paper. The strategy of approximating curved domains with polygonal domains is taken into consideration, and to overcome the issue of suboptimal convergence caused by enforcing Dirichlet boundary conditions strongly, Nitsche-based projection method is employed to impose the boundary conditions weakly. For time discretization, Crank-Nicolson scheme incorporating trapezoidal quadrature rule is adopted. Based on the concrete formulation of Nitsche-based projection method, a Ritz-Volterra projection is introduced and its approximation properties are rigorously analyzed. Building upon these approximation properties, error estimates are derived for the fully discrete scheme. Additionally, the extension of the fully discrete scheme to 3D case is also included. Finally, we present two numerical experiments to corroborate the theoretical findings.

Mathematics subject classification: 65M15, 65M60.
Key words: Serendipity virtual element method, Curved domain, Nitsche-based projection method, Semilinear parabolic integro-differential equation.

1. Introduction

Parabolic integro-differential equations (PIDEs) are widely used in various scientific disciplines to model phenomena with memory effects, such as heat transfer in materials with memory [29], nonlocal flow in porous media [20], temperature changes within nuclear reactors [32], and the dynamics of epidemic spread and evolution [18].

In this study, we focus on the following semilinear PIDEs with nonhomogeneous initial-boundary value conditions:

* Received July 9, 2024 / Revised version received November 13, 2024 / Accepted February 17, 2025 / Published online March 17, 2025 /
1) Corresponding author

$$a_0 u_t - \nabla \cdot (a_1 \nabla u) - \int_0^t \nabla \cdot \big(a_2\ \nabla u(\tau)\big) \mathrm{d}\tau + b(u) = f \quad \text{in } \Omega \times (0,T), \tag{1.1a}$$

$$u = g \quad \text{on } \partial\Omega \times (0,T), \tag{1.1b}$$

$$u(\cdot,0) = u_0 \quad \text{in } \Omega, \tag{1.1c}$$

where we consider Ω as a bounded, convex, and open subset of $\mathbb{R}^d$ ($d \in \{2,3\}$), with its boundary $\partial\Omega$ consisting of a finite number of curves (surfaces) $\{(\partial\Omega)_i\}_{i=1}^{N_\Omega}$. It is assumed that each curve (surface) $(\partial\Omega)_i$ is sufficiently smooth, and the overall boundary $\partial\Omega$ possesses Lipschitz continuity. The coefficients a_0, a_1 and a_2 are dependent solely on the spatial variable $\boldsymbol{x}$. The finite terminal time is denoted by T. The source function f, boundary value g, and initial value u_0 are provided as given information. The term $b(u)$ represents the nonlinearity in the equation.

Research interest in the field of mathematics has been significantly driven by the practical importance of PIDEs. For the analysis of PIDEs regarding existence, uniqueness, and regularity, some relevant results can be found in [23, 31, 40] as well as the cited references therein. Nevertheless, due to the intricate nature of the shape of the domain Ω and the presence of nonlinear terms, it is challenging to provide an explicit solution for the problem (1.1). Hence, it is imperative to consider efficient and accurate numerical methods for (1.1). The methods for discretization in temporal direction of PIDEs include backward-Euler scheme with rectangular quadrature rule [25], Crank-Nicolson scheme with trapezoidal quadrature rule [35], discontinuous Galerkin time-stepping scheme [30], and Laplace transformation [28]. Spatial discretization approaches range from finite element methods [36] to weak Galerkin finite element methods [41], mixed finite element methods [34] and hybridizable discontinuous Galerkin methods [26].

Despite the increasing interest in numerical methods for PIDEs, there has been a notable lack of focus on methods that can effectively handle polygonal or polyhedral meshes. These types of meshes offer more flexibility and accuracy in representing complex geometries compared to traditional triangular or quadrilateral meshes. As a result, the field of computational mathematics has experienced a growing interest in developing the numerical methods that are able to accommodate polygonal (polyhedral) meshes in recent years. Among these approaches, one particularly effective method is virtual element method (VEM) [4]. This method has gained popularity in various scientific and engineering applications, as discussed comprehensively in [8]. The use of L^2-projection operator is a common strategy in virtual element methods for handling nonlinear terms. It has been employed in a wide variety of initial boundary value problems, such as semilinear parabolic equations [1], N-coupled nonlinear Schrödinger-Boussinesq equations [27] and nematic liquid crystal flows [42]. However, this strategy comes with increased computational complexity of Newton's iteration algorithms for the resulting system, due to the need for element-wise integral computations, see [2].

Recently, a new strategy was proposed in [22] to address the aforementioned limitations by employing interpolation operators in serendipity virtual element method (SVEM) spaces to approximate the nonlinear terms [7]. As a modified version of VEM, SVEM strives to minimize the dimension of approximation spaces. SVEM has demonstrated its applicability in a wide range of physics problems, including linear magneto-static models [5], nonlinear elasticity [38], and general second order elliptic equations [6], among others. This study specifically focuses on a specialized type of SVEM that imposes specific requirements on the relationship between the mesh element shape and the SVEM order, thereby enabling the complete elimination of the internal-moment degrees of freedom. This specific method, also known as SVEM in the ideal case [22], simplifies the implementation of Newton's iteration algorithms if the interpolation operators are utilized to approximate the nonlinear terms, in comparison with the strategies utilizing L^2-projection operators, as discussed in [2, 22].

To handle the problem (1.1) on curved domains, we adopt polygonal (polyhedral) domain approximations for curved domains. And to tackle the suboptimal convergence for high order methods caused by imposing Dirichlet boundary conditions in a strong manner, we employ Nitsche-based projection method to impose the boundary conditions weakly, which was first proposed in [13] and then extended into the framework of VEM in [11, 12]. In order to implement the Nitsche-based projection method, it is necessary to determine the higher-order derivatives of virtual element functions at the element boundaries. However, we do not have access to the closed-form expressions of virtual element functions according to the construction of VEM spaces, let alone their higher-order derivatives. Therefore, in order to ensure the computability of the scheme, we employ the higher-order derivatives of L^2-projection of virtual element functions.

Crank-Nicolson scheme coupled with trapezoidal quadrature rule is utilized for temporal discretization. The key tool for error analysis is a special Ritz-Volterra projection, which is constructed based on the concrete form of Nitsche-based projection method. By establishing some approximation properties of this projection, we provide error analysis for the fully discrete scheme.

The subsequent sections of this paper are organized as follows. Section 2 provides the construction of the fully discrete scheme in 2D case. The optimal a priori error estimates for the fully discrete scheme in 2D case are discussed in Section 3. The extension of the fully discrete scheme to 3D case is addressed in Section 4. In Section 5, two numerical experiments are conducted to validate the theoretical derivations. Section 6 concludes with some remarks.

2. 2D Fully Discrete Scheme

2.1. Preliminaries

Let ω be a 2D or 3D domain. The seminorm and norm in Sobolev space $W^{s,p}(\omega)$, where the indices $s \geq 1$ and $p \geq 1$, are denoted as $|\cdot|_{s,p,\omega}$ and $\|\cdot\|_{s,p,\omega}$, respectively. The domain $\omega \subset \mathbb{R}^d$ ($d \in \{2,3\}$) is assumed to be bounded. In the case $p = 2$, the Sobolev space $W^{s,2}(\omega)$ is denoted as $H^s(\omega)$. In $H^s(\omega)$, we denote the seminorm and norm as $|\cdot|_{s,\omega}$ and $\|\cdot\|_{s,\omega}$, respectively. $\|\cdot\|_\omega$ and $(\cdot\,,\cdot)_\omega$ are used to represent L^2-norm and inner product in $L^2(\omega)$, respectively. The space of the traces of $H^s(\omega)$-functions is denoted as $H^{s-1/2}(\partial\omega)$. Denote the space of polynomials of degree m on ω as $\mathbb{P}_m(\omega)$ in which $m \geq 0$ is an integer. In the space $L^p((0,\mathcal{T});\mathcal{H})$ $(1 \leq p < \infty)$, we denote its norm as

$$\|u\|_{L^p((0,\mathcal{T});\mathcal{H})} = \left(\int_0^{\mathcal{T}} \|u(t)\|_{\mathcal{H}}^p \mathrm{d}t\right)^{\frac{1}{p}},$$

where the Hilbert space $\mathcal{H}$ is equipped with norm $\|\cdot\|_{\mathcal{H}}$ and the real number $\mathcal{T} > 0$. In addition, we denote the norm in the Bochner space $L^\infty((0,\mathcal{T});\mathcal{H})$ as

$$\|u\|_{L^\infty((0,\mathcal{T});\mathcal{H}} = \text{ess sup}_{t\in(0,\mathcal{T})}\|u(t)\|_{\mathcal{H}}.$$

To carry out the subsequent analysis of this paper, we put forth the following assumptions.

Assumption 2.1. The following conditions are assumed to be satisfied by the coefficients and data in (1.1):

(A1) a_0, a_1, and a_2 belong to $L^\infty(\Omega)$ and satisfy the following inequalities:

$$\underline{a_0} \leq a_0(\boldsymbol{x}) \leq \overline{a_0}, \quad \underline{a_1} \leq a_1(\boldsymbol{x}) \leq \overline{a_1}, \quad \underline{a_2} \leq a_2(\boldsymbol{x}) \leq \overline{a_2}, \quad \forall\, \boldsymbol{x} \in \overline{\Omega}, \tag{2.1}$$

where $\underline{a_0}, \overline{a_0}, \underline{a_1}, \overline{a_1}, \underline{a_2}$, and $\overline{a_2}$ are all strictly positive constants.

(A2) $g \in H^{1/2}(\partial\Omega)$ for any $t \in (0,T), f \in L^2((0,T); L^2(\Omega)), u_0 \in H^1(\Omega)$.

(A3) $b(u)$ is Lipschitz continuous in regard to u for any $u \in \mathbb{R}$.

The existence and uniqueness of the weak solution for problem (1.1) can be obtained by Assumption 2.1, the standard lift argument [21] and [39, Theorem A.1].

2.2. Serendipity virtual element space

In order to approximate the curved domain Ω, we introduce a sequence of polygonal domains $\{\Omega_h\}_h$ with vertices located on the boundary $\partial\Omega$. The subscript h $(0 < h \leq 1)$ signifies the proximity of Ω_h to Ω, with smaller values of h indicating a closer approximation. It is worth noting that the convexity of Ω guarantees the convexity of Ω_h and that Ω_h is a subset of Ω. To decompose each polygonal domain Ω_h, we utilize a polygonal mesh denoted as $\mathcal{T}_{h^*}$. The subscript h^* corresponds to the size of the polygonal mesh, which is defined as $h^* := \max_{E \in \mathcal{T}_{h^*}} h_E$, where h_E represents the diameter of a polygonal element E. For simplicity, we set $h = h^*$. In other words, the finer the mesh $\mathcal{T}_{h^*}$, the closer its corresponding polygonal domain Ω_h is to Ω. For any point $\boldsymbol{x}$ belonging to the boundary $\partial\Omega_h$ of Ω_h, it is assumed that there is a nonnegative function $\rho(\boldsymbol{x})$ which depends on $\boldsymbol{x}$ such that $\boldsymbol{x} + \rho(\boldsymbol{x})\boldsymbol{n} \in \partial\Omega$, where $\boldsymbol{n}$ represents the outward unit normal on $\partial\Omega_h$. From [11–13], it is known that the function $\rho(\boldsymbol{x})$ satisfies

$$\rho(\boldsymbol{x}) \leq C_\Omega h^2, \tag{2.2}$$

where C_Ω is a positive constant that does not depend on h.

The mesh $\mathcal{T}_h$ is assumed to have the shape regularity described in [12]. To be more specific, besides assuming a uniform bound on the number of edges in each element of the mesh, we also assume that each element $E \in \mathcal{T}_h$ is star-shaped with respect to a sphere with radius greater than or equal to βh_E, and that the length h_e of any edge e on the boundary of E satisfies $h_e \geq \beta h_E$, in which β is a positive constant. Additionally, we assume the existence of a positive constant $\hat{\beta}$ such that $\hat{\beta} h_E \geq h$ for every element $E \in \mathcal{T}_h$. The set of mesh edges in $\mathcal{T}_h$ is denoted as $\mathcal{E}_h$ and gather the edges lying on $\partial\Omega_h$ into the set $\mathcal{E}_h^{\mathtt{b}}$. The set of mesh vertices of $\mathcal{T}_h$ is denoted by $\mathcal{V}_h$. We introduce the notation $\mathcal{N}_{\mathtt{lines}}(\partial E)$ to represent minimum number of straight lines needed to completely enclose ∂E (the boundary of E) for each mesh element $E \in \mathcal{T}_h$. We then define

$$\mathcal{N}_{\mathtt{lines}}^h := \min_{E \in \mathcal{T}_h} \mathcal{N}_{\mathtt{lines}}(\partial E).$$

It is evident that $\mathcal{N}_{\mathtt{lines}}^h \geq 3$.

We make the assumption that k is a positive integer representing the order of SVEM, and require that $1 \leq k < \mathcal{N}_{\mathtt{lines}}^h$. As described in [7], we first define an auxiliary space $\widetilde{V}(E)$ for any element $E \in \mathcal{T}_h$ in the following manner:

$$\widetilde{V}(E) := \big\{ v_h \in H^1(E) : \Delta v_h \in \mathbb{P}_k(E),\ v_h|_{\partial E} \in C^0(\partial E),\ v_h|_e \in \mathbb{P}_k(e),\ \forall\, e \subset \partial E \big\},$$

where $C^0(\partial E)$ refers to the space of continuous functions on the boundary ∂E. Actually, $\widetilde{V}(E)$ can be viewed as a class of local virtual element spaces [8], and in order to uniquely determine a function v_h in $\widetilde{V}(E)$, we need the following degrees of freedom:

(L1) Values of v_h taken at all vertices of E.

(L2) Values of v_h taken at $k-1$ distinct internal points on every edge $e \subset \partial E$.

(L3) Moments $(v_h, p)_E/|E|, \forall\, p \in \mathbb{P}_k(E)$.

Nevertheless, the inclusion of degrees of freedom (L3) complicates the computation of the Jacobian matrix if the interpolation operators are utilized to approximate the nonlinear terms, see [1,2,22]. Fortunately, since we assume that $k < \mathcal{N}^h_{\texttt{lines}}$, it is possible to uniquely determine a polynomial of degree k using only the information from degree of freedom (L1) and (L2), see [7]. As a result, we can further completely eliminate the degrees of freedom (L3).

To do this, we introduce some notations. Let N_E^e represent the number of edges in E. It is widely recognized that the number of vertices in E is equal to N_E^e as well. Furthermore, it can be observed that the number of degrees of freedom (L1)-(L2) is equal to kN_E^e. These degrees of freedom (L1)-(L2) can be ordered and labeled as $s_1(v_h), s_2(v_h), \ldots, s_{kN_E^e}(v_h)$. We introduce an operator $\mathcal{S}_E : \widetilde{V}(E) \to \mathbb{R}^{kN_E^e}$, defined as

$$[\mathcal{S}_E v_h]_i = s_i(v_h), \quad 1 \le i \le kN_E^e. \tag{2.3}$$

We then define a projection operator $\Pi_{\mathcal{S}}^{k,E} : \widetilde{V}(E) \to \mathbb{P}_k(E)$ as

$$\big(\mathcal{S}_E\big(\Pi_{\mathcal{S}}^{k,E} v_h\big), \mathcal{S}_E p\big)_{\mathbb{R}^{kN_E^e}} = (\mathcal{S}_E v_h, \mathcal{S}_E p)_{\mathbb{R}^{kN_E^e}}, \quad \forall\, p \in \mathbb{P}_k(E), \tag{2.4}$$

where $(\cdot\,,\cdot)_{\mathbb{R}^{kN_E^e}}$ denotes the Euclidean scalar product in $\mathbb{R}^{kN_E^e}$. Based on the analysis in [7], it is established that the projection $\Pi_{\mathcal{S}}^{k,E} v_h$ can be uniquely determined by the degrees of freedom (L1) and (L2).

We define the k-th order local serendipity virtual element space $V(E)$ using the operator $\Pi_{\mathcal{S}}^{k,E}$ as,

$$V(E) := \big\{ v_h \in \widetilde{V}(E) : (v_h, p)_E = \big(\Pi_{\mathcal{S}}^{k,E} v_h, p\big)_E, \ \forall\, p \in \mathbb{P}_k(E) \big\}. \tag{2.5}$$

The unisolvency of the degrees of freedom (L1)-(L2) for the local serendipity virtual element space $V(E)$ is established in [7].

We define the global space $V_{\mathcal{S}}$ as

$$V_{\mathcal{S}} := \big\{ v_h \in H^1(\Omega_h) : v_h|_E \in V(E), \ \forall\, E \in \mathcal{T}_h \big\}. \tag{2.6}$$

The global degrees of freedom in $V_{\mathcal{S}}$ are determined by standard coupling of the local degrees of freedom specified by (L1) and (L2).

Next, we introduce some L^2-projection and interpolation operators that are necessary for constructing the discrete scheme. Recall the following definitions of standard L^2-projection operators $\Pi_0^{k,E}$ and $\Pi_1^{k-1,E}$ for scalar and vector fields on any element $E \in \mathcal{T}_h$:

$$(w, p)_E = \big(\Pi_0^{k,E} w, p\big)_E, \qquad \forall\, w \in L^2(E), \qquad \forall\, p \in \mathbb{P}_k(E), \tag{2.7}$$

$$(\boldsymbol{w}, \boldsymbol{p})_E = \big(\Pi_1^{k-1,E} \boldsymbol{w}, \boldsymbol{p}\big)_E, \quad \forall\, \boldsymbol{w} \in [L^2(E)]^2, \quad \forall\, \boldsymbol{p} \in [\mathbb{P}_{k-1}(E)]^2. \tag{2.8}$$

Through an examination of the definition of $V(E)$, for any $v_h \in V(E)$ and its gradient ∇v_h, the computation of $\Pi_0^{k,E} v_h$ and $\Pi_1^{k-1,E} \nabla v_h$ can be achieved by utilizing $\Pi_{\mathcal{S}}^{k,E} v_h$.

Lemma 2.1 ([14, 15]). *The L^2-projection operators $\Pi_0^{k,E}$ and $\Pi_1^{k-1,E}$ have the following properties for any sufficiently regular function v defined on $E \in \mathcal{T}_h$:*

$$\left\|\Pi_0^{k,E} v\right\|_E \le \|v\|_E, \tag{2.9}$$

$$\left\|\Pi_1^{k-1,E} \nabla v\right\|_E \le \|\nabla v\|_E, \tag{2.10}$$

$$\left|\Pi_0^{k,E} v\right|_{1,E} \le C_{*,1}|v|_{1,E}, \tag{2.11}$$

$$\left\|\nabla v - \Pi_1^{k-1,E}\nabla v\right\|_E \le C_{*,2} h_E^r |v|_{r+1,E}, \quad r \in \{0,1,\ldots,k\}, \tag{2.12}$$

$$\left|v - \Pi_0^{k,E} v\right|_{s,E} \le C_{*,3} h_E^{r-s}|v|_{r,E}, \qquad s,r \in \{0,1,\ldots,k+1\}, \quad s \le r, \tag{2.13}$$

where $C_{*,1}, C_{*,2}$, and $C_{*,3}$ are positive constants that are independent of h_E and $|\cdot|_{0,E} = \|\cdot\|_E$.

It is evident that the total number of global degrees of freedom $N_{\mathcal{S}}$ for $V_{\mathcal{S}}$ is equal to $(k-1)N^e + N^v$, where N^v and N^e represent the number of vertices and edges in $\mathcal{T}_h$, respectively. Let $\mathtt{DOF}_i$ be the i-th global degree of freedom for $V_{\mathcal{S}}$, then the interpolation operator $I_{\mathcal{S}} : H^1(\Omega) \rightarrow V_{\mathcal{S}}$ is defined by

$$\mathtt{DOF}_i(\phi) = \mathtt{DOF}_i(I_{\mathcal{S}}\phi), \quad i = 1,2,\ldots,N_{\mathcal{S}}. \tag{2.14}$$

Lemma 2.2 ([19, 22]). *For any function $\phi \in H^r(\Omega)$ with $r \in \{2,3,\ldots,k+1\}$, the interpolation $I_{\mathcal{S}}\phi$ satisfies*

$$\|\phi - I_{\mathcal{S}}\phi\|_E + h_E|\phi - I_{\mathcal{S}}\phi|_{1,E} \le C_I h_E^r |\phi|_{r,E}, \tag{2.15}$$

where C_I is a positive constant that is independent of h_E.

2.3. Discrete bilinear forms

The definition of the virtual element space $V_{\mathcal{S}}$ implies that the closed form of functions within it cannot be obtained. As a result, the computability of bilinear form $(a_0 v_h, w_h)_{\Omega_h}$, $(a_1\nabla v_h, \nabla w_h)_{\Omega_h}$ and $(a_2\nabla v_h, \nabla w_h)_{\Omega_h}$ cannot be guaranteed for any $v_h, w_h \in V_{\mathcal{S}}$. To address this issue, it is necessary to construct the corresponding approximate discrete bilinear forms.

Following [17, 39], for each element $E \in \mathcal{T}_h$, define local bilinear forms $\mathcal{A}_0^E(\cdot\,,\cdot)$, $\mathcal{A}_1^E(\cdot\,,\cdot)$ and $\mathcal{A}_2^E(\cdot\,,\cdot)$ on $V(E)\times V(E)$ as

$$\begin{aligned}
\mathcal{A}_0^E(v_h,w_h) &:= \left(a_0\Pi_0^{k,E}v_h, \Pi_0^{k,E}w_h\right)_E + \hat{a}_0 h_E^2\left(\mathcal{S}_E\left(v_h - \Pi_0^{k,E}v_h\right), \mathcal{S}_E\left(w_h - \Pi_0^{k,E}w_h\right)\right)_{\mathbb{R}^{kN_E^e}},\\
\mathcal{A}_1^E(v_h,w_h) &:= \left(a_1\Pi_1^{k-1,E}\nabla v_h, \Pi_1^{k-1,E}\nabla w_h\right)_E + \hat{a}_1\left(\mathcal{S}_E\left(v_h - \Pi_0^{k,E}v_h\right), \mathcal{S}_E\left(w_h - \Pi_0^{k,E}w_h\right)\right)_{\mathbb{R}^{kN_E^e}},\\
\mathcal{A}_2^E(v_h,w_h) &:= \left(a_2\Pi_1^{k-1,E}\nabla v_h, \Pi_1^{k-1,E}\nabla w_h\right)_E + \hat{a}_2\left(\mathcal{S}_E\left(v_h - \Pi_0^{k,E}v_h\right), \mathcal{S}_E\left(w_h - \Pi_0^{k,E}w_h\right)\right)_{\mathbb{R}^{kN_E^e}},
\end{aligned}$$

where

$$\hat{a}_0 = \frac{1}{|E|}\int_E a_0(\boldsymbol{x})\mathrm{d}\boldsymbol{x}, \quad \hat{a}_1 = \frac{1}{|E|}\int_E a_1(\boldsymbol{x})\mathrm{d}\boldsymbol{x}, \quad \hat{a}_2 = \frac{1}{|E|}\int_E a_2(\boldsymbol{x})\mathrm{d}\boldsymbol{x}.$$

By summing up the above local bilinear forms for each element $E \in \mathcal{T}_h$, we obtain the global bilinear forms $\mathcal{A}_0^h(\cdot\,,\cdot)$, $\mathcal{A}_1^h(\cdot\,,\cdot)$ and $\mathcal{A}_2^h(\cdot\,,\cdot)$, i.e.

$$\begin{aligned}
\mathcal{A}_0^h(v_h,w_h) &:= \sum_{E\in\mathcal{T}_h}\mathcal{A}_0^E(v_h,w_h), \quad \forall\, v_h,w_h \in V_{\mathcal{S}},\\
\mathcal{A}_1^h(v_h,w_h) &:= \sum_{E\in\mathcal{T}_h}\mathcal{A}_1^E(v_h,w_h), \quad \forall\, v_h,w_h \in V_{\mathcal{S}},\\
\mathcal{A}_2^h(v_h,w_h) &:= \sum_{E\in\mathcal{T}_h}\mathcal{A}_2^E(v_h,w_h), \quad \forall\, v_h,w_h \in V_{\mathcal{S}}.
\end{aligned}$$

Based on the continuity and coercivity of the stabilization terms with respect to the energy norm established in [9] and the norm equivalence of the stabilization terms given in [19], we can obtain the continuity and coercivity of $\mathcal{A}_0^h(\cdot\,,\cdot)$, $\mathcal{A}_1^h(\cdot\,,\cdot)$ and $\mathcal{A}_2^h(\cdot\,,\cdot)$ (see also [17, 22, 37]). Specifically, we have

$$
\begin{aligned}
&\left|\mathcal{A}_0^h(v_h, w_h)\right| \le C_0^{\mathtt{u}}\|v_h\|_{\Omega_h}\|w_h\|_{\Omega_h}, && \forall\, v_h, w_h \in V_{\mathcal{S}}, && (2.16)\\
&\mathcal{A}_0^h(w_h, w_h) \ge C_0^{\mathtt{d}}\|w_h\|_{\Omega_h}^2, && \forall\, w_h \in V_{\mathcal{S}}, && (2.17)\\
&\left|\mathcal{A}_1^h(v_h, w_h)\right| \le C_1^{\mathtt{u}}|v_h|_{1,\Omega_h}|w_h|_{1,\Omega_h}, && \forall\, v_h, w_h \in V_{\mathcal{S}}, && (2.18)\\
&\mathcal{A}_1^h(w_h, w_h) \ge C_1^{\mathtt{d}}|w_h|_{1,\Omega_h}^2, && \forall\, w_h \in V_{\mathcal{S}}, && (2.19)\\
&\left|\mathcal{A}_2^h(v_h, w_h)\right| \le C_2^{\mathtt{u}}|v_h|_{1,\Omega_h}|w_h|_{1,\Omega_h}, && \forall\, v_h, w_h \in V_{\mathcal{S}}, && (2.20)\\
&\mathcal{A}_2^h(w_h, w_h) \ge C_2^{\mathtt{d}}|w_h|_{1,\Omega_h}^2, && \forall\, w_h \in V_{\mathcal{S}}, && (2.21)
\end{aligned}
$$

where $C_0^{\mathtt{u}}, C_0^{\mathtt{d}}, C_1^{\mathtt{u}}, C_1^{\mathtt{d}}, C_2^{\mathtt{u}}$ and $C_2^{\mathtt{d}}$ are all positive constants that are independent of h.

We now shift our focus to the construction of bilinear forms $\mathcal{N}_1^h(\cdot\,,\cdot)$ and $\mathcal{N}_2^h(\cdot\,,\cdot)$ based on the Nitsche-based projection method [11, 12]. Set $\bar{m} = \lfloor (k+1)/2 \rfloor$. For any $v_h, w_h \in V_{\mathcal{S}}$, the bilinear form $\mathcal{N}_1^h(v_h, w_h)$ is defined as

$$
\begin{aligned}
\mathcal{N}_1^h(v_h, w_h) \coloneqq \mathcal{A}_1^h(v_h, w_h) &- \sum_{e\in\mathcal{E}_h^{\mathtt{b}}} \int_e a_1 \nabla\big(\Pi_0^{k,E_e} v_h\big)\cdot \boldsymbol{n} w_h \mathrm{d}s \\
&- \sum_{e\in\mathcal{E}_h^{\mathtt{b}}} \int_e \left(v_h + \sum_{j=1}^{\bar{m}} \frac{\rho^j}{j!} \partial_{\boldsymbol{n}}^j \big(\Pi_0^{k,E_e} v_h\big) \right) \big(a_1 \nabla\big(\Pi_0^{k,E_e} w_h\big)\cdot \boldsymbol{n} - \gamma_1 h_e^{-1} w_h\big) \mathrm{d}s,
\end{aligned}
$$

where $\partial_{\boldsymbol{n}}^j$ denotes the j-th order normal derivative, $E_e \in \mathcal{T}_h$ represents the unique element satisfying $e \subset \partial E_e$, h_e denotes the length of e, and γ_1 is the penalty parameter in the Nitsche-based projection method.

In a similar fashion, for any $v_h, w_h \in V_{\mathcal{S}}$, we define the bilinear form $\mathcal{N}_2^h(v_h, w_h)$ as

$$
\begin{aligned}
\mathcal{N}_2^h(v_h, w_h) \coloneqq \mathcal{A}_2^h(v_h, w_h) &- \sum_{e\in\mathcal{E}_h^{\mathtt{b}}} \int_e a_2 \nabla\big(\Pi_0^{k,E_e} v_h\big)\cdot \boldsymbol{n} w_h \mathrm{d}s \\
&- \sum_{e\in\mathcal{E}_h^{\mathtt{b}}} \int_e \left(v_h + \sum_{j=1}^{\bar{m}} \frac{\rho^j}{j!} \partial_{\boldsymbol{n}}^j \big(\Pi_0^{k,E_e} v_h\big) \right) \big(a_2 \nabla\big(\Pi_0^{k,E_e} w_h\big)\cdot \boldsymbol{n} - \gamma_2 h_e^{-1} w_h\big) \mathrm{d}s,
\end{aligned}
$$

where γ_2 is the penalty parameter in the Nitsche-based projection method.

We are now in a position to present the proofs for the continuity and coercivity of $\mathcal{N}_1^h(\cdot\,,\cdot)$ and $\mathcal{N}_2^h(\cdot\,,\cdot)$. Prior to that, we define an energy norm for $V_{\mathcal{S}}$, which takes the form

$$
\|v_h\|_{\mathcal{N}}^2 \coloneqq |v_h|_{1,\Omega_h}^2 + |v_h|_{\partial\Omega_h}^2, \quad \forall\, v_h \in V_{\mathcal{S}}, \tag{2.22}
$$

where

$$
|v_h|_{\partial\Omega_h}^2 \coloneqq \sum_{e\in\mathcal{E}_h^{\mathtt{b}}} h_e^{-1}\|v_h\|_e^2.
$$

If we have $\|v_h\|_{\mathcal{N}} = 0$, it implies that v_h is constant in Ω_h and vanishes on $\partial\Omega_h$. As a result, we can conclude that $v_h \equiv 0$ in Ω_h. It is clear that $\|\cdot\|_{\mathcal{N}}$ defines a norm on $V_{\mathcal{S}}$. Furthermore, in accordance with [12], $\|\cdot\|_{\mathcal{N}}$ is in fact also a norm on $H^1(\Omega_h)$. More specifically, $\|v\|_{1,\Omega_h} \le \hat{C}\|v\|_{\mathcal{N}}$ for any $v \in H^1(\Omega_h)$, where $\hat{C}$ is a positive constant independent of h.

Lemma 2.3 ([14, 16]). *We have the following discrete trace inequality:*

$$\|\nabla p\|_{\partial E} \leq C_{\mathrm{dt}} h_E^{-\frac{1}{2}} |p|_{1,E}, \quad \forall\, p \in \mathbb{P}_k(E), \quad \forall\, E \in \mathcal{T}_h, \tag{2.23}$$

where the positive constant C_{dt} is independent of h.

Lemma 2.4. *For any $e \in \mathcal{E}_h^{\mathtt{b}}$ and any $p \in \mathbb{P}_k(E_e)$, we have*

$$h_{E_e}^{-1} \sum_{j=1}^{\bar{m}} \left\|\rho^j \partial_{\boldsymbol{n}}^j p\right\|_e^2 \leq C_{\mathrm{in}} |p|_{1,E_e}^2 \sum_{j=1}^{\bar{m}} (C_\Omega \hat{\beta} h)^{2j}, \tag{2.24}$$

where the positive constant C_{in} is independent of h.

Proof. From [12, Lemma 4.3], we know that

$$h_{E_e}^{-1} \left\|\rho^j \partial_{\boldsymbol{n}}^j p\right\|_e^2 \leq C_{\mathrm{in}} \hat{\varrho}^{2j} |p|_{1,E_e}^2, \tag{2.25}$$

where $\hat{\varrho}$ satisfies that

$$\max_{e \in \mathcal{E}_h^{\mathtt{b}}} \max_{\boldsymbol{x} \in e} \frac{\rho\,(\boldsymbol{x})}{h_{E_e}} \leq \hat{\varrho}.$$

By (2.2), we have

$$\frac{\rho(\boldsymbol{x})}{h_{E_e}} \leq C_\Omega h \frac{h}{h_{E_e}} \leq C_\Omega \hat{\beta} h,$$

thus we can select $\hat{\varrho} = C_\Omega \hat{\beta} h$. Summing up (2.25) for $j = 1, 2, \ldots, \bar{m}$, yields (2.24). □

Theorem 2.1. *If the penalty parameters γ_1 and γ_2 satisfy that*

$$\gamma_1 > \gamma_1^0 := \frac{2(\overline{a_1} C_{\mathrm{dt}} C_{*,1})^2}{C_1^{\mathtt{d}}}, \quad \gamma_2 > \gamma_2^0 := \frac{2(\overline{a_2} C_{\mathrm{dt}} C_{*,1})^2}{C_2^{\mathtt{d}}},$$

and h ($h \leq 1$) is sufficiently small such that

$$\begin{aligned}
&h C_{*,1} \bar{m} \sqrt{\frac{C_{\mathrm{in}}}{\beta}} C_\Omega \hat{\beta} \left(\overline{a_1} C_{\mathrm{dt}} (C_{*,1}) + \frac{1}{2}\gamma_1\right) < \frac{C_1^{\mathtt{d}}}{2}, \\
&h C_{*,1} \bar{m} \sqrt{\frac{C_{\mathrm{in}}}{\beta}} C_\Omega \hat{\beta} \left(\overline{a_2} C_{\mathrm{dt}} (C_{*,1}) + \frac{1}{2}\gamma_2\right) < \frac{C_2^{\mathtt{d}}}{2}, \\
&\frac{h}{2} \gamma_1 \bar{m} C_{*,1} \sqrt{\frac{C_{\mathrm{in}}}{\beta}} C_\Omega \hat{\beta} < \gamma_1 - \gamma_1^0, \\
&\frac{h}{2} \gamma_2 \bar{m} C_{*,1} \sqrt{\frac{C_{\mathrm{in}}}{\beta}} C_\Omega \hat{\beta} < \gamma_2 - \gamma_2^0,
\end{aligned}$$

and $C_\Omega \hat{\beta} h < 1$, then $\mathcal{N}_1^h(\cdot\,,\cdot)$ and $\mathcal{N}_2^h(\cdot\,,\cdot)$ are coercive and bounded.

Proof. We will only present the analysis process for $\mathcal{N}_1^h(\cdot\,,\cdot)$, as the analysis for $\mathcal{N}_2^h(\cdot\,,\cdot)$ follows a similar approach. By (2.1), Cauchy-Schwarz inequality, (2.11) and (2.23), we have for any $v_h, w_h \in V_{\mathcal{S}}$,

$$\left| \sum_{e \in \mathcal{E}_h^{\mathtt{b}}} \int_e a_1 \nabla\big(\Pi_0^{k,E_e} v_h\big) \cdot \boldsymbol{n} w_h \mathrm{d}s \right|$$

$$\leq \overline{a_1} \sum_{e\in\mathcal{E}_h^{\mathrm{b}}} h_e^{\frac{1}{2}} \big\|\nabla\big(\Pi_0^{k,E_e} v_h\big)\big\|_e h_e^{-\frac{1}{2}} \|w_h\|_e$$

$$\leq \overline{a_1} C_{\mathrm{dt}} C_{*,1} |v_h|_{1,\Omega_h} |w_h|_{\partial\Omega_h}. \tag{2.26}$$

Similarly, we can derive that

$$\left|\sum_{e\in\mathcal{E}_h^{\mathrm{b}}} \int_e v_h a_1 \nabla\big(\Pi_0^{k,E_e} w_h\big)\cdot \boldsymbol{n} \mathrm{d}s\right| \leq \overline{a_1} C_{\mathrm{dt}} C_{*,1} |w_h|_{1,\Omega_h} |v_h|_{\partial\Omega_h}. \tag{2.27}$$

By Cauchy-Schwarz inequality, it is simple to observe that

$$\sum_{e\in\mathcal{E}_h^{\mathrm{b}}} \int_e v_h \gamma_1 h_e^{-1} w_h \mathrm{d}s \leq \gamma_1 |v_h|_{\partial\Omega_h} |w_h|_{\partial\Omega_h}. \tag{2.28}$$

From (2.1), (2.11), (2.23), (2.24) and the assumption $C_\Omega \hat{\beta} h < 1$, we obtain

$$\begin{aligned}
&\left|\sum_{e\in\mathcal{E}_h^{\mathrm{b}}} \int_e \left(\sum_{j=1}^{\bar{m}} \frac{\rho^j}{j!} \partial_{\boldsymbol{n}}^j \big(\Pi_0^{k,E_e} v_h\big)\right) a_1 \nabla\big(\Pi_0^{k,E_e} w_h\big)\cdot \boldsymbol{n} \mathrm{d}s\right| \\
&\leq \overline{a_1} \sum_{e\in\mathcal{E}_h^{\mathrm{b}}} h_e^{\frac{1}{2}} \big\|\nabla\big(\Pi_0^{k,E_e} w_h\big)\big\|_e h_e^{-\frac{1}{2}} \left(\sum_{j=1}^{\bar{m}} \big\|\rho^j \partial_{\boldsymbol{n}}^j \big(\Pi_0^{k,E_e} v_h\big)\big\|_e\right) \\
&\leq \overline{a_1} \left(\sum_{e\in\mathcal{E}_h^{\mathrm{b}}} h_e \big\|\nabla\big(\Pi_0^{k,E_e} w_h\big)\big\|_e^2\right)^{\frac{1}{2}} \left(\sum_{e\in\mathcal{E}_h^{\mathrm{b}}} h_e^{-1} \left(\sum_{j=1}^{\bar{m}} \big\|\rho^j \partial_{\boldsymbol{n}}^j \big(\Pi_0^{k,E_e} v_h\big)\big\|_e\right)^2\right)^{\frac{1}{2}} \\
&\leq \overline{a_1} \sqrt{\frac{\bar{m}}{\beta}} \left(\sum_{e\in\mathcal{E}_h^{\mathrm{b}}} h_e \big\|\nabla\big(\Pi_0^{k,E_e} w_h\big)\big\|_e^2\right)^{\frac{1}{2}} \left(\sum_{e\in\mathcal{E}_h^{\mathrm{b}}} h_{E_e}^{-1} \sum_{j=1}^{\bar{m}} \big\|\rho^j \partial_{\boldsymbol{n}}^j \big(\Pi_0^{k,E_e} v_h\big)\big\|_e^2\right)^{\frac{1}{2}} \\
&\leq \overline{a_1} \bar{m} C_{\mathrm{dt}} (C_{*,1})^2 \sqrt{\frac{C_{\mathrm{in}}}{\beta}} C_\Omega \hat{\beta} h |w_h|_{1,\Omega_h} |v_h|_{1,\Omega_h}.
\end{aligned} \tag{2.29}$$

In a manner similar to (2.29), we can find that

$$\begin{aligned}
&\left|\sum_{e\in\mathcal{E}_h^{\mathrm{b}}} \int_e \left(\sum_{j=1}^{\bar{m}} \frac{\rho^j}{j!} \partial_{\boldsymbol{n}}^j \big(\Pi_0^{k,E_e} v_h\big)\right) \frac{\gamma_1}{h_e} w_h \mathrm{d}s\right| \\
&\leq \gamma_1 \bar{m} C_{*,1} \sqrt{\frac{C_{\mathrm{in}}}{\beta}} C_\Omega \hat{\beta} h |v_h|_{1,\Omega_h} |w_h|_{\partial\Omega_h}.
\end{aligned} \tag{2.30}$$

By utilizing (2.18) and (2.26)-(2.30), we can establish the following continuity of $\mathcal{N}_1^h(\cdot,\cdot)$ for any $v_h, w_h \in V_{\mathcal{S}}$:

$$\big|\mathcal{N}_1^h(v_h, w_h)\big| \leq \overline{C_1^{\mathcal{N}}} \|v_h\|_{\mathcal{N}} \|w_h\|_{\mathcal{N}},$$

where

$$\overline{C_1^{\mathcal{N}}} = \max\left\{C_1^{\mathfrak{u}}, \overline{a_1} C_{\mathrm{dt}} C_{*,1}, \overline{a_1} \bar{m} C_{\mathrm{dt}} (C_{*,1})^2 \sqrt{\frac{C_{\mathrm{in}}}{\beta}} C_\Omega \hat{\beta}, \gamma_1 \bar{m} C_{*,1} \sqrt{\frac{C_{\mathrm{in}}}{\beta}} C_\Omega \hat{\beta}, \gamma_1\right\}.$$

Based on (2.26), (2.27), (2.29), (2.30), and noticing (2.19), we arrive at

$$\begin{aligned}\mathcal{N}_1^h(w_h,w_h) \geq & \left(C_1^{\mathrm{d}} - \overline{a_1}\bar{m}C_{\mathrm{dt}}(C_{*,1})^2\sqrt{\frac{C_{\mathrm{in}}}{\beta}}C_\Omega\hat{\beta}h\right)|w_h|_{1,\Omega_h}^2 \\ & - 2\overline{a_1}C_{\mathrm{dt}}C_{*,1}|w_h|_{1,\Omega_h}|w_h|_{\partial\Omega_h} \\ & - \gamma_1\bar{m}C_{*,1}\sqrt{\frac{C_{\mathrm{in}}}{\beta}}C_\Omega\hat{\beta}h|w_h|_{1,\Omega_h}|w_h|_{\partial\Omega_h} + \gamma_1|w_h|_{\partial\Omega_h}^2,\end{aligned}$$

then the application of Young's inequality results in

$$\begin{aligned}\mathcal{N}_1^h(w_h,w_h) \geq & \left(C_1^{\mathrm{d}} - \overline{a_1}\bar{m}C_{\mathrm{dt}}(C_{*,1})^2\sqrt{\frac{C_{\mathrm{in}}}{\beta}}C_\Omega\hat{\beta}h - \varepsilon\overline{a_1}C_{\mathrm{dt}}C_{*,1}\right. \\ & \left. - \frac{1}{2}\gamma_1\bar{m}C_{*,1}\sqrt{\frac{C_{\mathrm{in}}}{\beta}}C_\Omega\hat{\beta}h\right)|w_h|_{1,\Omega_h}^2 \\ & + \left(\gamma_1 - \varepsilon^{-1}\overline{a_1}C_{\mathrm{dt}}C_{*,1} - \frac{1}{2}\gamma_1\bar{m}C_{*,1}\sqrt{\frac{C_{\mathrm{in}}}{\beta}}C_\Omega\hat{\beta}h\right)|w_h|_{\partial\Omega_h}^2.\end{aligned}$$

Choosing ε as $C_1^{\mathrm{d}}/(2\overline{a_1}C_{\mathrm{dt}}C_{*,1})$ and recalling the assumption for γ_1 and h and the setting of γ_1^0, we get the following coercivity of $\mathcal{N}_1^h(\cdot\,,\cdot)$ for any $w_h \in V_{\mathcal{S}}$:

$$\mathcal{N}_1^h(w_h,w_h) > \underline{C_1^{\mathcal{N}}}\|w_h\|_{\mathcal{N}}^2,$$

where

$$\underline{C_1^{\mathcal{N}}} = \min\left\{\frac{C_1^{\mathrm{d}}}{2} - hC_{*,1}\bar{m}\sqrt{\frac{C_{\mathrm{in}}}{\beta}}C_\Omega\hat{\beta}\left(\overline{a_1}C_{\mathrm{dt}}\left(C_{*,1}\right) + \frac{1}{2}\gamma_1\right), \gamma_1 - \gamma_1^0 - \frac{1}{2}\gamma_1\bar{m}C_{*,1}\sqrt{\frac{C_{\mathrm{in}}}{\beta}}C_\Omega\hat{\beta}h\right\}.$$

The proof is complete. □

2.4. Fully discrete scheme

Prior to presenting the construction of the discrete scheme, it is necessary to introduce the strategy mentioned in [22] that utilizes the interpolation operator $I_{\mathcal{S}}$ defined in (2.14) to approximate the nonlinear terms.

By substituting a_0 with 1 in the bilinear form $\mathcal{A}_0^h(\cdot\,,\cdot)$, we obtain an approximation $\mathcal{B}_0^h(\cdot\,,\cdot)$ for the inner product $(\cdot\,,\cdot)_{\Omega_h}$. Then we approximate the nonlinear term $(b(\cdot),\cdot)_{\Omega_h}$ as

$$\big(b(v_h),w_h\big)_{\Omega_h} \approx \mathcal{B}_0^h\big(I_{\mathcal{S}}b(v_h),w_h\big), \quad \forall\, v_h, w_h \in V_{\mathcal{S}}.$$

For any $w_h \in V_{\mathcal{S}}$, an approximation $f^h(t;w_h)$ can be constructed for the inner product $(f(t),w_h)_{\Omega_h}$ as follows:

$$f^h(t;w_h) := \sum_{E\in\mathcal{T}_h}\int_E \big(\Pi_0^{k,E}f(t)\big)w_h\mathrm{d}\boldsymbol{x}.$$

Consider the uniform temporal partition $t_n = n\Delta t$ for $n = 0,1,\ldots,N_T$, where $\Delta t = T/N_T$ and N_T is a positive integer. Then we define the fully discrete scheme as finding a sequence

$\{u_h^n\}_{n=1}^{N_T}$ of functions in $V_{\mathcal{S}}$ such that

$$\begin{cases} \mathcal{A}_0^h\left(\dfrac{u_h^n - u_h^{n-1}}{\Delta t}, v_h\right) + \mathcal{N}_1^h\left(\dfrac{u_h^n + u_h^{n-1}}{2}, v_h\right) + \mathcal{N}_2^h\left(\mathbb{Q}_n^h, v_h\right) \\ \quad +\mathcal{B}_0^h\left(\dfrac{I_{\mathcal{S}} b\big(u_h^n\big) + I_{\mathcal{S}} b\big(u_h^{n-1}\big)}{2}, v_h\right) = \mathcal{L}_n^h(t_n; v_h), \quad \forall\, v_h \in V_{\mathcal{S}}, \\ u_h^0 = I_{\mathcal{S}} u_0, \end{cases} \tag{2.31}$$

where the linear form $\mathcal{L}_n^h(t_n; v_h)$ is defined as

$$\begin{aligned} \mathcal{L}_n^h(t_n; v_h) \coloneqq{}& \frac{1}{2}\big(f^h(t_n; v_h) + f^h(t_{n-1}; v_h)\big) \\ &- \sum_{e\in\mathcal{E}_h^{\mathrm{b}}} \int_e \frac{1}{2}\big(\hat{g}(t_n) + \hat{g}(t_{n-1})\big)\big(a_1\nabla\big(\Pi_0^{k,E_e} v_h\big)\cdot \boldsymbol{n} - \gamma_1 h_e^{-1} v_h\big)\mathrm{d}s \\ &- \frac{1}{2}\int_0^{t_n} \sum_{e\in\mathcal{E}_h^{\mathrm{b}}} \int_e \hat{g}(\tau)\big(a_2\nabla\big(\Pi_0^{k,E_e} v_h\big)\cdot \boldsymbol{n} - \gamma_2 h_e^{-1} v_h\big)\mathrm{d}s\mathrm{d}\tau \\ &- \frac{1}{2}\int_0^{t_{n-1}} \sum_{e\in\mathcal{E}_h^{\mathrm{b}}} \int_e \hat{g}(\tau)\big(a_2\nabla\big(\Pi_0^{k,E_e} v_h\big)\cdot \boldsymbol{n} - \gamma_2 h_e^{-1} v_h\big)\mathrm{d}s\mathrm{d}\tau, \end{aligned}$$

in which

$$\hat{g}(\tau) = g\big(\boldsymbol{x} + \rho(\boldsymbol{x})\boldsymbol{n}, \tau\big), \quad \tau \in [0, t_n].$$

Here, the definition of the trapezoidal quadrature rule $\mathbb{Q}_n^h$ is as follows:

$$\mathbb{Q}_n^h \coloneqq \begin{cases} \dfrac{\Delta t}{4} u_h^0 + \dfrac{\Delta t}{4} u_h^1, & n = 1, \\ \dfrac{\Delta t}{2} u_h^0 + \dfrac{3\Delta t}{4} u_h^1 + \dfrac{\Delta t}{4} u_h^2, & n = 2, \\ \dfrac{\Delta t}{2} u_h^0 + \Delta t \displaystyle\sum_{q=1}^{n-2} u_h^q + \dfrac{3\Delta t}{4} u_h^{n-1} + \dfrac{\Delta t}{4} u_h^n, & n \geq 3. \end{cases} \tag{2.32}$$

Next, we will present the Newton's iteration algorithm for solving (2.31) and briefly introduce the Newton's iteration algorithm for the fully discrete scheme based on the strategy of imposing Dirichlet boundary conditions strongly. Any function $\varphi_h \in V_{\mathcal{S}}$ can be expressed as

$$\varphi_h = \sum_{i=1}^{N_{\mathcal{S}}} \mathtt{DOF}_i(\varphi_h)\phi_i, \tag{2.33}$$

where ϕ_i represents the i-th basis function for $V_{\mathcal{S}}$. Let $\boldsymbol{A^0}, \boldsymbol{N^1}, \boldsymbol{N^2}$ and $\boldsymbol{B^h}$ be the matrices corresponding to the bilinear forms $\mathcal{A}_0^h(\cdot\,,\cdot)$, $\mathcal{N}_1^h(\cdot\,,\cdot)$, $\mathcal{N}_2^h(\cdot\,,\cdot)$ and $\mathcal{B}_0^h(\cdot\,,\cdot)$, respectively, and introduce the following vector notations:

$$\begin{aligned} &\boldsymbol{D}(\varphi_h) = [d_1, d_2, \ldots, d_{N_{\mathcal{S}}}]^\top, && d_i = \mathtt{DOF}_i(\varphi_h), && i = 1, 2, \ldots, N_{\mathcal{S}}, \\ &\boldsymbol{B}(\varphi_h) = [b_1, b_2, \ldots, b_{N_{\mathcal{S}}}]^\top, && b_i = b\big(\mathtt{DOF}_i(\varphi_h)\big), && i = 1, 2, \ldots, N_{\mathcal{S}}, \\ &\boldsymbol{L}(t_n) = [L_1, L_2, \ldots, L_{N_{\mathcal{S}}}]^\top, && L_i = \mathcal{L}_n^h(t_n; \phi_i), && i = 1, 2, \ldots, N_{\mathcal{S}}. \end{aligned}$$

Then according to (2.14), (2.33) and [22], we can rewrite the nonlinear term $\mathcal{B}_0^h(I_{\mathcal{S}}b(\varphi_h), v_h)$ as

$$\mathcal{B}_0^h\big(I_{\mathcal{S}}b(\varphi_h), v_h\big) = \sum_{i=1}^{N_{\mathcal{S}}} \mathtt{DOF}_i\big(b(\varphi_h)\big)\mathcal{B}_0^h(\phi_i, v_h) = \sum_{i=1}^{N_{\mathcal{S}}} b\big(\mathtt{DOF}_i(\varphi_h)\big)\mathcal{B}_0^h(\phi_i, v_h).$$

Therefore, we can express the fully discrete scheme (2.31) as

$$\begin{aligned}&\left(\boldsymbol{A^0} + \frac{\Delta t}{2}\boldsymbol{N^1} + \frac{(\Delta t)^2}{4}\boldsymbol{N^2}\right)\boldsymbol{D}\big(u_h^n\big) + \frac{\Delta t}{2}\boldsymbol{B^h}\boldsymbol{B}\big(u_h^n\big)\\ &= \left(\boldsymbol{A^0} - \frac{\Delta t}{2}\boldsymbol{N^1}\right)\boldsymbol{D}\big(u_h^{n-1}\big) - \frac{\Delta t}{2}\boldsymbol{B^h}\boldsymbol{B}\big(u_h^{n-1}\big) + \Delta t\boldsymbol{L}(t_n) - \Delta t\boldsymbol{N^2}\hat{\mathbb{Q}}_{n-1}^h,\end{aligned}$$

where

$$\hat{\mathbb{Q}}_{n-1}^h := \begin{cases}\dfrac{\Delta t}{4}\boldsymbol{D}\big(u_h^0\big), & n=1,\\ \dfrac{\Delta t}{2}\boldsymbol{D}\big(u_h^0\big) + \dfrac{3\Delta t}{4}\boldsymbol{D}\big(u_h^1\big), & n=2,\\ \dfrac{\Delta t}{2}\boldsymbol{D}\big(u_h^0\big) + \Delta t\displaystyle\sum_{q=1}^{n-2}\boldsymbol{D}\big(u_h^q\big) + \dfrac{3\Delta t}{4}\boldsymbol{D}\big(u_h^{n-1}\big), & n\geq 3.\end{cases}$$

For $n = 1, 2, \ldots, N_T$, setting $u_h^{n,0} = u_h^{n-1}$, the Newton's iteration algorithm for (2.31) is then defined by finding $u_h^{n,r} \in V_{\mathcal{S}}$ for $r \geq 1$ such that

$$\boldsymbol{J}\boldsymbol{D}\big(u_h^{n,r}\big) = \boldsymbol{J}\boldsymbol{D}\big(u_h^{n,r-1}\big) - \boldsymbol{F}, \tag{2.34}$$

where Jacobian $\boldsymbol{J}$ takes the following form:

$$\boldsymbol{J} = \boldsymbol{A^0} + \frac{\Delta t}{2}\boldsymbol{N^1} + \frac{(\Delta t)^2}{4}\boldsymbol{N^2} + \frac{\Delta t}{2}\widetilde{\boldsymbol{B}}^{\boldsymbol{h}}$$

with

$$\widetilde{\boldsymbol{B}}^{\boldsymbol{h}} = \big[\widetilde{B}_{i,j}\big] = \mathcal{B}_0^h(\phi_i, \phi_j)b'\big(\mathtt{DOF}_j\big(u_h^{n,r-1}\big)\big), \quad i,j = 1,2,\ldots,N_{\mathcal{S}},$$

and the term $\boldsymbol{F}$ is defined as

$$\begin{aligned}\boldsymbol{F} = &\left(\boldsymbol{A^0} + \frac{\Delta t}{2}\boldsymbol{N^1} + \frac{(\Delta t)^2}{4}\boldsymbol{N^2}\right)\boldsymbol{D}\big(u_h^{n,r-1}\big)\\ &+ \frac{\Delta t}{2}\boldsymbol{B^h}\boldsymbol{B}\big(u_h^{n,r-1}\big) - \left(\boldsymbol{A^0} - \frac{\Delta t}{2}\boldsymbol{N^1}\right)\boldsymbol{D}\big(u_h^{n-1}\big)\\ &+ \frac{\Delta t}{2}\boldsymbol{B^h}\boldsymbol{B}\big(u_h^{n-1}\big) - \Delta t\boldsymbol{L}(t_n) + \Delta t\boldsymbol{N^2}\hat{\mathbb{Q}}_{n-1}^h.\end{aligned}$$

Apparently, the computation of the Jacobian $\boldsymbol{J}$ here is simple and does not require looping over all mesh elements in $\mathcal{T}_h$ and calculating some numerical integrals within each element, which is exactly what needs to be done for the strategies utilizing L^2-projection operators, see [1, 2].

Now we turn to the strategy of imposing Dirichlet boundary conditions in a strong manner. The corresponding fully discrete scheme is defined as finding a sequence $\{u_h^n\}_{n=1}^{N_T}$ of functions in $V_{\mathcal{S}}$ such that

$$\begin{cases}\mathcal{A}_0^h\left(\dfrac{u_h^n - u_h^{n-1}}{\Delta t}, v_h\right) + \mathcal{A}_1^h\left(\dfrac{u_h^n + u_h^{n-1}}{2}, v_h\right) + \mathcal{A}_2^h\big(\mathbb{Q}_n^h, v_h\big)\\ \quad + \mathcal{B}_0^h\left(\dfrac{I_{\mathcal{S}}b\big(u_h^n\big) + I_{\mathcal{S}}b\big(u_h^{n-1}\big)}{2}, v_h\right) = \dfrac{f^h(t_n; v_h) + f^h(t_{n-1}; v_h)}{2}, \quad \forall\, v_h \in V_{\mathcal{S}},\\ u_h^0 = I_{\mathcal{S}}u_0.\end{cases}$$

For $n = 1, 2, \ldots, N_T$ and $r \geq 1$, setting $u_h^{n,0} = u_h^{n-1}$, the corresponding Newton's iteration algorithm is defined as finding $u_h^{n,r} \in V_{\mathcal{S}}$ such that

$$\boldsymbol{J_s} \boldsymbol{D}\big(u_h^{n,r}\big) = \hat{\boldsymbol{F}}, \tag{2.35}$$

where

$$\boldsymbol{J_s} = \boldsymbol{A^0} + \frac{\Delta t}{2}\boldsymbol{A^1} + \frac{(\Delta t)^2}{4}\boldsymbol{A^2} + \frac{\Delta t}{2}\widetilde{\boldsymbol{B}}^{\boldsymbol{h}}, \quad \hat{\boldsymbol{F}} = \boldsymbol{J_s}\boldsymbol{D}\big(u_h^{n,r-1}\big) - \boldsymbol{F_s},$$

in which

$$\begin{aligned}\boldsymbol{F_s} = &\left(\boldsymbol{A^0} + \frac{\Delta t}{2}\boldsymbol{A^1} + \frac{(\Delta t)^2}{4}\boldsymbol{A^2}\right)\boldsymbol{D}\big(u_h^{n,r-1}\big)\\ &+ \frac{\Delta t}{2}\boldsymbol{B^h}\boldsymbol{B}\big(u_h^{n,r-1}\big) - \left(\boldsymbol{A^0} - \frac{\Delta t}{2}\boldsymbol{A^1}\right)\boldsymbol{D}\big(u_h^{n-1}\big)\\ &+ \frac{\Delta t}{2}\boldsymbol{B^h}\boldsymbol{B}\big(u_h^{n-1}\big) - \frac{\Delta t}{2}\big(\boldsymbol{f}(t_n) + \boldsymbol{f}(t_{n-1})\big) + \Delta t\boldsymbol{A^2}\hat{\mathbb{Q}}_{n-1}^h.\end{aligned}$$

Here, $\boldsymbol{A^1}$ and $\boldsymbol{A^2}$ are the matrices corresponding to the bilinear forms $\mathcal{A}_1^h(\cdot\,,\cdot)$ and $\mathcal{A}_2^h(\cdot\,,\cdot)$, respectively, and

$$\boldsymbol{f}(t_j) = [f_1, f_2, \ldots, f_{N_{\mathcal{S}}}]^\top, \quad f_i = f^h(t_j; \phi_i), \quad i = 1, 2, \ldots, N_{\mathcal{S}}, \quad j \in \{n-1, n\}.$$

Decompose the vector $\boldsymbol{D}(u_h^{n,r})$ as

$$\boldsymbol{D}\big(u_h^{n,r}\big) = \begin{bmatrix}\boldsymbol{D}^{\mathfrak{I}}\\ \boldsymbol{D}^{\mathfrak{B}}\end{bmatrix},$$

where $\mathfrak{B}$ denotes the set of indices for degrees of freedom associated with the points on the boundary $\partial\Omega_h$ and $\mathfrak{I}$ denotes the set of indices for degrees of freedom associated with the points inside Ω_h. Then (2.35) can be rewritten as

$$\begin{bmatrix}\boldsymbol{J_s}^{\mathfrak{I}\mathfrak{I}} & \boldsymbol{J_s}^{\mathfrak{I}\mathfrak{B}}\\ \boldsymbol{J_s}^{\mathfrak{B}\mathfrak{I}} & \boldsymbol{J_s}^{\mathfrak{B}\mathfrak{B}}\end{bmatrix}\begin{bmatrix}\boldsymbol{D}^{\mathfrak{I}}\\ \boldsymbol{D}^{\mathfrak{B}}\end{bmatrix} = \begin{bmatrix}\hat{\boldsymbol{F}}^{\mathfrak{I}}\\ \hat{\boldsymbol{F}}^{\mathfrak{B}}\end{bmatrix}.$$

To impose the Dirichlet boundary conditions, we need to specify the value of $\boldsymbol{D}^{\mathfrak{B}}$. For any index $j \in \mathfrak{B}$, we use $\boldsymbol{x}_j = (x_j, y_j)$ to represent its corresponding boundary point. It should be noted that unless $\boldsymbol{x}_j$ is a vertex of Ω_h, the value of the true boundary conditions taken at $\boldsymbol{x}_j$ is not available. Therefore, we assign the value to $\boldsymbol{D}^{\mathfrak{B}}$ in the following approximate way:

$$(\boldsymbol{D}^{\mathfrak{B}})_j = \mathtt{DOF}_j\big(u_h^{n,r}\big) \approx g\big(\boldsymbol{x}_j + \rho(\boldsymbol{x}_j)\boldsymbol{n}, t_n\big), \quad \forall\, j \in \mathfrak{B}. \tag{2.36}$$

Then $\boldsymbol{D}^{\mathfrak{I}}$ is obtained by solving the following problem:

$$\boldsymbol{J_s}^{\mathfrak{I}\mathfrak{I}}\boldsymbol{D}_{\mathfrak{I}} = \hat{\boldsymbol{F}}^{\mathfrak{I}} - \boldsymbol{J_s}^{\mathfrak{I}\mathfrak{B}}\boldsymbol{D}_{\mathfrak{B}}.$$

Remark 2.1. We remark that as k increases, the approximation error generated in (2.36) may dominate, and thus a suboptimal convergence order may occur, see also [10, 11]. In Section 5, we will verify this assertion with numerical results.

3. Error Analysis in 2D Case

We derive in this section the error estimates for the fully discrete scheme (2.31) in the norms $\|\cdot\|_{\mathcal{N}}$ and $\|\cdot\|_{\Omega_h}$. The tool utilised is a special Ritz-Volterra projection $\mathfrak{R}^h$ defined according the bilinear forms $\mathcal{N}_1^h(\cdot\,,\cdot)$ and $\mathcal{N}_2^h(\cdot\,,\cdot)$. Starting from here, the inequality $\mathfrak{a} \le C\mathfrak{b}$ is reduced to $\mathfrak{a} \lesssim \mathfrak{b}$ for a positive constant C with no dependence on h. Additionally, for the sake of error analysis, we assume that the coefficients and data in (1.1) have enough regularity so that the weak solution u of (1.1) satisfies the required regularity.

3.1. The Ritz-Volterra projection

For any function w satisfying $w(\cdot,t) \in H^{\bar{m}+1}(\Omega_h)$ where $t \in [0,T]$, Ritz-Volterra projection $\mathfrak{R}^h w$ is defined by finding $\mathfrak{R}^h w(t) \in V_{\mathcal{S}}$ such that

$$\begin{aligned}
&\mathcal{N}_1^h\big(\mathfrak{R}^h w, v_h\big) + \int_0^t \mathcal{N}_2^h\big(\mathfrak{R}^h w(\tau), v_h\big)\mathrm{d}\tau \\
&= \mathcal{N}_1(w, v_h) + \int_0^t \mathcal{N}_2\big(w(\tau), v_h\big)\mathrm{d}\tau, \quad \forall\, v_h \in V_{\mathcal{S}},
\end{aligned} \tag{3.1}$$

where

$$\begin{aligned}
\mathcal{N}_1(w,v_h) &= (a_1\nabla w, \nabla v_h)_{\Omega_h} - \sum_{e\in\mathcal{E}_h^{\mathfrak{b}}}\int_e a_1\nabla w\cdot\boldsymbol{n} v_h \mathrm{d}s \\
&\quad - \sum_{e\in\mathcal{E}_h^{\mathfrak{b}}}\int_e \left(w + \sum_{j=1}^{\bar{m}}\frac{\rho^j}{j!}\partial_{\boldsymbol{n}}^j w\right)\big(a_1\nabla\big(\Pi_0^{k,E_e}v_h\big)\cdot\boldsymbol{n} - \gamma_1 h_e^{-1}v_h\big)\mathrm{d}s, \\
\mathcal{N}_2(w,v_h) &= (a_2\nabla w, \nabla v_h)_{\Omega_h} - \sum_{e\in\mathcal{E}_h^{\mathfrak{b}}}\int_e a_2\nabla w\cdot\boldsymbol{n} v_h \mathrm{d}s \\
&\quad - \sum_{e\in\mathcal{E}_h^{\mathfrak{b}}}\int_e \left(w + \sum_{j=1}^{\bar{m}}\frac{\rho^j}{j!}\partial_{\boldsymbol{n}}^j w\right)\big(a_2\nabla\big(\Pi_0^{k,E_e}v_h\big)\cdot\boldsymbol{n} - \gamma_2 h_e^{-1}v_h\big)\mathrm{d}s.
\end{aligned}$$

Next, we will establish the continuity of the right-hand side of Eq. (3.1). Before that, we recall the following trace inequality.

Lemma 3.1 ([14]). *For a function $v \in H^1(E)$ with any $E \in \mathcal{T}_h$, we have*

$$\|v\|_{\partial E} \lesssim h_E^{-\frac{1}{2}}\|v\|_E + h_E^{\frac{1}{2}}|v|_{1,E}. \tag{3.2}$$

It is easy to derive from (2.23), (3.2) and the fact $0 < h \le 1$ that

$$\begin{aligned}
|\mathcal{N}_1(w,v_h)| &\lesssim |w|_{1,\Omega_h}|v_h|_{1,\Omega_h} + \sum_{e\in\mathcal{E}_h^{\mathfrak{b}}}\big(|w|_{1,E_e} + h_{E_e}|w|_{2,E_e}\big)h_e^{-\frac{1}{2}}\|v_h\|_e \\
&\quad + \sum_{e\in\mathcal{E}_h^{\mathfrak{b}}} h_e^{-\frac{1}{2}}\|w\|_e\Big(h_e^{\frac{1}{2}}\big\|\nabla\big(\Pi_0^{k,E_e}v_h\big)\big\|_e + h_e^{-\frac{1}{2}}\|v_h\|_e\Big) \\
&\quad + \sum_{e\in\mathcal{E}_h^{\mathfrak{b}}}\left(\sum_{j=1}^{\bar{m}} h^{2j}\big(h_{E_e}^{-1}|w|_{j,E_e} + |w|_{j+1,E_e}\big)\right)\Big(h_e^{\frac{1}{2}}\big\|\nabla\big(\Pi_0^{k,E_e}v_h\big)\big\|_e + h_e^{-\frac{1}{2}}\|v_h\|_e\Big) \\
&\lesssim \big(\|w\|_{\bar{m}+1,\Omega_h} + \|w\|_{\mathcal{N}}\big)\|v_h\|_{\mathcal{N}},
\end{aligned}$$

then we obtain the continuity of the right-hand side of (3.1), i.e.

$$\begin{aligned}&\left|\mathcal{N}_1(w,v_h)+\int_0^t\mathcal{N}_2\big(w(\tau),v_h\big)\mathrm{d}\tau\right|\\ \lesssim&\left(\|w\|_{\bar{m}+1,\Omega_h}+\|w\|_{\mathcal{N}}+\int_0^t\big(\|w(\tau)\|_{\bar{m}+1,\Omega_h}+\|w(\tau)\|_{\mathcal{N}}\big)\mathrm{d}\tau\right)\|v_h\|_{\mathcal{N}}.\end{aligned}\tag{3.3}$$

Recalling the continuity and coercivity of $\mathcal{N}_1^h(\cdot\,,\cdot)$ and $\mathcal{N}_2^h(\cdot\,,\cdot)$ established in Theorem 2.1, one can conclude that $\mathfrak{R}^h$ is well posed [41]. The lemma below establishes the stability of $\mathfrak{R}^h$.

Lemma 3.2. *For any $w\in L^\infty((0,T);H^{\bar{m}+1}(\Omega_h))$ with $w_t,w_{tt}\in L^\infty((0,T);H^{\bar{m}+1}(\Omega_h))$ and any $t\in(0,T)$, we have*

$$\|\mathfrak{R}^h w\|_{\mathcal{N}}^2\lesssim\|w\|_{\bar{m}+1,\Omega_h}^2+\|w\|_{\mathcal{N}}^2+\int_0^t\big(\|w(\tau)\|_{\bar{m}+1,\Omega_h}^2+\|w(\tau)\|_{\mathcal{N}}^2\big)\mathrm{d}\tau,\tag{3.4}$$

$$\begin{aligned}\big\|(\mathfrak{R}^h w)_t\big\|_{\mathcal{N}}^2\lesssim&\|w\|_{\bar{m}+1,\Omega_h}^2+\|w\|_{\mathcal{N}}^2+\|w_t\|_{\bar{m}+1,\Omega_h}^2+\|w_t\|_{\mathcal{N}}^2\\&+\int_0^t\big(\|w(\tau)\|_{\bar{m}+1,\Omega_h}^2+\|w(\tau)\|_{\mathcal{N}}^2\big)\,\mathrm{d}\tau,\end{aligned}\tag{3.5}$$

$$\begin{aligned}\big\|(\mathfrak{R}^h w)_{tt}\big\|_{\mathcal{N}}^2\lesssim&\|w\|_{\bar{m}+1,\Omega_h}^2+\|w\|_{\mathcal{N}}^2+\|w_t\|_{\bar{m}+1,\Omega_h}^2+\|w_t\|_{\mathcal{N}}^2+\|w_{tt}\|_{\bar{m}+1,\Omega_h}^2+\|w_{tt}\|_{\mathcal{N}}^2\\&+\int_0^t\big(\|w(\tau)\|_{\bar{m}+1,\Omega_h}^2+\|w(\tau)\|_{\mathcal{N}}^2\big)\mathrm{d}\tau.\end{aligned}\tag{3.6}$$

Proof. Replacing v_h with $\mathfrak{R}^h w$ in (3.1), we obtain by (3.3), the coercivity of $\mathcal{N}_1^h(\cdot\,,\cdot)$ and the continuity of $\mathcal{N}_2^h(\cdot\,,\cdot)$

$$\begin{aligned}\|\mathfrak{R}^h w\|_{\mathcal{N}}^2\lesssim&(\|w\|_{\bar{m}+1,\Omega_h}+\|w\|_{\mathcal{N}})\|\mathfrak{R}^h w\|_{\mathcal{N}}\\&+\int_0^t(\|w(\tau)\|_{\bar{m}+1,\Omega_h}+\|w(\tau)\|_{\mathcal{N}})\|\mathfrak{R}^h w(t)\|_{\mathcal{N}}\mathrm{d}\tau\\&+\int_0^t\|\mathfrak{R}^h w(\tau)\|_{\mathcal{N}}\|\mathfrak{R}^h w(t)\|_{\mathcal{N}}\mathrm{d}\tau,\end{aligned}$$

then employing Young's inequality and the continuous Grönwall's inequality leads to (3.4). Differentiating (3.1) with respect to t, we have

$$\mathcal{N}_1^h\big((\mathfrak{R}^h w)_t,v_h\big)+\mathcal{N}_2^h\big(\mathfrak{R}^h w,v_h\big)=\mathcal{N}_1(w_t,v_h)+\mathcal{N}_2(w,v_h),\quad\forall\,v_h\in V_{\mathcal{S}}.\tag{3.7}$$

Then taking $v_h=(\mathfrak{R}^h w)_t$, (3.5) follows from Young's inequality and (3.4). Differentiating (3.7) with respect to t, we get

$$\mathcal{N}_1^h\big((\mathfrak{R}^h w)_{tt},v_h\big)+\mathcal{N}_2^h\big((\mathfrak{R}^h w)_t,v_h\big)=\mathcal{N}_1(w_{tt},v_h)+\mathcal{N}_2(w_t,v_h),\quad\forall\,v_h\in V_{\mathcal{S}}.\tag{3.8}$$

Replacing v_h with $(\mathfrak{R}^h w)_{tt}$ in (3.8), (3.6) can be obtained from Young's inequality and (3.5). The proof is complete. □

Next, we move on to analyzing the approximation properties of $\mathfrak{R}^h$ for the solution of (1.1).

Lemma 3.3. *Assume the weak solution u of (1.1) satisfies $u\in L^\infty((0,T);H^{k+1}(\Omega))$, then for any $t\in(0,T)$, the following estimates hold:*

$$\|u(t)-\mathfrak{R}^h u(t)\|_{\mathcal{N}}\lesssim h^k\left(|u|_{k+1,\Omega}^2+\int_0^t|u(\tau)|_{k+1,\Omega}^2\mathrm{d}\tau\right)^{\frac{1}{2}}.\tag{3.9}$$

Proof. Utilizing the interpolation operator $I_{\mathcal{S}}$, we can split $u - \mathfrak{R}^h u$ as

$$u - \mathfrak{R}^h u = u - I_{\mathcal{S}} u + I_{\mathcal{S}} u - \mathfrak{R}^h u,$$

then in light of (2.15) and (3.2), we have

$$\begin{aligned} \|u - I_{\mathcal{S}} u\|_{\mathcal{N}}^2 &= |u - I_{\mathcal{S}} u|_{1,\Omega_h}^2 + \sum_{e \in \mathcal{E}_h^{\mathrm{b}}} h_e^{-1} \|u - I_{\mathcal{S}} u\|_e^2 \\ &\lesssim h^{2k} |u|_{k+1,\Omega}^2 + \sum_{e \in \mathcal{E}_h^{\mathrm{b}}} h_e^{-1} \big(h_{E_e}^{-1} \|u - I_{\mathcal{S}} u\|_{E_e}^2 + h_{E_e} |u - I_{\mathcal{S}} u|_{1,E_e}^2 \big) \\ &\lesssim h^{2k} |u|_{k+1,\Omega}^2. \end{aligned} \tag{3.10}$$

We now proceed to estimate $\eta^h = I_{\mathcal{S}} u - \mathfrak{R}^h u$. It follows from (3.1) that

$$\mathcal{N}_1^h\big(\eta^h, v_h\big) + \int_0^t \mathcal{N}_2^h\big(\eta^h(\tau), v_h\big) \mathrm{d}\tau = T^1 + T^2$$

with

$$\begin{aligned} T^1 &= \mathcal{N}_1^h(I_{\mathcal{S}} u, v_h) - \mathcal{N}_1(u, v_h), \\ T^2 &= \int_0^t \mathcal{N}_2^h\big(I_{\mathcal{S}} u(\tau), v_h\big) - \mathcal{N}_2\big(u(\tau), v_h\big) \mathrm{d}\tau. \end{aligned}$$

By the concrete forms of $\mathcal{N}_1^h(\cdot\,,\cdot)$ and $\mathcal{N}_1(\cdot\,,\cdot)$, T^1 can be written as

$$T^1 = T_1^1 + T_2^1 + T_3^1 + T_4^1$$

with

$$\begin{aligned} T_1^1 &= \mathcal{A}_1^h(I_{\mathcal{S}} u, v_h) - (a_1 \nabla u, \nabla v_h)_{\Omega_h}, \\ T_2^1 &= \sum_{e \in \mathcal{E}_h^{\mathrm{b}}} \int_e a_1 \nabla\big(u - \Pi_0^{k,E_e} I_{\mathcal{S}} u\big) \cdot \boldsymbol{n} v_h \mathrm{d}s, \\ T_3^1 &= \sum_{e \in \mathcal{E}_h^{\mathrm{b}}} \int_e (u - I_{\mathcal{S}} u)\big(a_1 \nabla\big(\Pi_0^{k,E_e} v_h\big) \cdot \boldsymbol{n} - \gamma_1 h_e^{-1} v_h\big) \mathrm{d}s, \\ T_4^1 &= \sum_{e \in \mathcal{E}_h^{\mathrm{b}}} \int_e \left(\sum_{j=1}^{\bar{m}} \frac{\rho^j}{j!} \partial_{\boldsymbol{n}}^j \big(u - \Pi_0^{k,E_e} I_{\mathcal{S}} u\big) \right) \big(a_1 \nabla\big(\Pi_0^{k,E_e} v_h\big) \cdot \boldsymbol{n} - \gamma_1 h_e^{-1} v_h\big) \mathrm{d}s. \end{aligned}$$

In line with [39, Lemma 4.1], the upper bound of T_1^1 can be determined as

$$T_1^1 \lesssim h^k |u|_{k+1,\Omega_h} |v_h|_{1,\Omega_h} \lesssim h^k |u|_{k+1,\Omega} \|v_h\|_{\mathcal{N}}.$$

The estimate of T_2^1 can be obtained by utilizing the trace inequalities (2.23) and (3.2) in the following manner:

$$\begin{aligned} T_2^1 &\lesssim \sum_{e \in \mathcal{E}_h^{\mathrm{b}}} \big\| \nabla\big(u - \Pi_0^{k,E_e} I_{\mathcal{S}} u\big) \big\|_e \|v_h\|_e \\ &\lesssim \sum_{e \in \mathcal{E}_h^{\mathrm{b}}} \big(\big|u - \Pi_0^{k,E_e} u\big|_{1,E_e} + h_{E_e} \big|u - \Pi_0^{k,E_e} u\big|_{2,E_e} + |u - I_{\mathcal{S}} u|_{1,E_e} \big) h_e^{-\frac{1}{2}} \|v_h\|_e \\ &\lesssim h^k |u|_{k+1,\Omega_h} |v_h|_{\partial\Omega_h} \lesssim h^k |u|_{k+1,\Omega} \|v_h\|_{\mathcal{N}}. \end{aligned}$$

Considering the trace inequality (3.2), we can estimate T_3^1 as

$$
\begin{aligned}
T_3^1 &\lesssim \sum_{e\in\mathcal{E}_h^{\mathrm{b}}} \|u - I_{\mathcal{S}}u\|_e\Big(\big\|\nabla\big(\Pi_0^{k,E_e}v_h\big)\big\|_e + h_e^{-1}\|v_h\|_e\Big)\\
&\lesssim \sum_{e\in\mathcal{E}_h^{\mathrm{b}}} \Big(h_{E_e}^{-1}\|u - I_{\mathcal{S}}u\|_{E_e} + |u - I_{\mathcal{S}}u|_{1,E_e}\Big)\Big(|v_h|_{1,E_e} + h_e^{-\frac{1}{2}}\|v_h\|_e\Big)\\
&\lesssim h^k|u|_{k+1,\Omega_h}(|v_h|_{1,\Omega_h} + |v_h|_{\partial\Omega_h}) \lesssim h^k|u|_{k+1,\Omega}\|v_h\|_{\mathcal{N}}.
\end{aligned}
$$

In order to estimate T_4^1, it is necessary to utilize the inequalities (2.24) and (3.2), and the estimation can be done in the following way:

$$
\begin{aligned}
T_4^1 &\lesssim \sum_{e\in\mathcal{E}_h^{\mathrm{b}}} \left(\sum_{j=1}^{\bar m} \big\|\rho^j\partial_{\boldsymbol{n}}^j\big(u - \Pi_0^{k,E_e}I_{\mathcal{S}}u\big)\big\|_e\right)\Big(\big\|\nabla\big(\Pi_0^{k,E_e}v_h\big)\big\|_e + h_e^{-1}\|v_h\|_e\Big)\\
&\lesssim \sum_{e\in\mathcal{E}_h^{\mathrm{b}}} \left(\sum_{j=1}^{\bar m} \big\|\rho^j\partial_{\boldsymbol{n}}^j\big(u - \Pi_0^{k,E_e}u\big)\big\|_e\right)\Big(\big\|\nabla\big(\Pi_0^{k,E_e}v_h\big)\big\|_e + h_e^{-1}\|v_h\|_e\Big)\\
&\quad + \sum_{e\in\mathcal{E}_h^{\mathrm{b}}} \left(\sum_{j=1}^{\bar m} \big\|\rho^j\partial_{\boldsymbol{n}}^j\big(\Pi_0^{k,E_e}(u - I_{\mathcal{S}}u)\big)\big\|_e\right)\Big(\big\|\nabla\big(\Pi_0^{k,E_e}v_h\big)\big\|_e + h_e^{-1}\|v_h\|_e\Big)\\
&\lesssim \sum_{e\in\mathcal{E}_h^{\mathrm{b}}} \left(\sum_{j=1}^{\bar m} h^{2j}h_{E_e}^{-1}\big|u - \Pi_0^{k,E_e}u\big|_{j,E_e}\right)\Big(|v_h|_{1,E_e} + h_e^{-\frac{1}{2}}\|v_h\|_e\Big)\\
&\quad + \sum_{e\in\mathcal{E}_h^{\mathrm{b}}} \left(\sum_{j=1}^{\bar m} h^{2j}\big|u - \Pi_0^{k,E_e}u\big|_{j+1,E_e}\right)\Big(|v_h|_{1,E_e} + h_e^{-\frac{1}{2}}\|v_h\|_e\Big)\\
&\quad + \sum_{e\in\mathcal{E}_h^{\mathrm{b}}} h_e^{-\frac{1}{2}}\left(\sum_{j=1}^{\bar m} \big\|\rho^j\partial_{\boldsymbol{n}}^j\big(\Pi_0^{k,E_e}(u - I_{\mathcal{S}}u)\big)\big\|_e\right)\Big(|v_h|_{1,E_e} + h_e^{-\frac{1}{2}}\|v_h\|_e\Big)\\
&\lesssim \sum_{e\in\mathcal{E}_h^{\mathrm{b}}} \left(\sum_{j=1}^{\bar m} h^{k+j}|u|_{k+1,E_e}\right)\Big(|v_h|_{1,E_e} + h_e^{-\frac{1}{2}}\|v_h\|_e\Big)\\
&\quad + \left(\sum_{e\in\mathcal{E}_h^{\mathrm{b}}} \left(\sum_{j=1}^{\bar m} h^{2j}\right)|u - I_{\mathcal{S}}u|_{1,E_e}^2\right)^{\frac{1}{2}}(|v_h|_{1,\Omega_h} + |v_h|_{\partial\Omega_h})\\
&\lesssim \left(\sum_{j=1}^{\bar m} h^{k+j}\right)|u|_{k+1,\Omega_h}(|v_h|_{1,\Omega_h} + |v_h|_{\partial\Omega_h})\\
&\lesssim h^{k+1}|u|_{k+1,\Omega}\|v_h\|_{\mathcal{N}} \lesssim h^k|u|_{k+1,\Omega}\|v_h\|_{\mathcal{N}},
\end{aligned}
$$

where the fact that $h \le 1$ has been used.

In a similar vein to the analysis of T^1, T^2 can be estimated as

$$
T^2 \lesssim h^k\int_0^t |u(\tau)|_{k+1,\Omega}\|v_h\|_{\mathcal{N}}\mathrm{d}\tau.
$$

Consequently, we can infer that

$$
\mathcal{N}_1^h(\eta^h, v_h) + \int_0^t \mathcal{N}_2^h(\eta^h(\tau), v_h)\mathrm{d}\tau \lesssim h^k\left(|u|_{k+1,\Omega}\|v_h\|_{\mathcal{N}} + \int_0^t |u(\tau)|_{k+1,\Omega}\|v_h\|_{\mathcal{N}}\mathrm{d}\tau\right),
$$

then substituting v_h with η^h and utilizing the coercivity of $\mathcal{N}_1^h(\cdot\,,\cdot)$ and the continuity of $\mathcal{N}_2^h(\cdot\,,\cdot)$, we have by Young's inequality that

$$\|\eta^h\|_{\mathcal{N}}^2 \lesssim h^{2k}\left(|u|_{k+1,\Omega}^2 + \int_0^t |u(\tau)|_{k+1,\Omega}^2 \mathrm{d}\tau\right) + \int_0^t \|\eta^h(\tau)\|_{\mathcal{N}}^2 \mathrm{d}\tau.$$

The desired result (3.9) can be obtained by further utilizing the continuous Grönwall's inequality and (3.10). □

Given Lemma 3.3, we are now ready to give the estimates for $\|u - \mathfrak{R}^h u\|_{\Omega_h}$ by the duality argument.

Lemma 3.4. *Suppose that for* (1.1)*, the weak solution* u *satisfies* $u \in L^\infty((0,T); H^{k+1}(\Omega))$*. Then for any* $t \in (0,T)$*, we have the following estimates:*

$$\|u(t) - \mathfrak{R}^h u(t)\|_{\Omega_h} \lesssim h^{k+1}\left(|u|_{k+1,\Omega}^2 + \int_0^t |u(\tau)|_{k+1,\Omega}^2 \mathrm{d}\tau\right)^{\frac{1}{2}}. \tag{3.11}$$

Proof. Consider the following dual problem with the solution $\zeta \in H^2(\Omega_h) \cap H_0^1(\Omega_h)$:

$$\begin{aligned} -\nabla\cdot(a_1(\boldsymbol{x})\nabla\zeta) &= u - \mathfrak{R}^h u, \quad && \boldsymbol{x} \in \Omega_h,\\ \zeta &= 0, && \boldsymbol{x} \in \partial\Omega_h. \end{aligned}$$

The convexity of the domain Ω_h leads to the following regularity result:

$$\|\zeta\|_{2,\Omega_h} \lesssim \|u - \mathfrak{R}^h u\|_{\Omega_h}. \tag{3.12}$$

By utilizing the boundary condition for ζ and the definition of the global degrees of freedom for $V_{\mathcal{S}}$, we can infer that the interpolation of ζ in $V_{\mathcal{S}}$, denoted as $I_{\mathcal{S}}\zeta$, satisfies $I_{\mathcal{S}}\zeta|_{\partial\Omega_h} = 0$. We further deduce from (2.15) and (3.12) that

$$|\zeta - I_{\mathcal{S}}\zeta|_{1,\Omega_h} \lesssim h\|u - \mathfrak{R}^h u\|_{\Omega_h}. \tag{3.13}$$

Taking into account (3.1) and the definition of $\mathcal{N}_1^h(\cdot\,,\cdot)$ and $\mathcal{N}_2^h(\cdot\,,\cdot)$, we have

$$\|u - \mathfrak{R}^h u\|_{\Omega_h}^2 = R^1 + R^2 + R^3 + R^4 + R^5 + R^6 + R^7 \tag{3.14}$$

with

$$\begin{aligned}
R^1 &= \big(a_1\nabla(u - \mathfrak{R}^h u), \nabla(\zeta - I_{\mathcal{S}}\zeta)\big)_{\Omega_h},\\
R^2 &= \mathcal{A}_1^h\big(\mathfrak{R}^h u, I_{\mathcal{S}}\zeta\big) - \big(a_1\nabla\mathfrak{R}^h u, \nabla I_{\mathcal{S}}\zeta\big)_{\Omega_h},\\
R^3 &= \sum_{e\in\mathcal{E}_h^{\mathrm{b}}}\int_e \big(a_1\nabla\big(\Pi_0^{k,E_e} I_{\mathcal{S}}\zeta\big)\cdot\boldsymbol{n} - a_1\nabla\zeta\cdot\boldsymbol{n}\big)(u - \mathfrak{R}^h u)\mathrm{d}s,\\
R^4 &= \sum_{e\in\mathcal{E}_h^{\mathrm{b}}}\int_e \left(\sum_{j=1}^{\bar{m}} \frac{\rho^j}{j!}\partial_{\boldsymbol{n}}^j\big(u - \Pi_0^{k,E_e}\mathfrak{R}^h u\big)\right) a_1\nabla\big(\Pi_0^{k,E_e} I_{\mathcal{S}}\zeta\big)\cdot\boldsymbol{n}\mathrm{d}s,\\
R^5 &= \int_0^t \mathcal{A}_2^h\big(\mathfrak{R}^h u(\tau), I_{\mathcal{S}}\zeta\big) - \big(a_2\nabla u(\tau), \nabla I_{\mathcal{S}}\zeta\big)_{\Omega_h}\mathrm{d}\tau,\\
R^6 &= \int_0^t \sum_{e\in\mathcal{E}_h^{\mathrm{b}}}\int_e \big(a_2\nabla\big(\Pi_0^{k,E_e} I_{\mathcal{S}}\zeta\big)\cdot\boldsymbol{n}\big)\big(u(\tau) - \mathfrak{R}^h u(\tau)\big)\mathrm{d}s\mathrm{d}\tau,\\
R^7 &= \int_0^t \sum_{e\in\mathcal{E}_h^{\mathrm{b}}}\int_e \left(\sum_{j=1}^{\bar{m}} \frac{\rho^j}{j!}\partial_{\boldsymbol{n}}^j\big(u(\tau) - \Pi_0^{k,E_e}\mathfrak{R}^h u(\tau)\big)\right) a_2\nabla\big(\Pi_0^{k,E_e} I_{\mathcal{S}}\zeta\big)\cdot\boldsymbol{n}\mathrm{d}s\mathrm{d}\tau.
\end{aligned}$$

The estimate for R^1 is straightforward by (2.15) and (3.9), and can be expressed as

$$\begin{aligned} R^1 &\lesssim |u-\mathfrak{R}^h u|_{1,\Omega_h}|\zeta - I_{\mathcal{S}}\zeta|_{1,\Omega_h} \\ &\lesssim h^{k+1}\left(|u|^2_{k+1,\Omega}+\int_0^t |u(\tau)|^2_{k+1,\Omega}\mathrm{d}\tau\right)^{\frac{1}{2}}\|u-\mathfrak{R}^h u\|_{\Omega_h}. \end{aligned} \tag{3.15}$$

According to [39, Lemma 4.2], we can establish the upper bound of R^2 as

$$R^2 \lesssim h^{k+1}\left(|u|^2_{k+1,\Omega}+\int_0^t |u(\tau)|^2_{k+1,\Omega}\mathrm{d}\tau\right)^{\frac{1}{2}}\|u-\mathfrak{R}^h u\|_{\Omega_h}. \tag{3.16}$$

For R^3, based on (2.13), (2.15), (3.2) and (3.9), it follows that

$$\begin{aligned} R^3 &\lesssim \sum_{e\in\mathcal{E}_h^{\mathrm{b}}} \left\|\nabla\big(\Pi_0^{k,E_e} I_{\mathcal{S}}\zeta\big)-\nabla\zeta\right\|_e \|u-\mathfrak{R}^h u\|_e \\ &\lesssim \sum_{e\in\mathcal{E}_h^{\mathrm{b}}}\left(\left|\Pi_0^{k,E_e} I_{\mathcal{S}}\zeta-\zeta\right|_{1,E_e}+h_{E_e}\left|\Pi_0^{k,E_e} I_{\mathcal{S}}\zeta-\zeta\right|_{2,E_e}\right)h_e^{-\frac{1}{2}}\|u-\mathfrak{R}^h u\|_e \\ &\lesssim h|\zeta|_{2,\Omega_h}\|u-\mathfrak{R}^h u\|_{\mathcal{N}} \\ &\lesssim h^{k+1}\left(|u|^2_{k+1,\Omega}+\int_0^t |u(\tau)|^2_{k+1,\Omega}\mathrm{d}\tau\right)^{\frac{1}{2}}\|u-\mathfrak{R}^h u\|_{\Omega_h}. \end{aligned} \tag{3.17}$$

Similar to the analysis of T_4^1 in Lemma 3.3, the estimation for R^4 can be performed in the following manner:

$$\begin{aligned} R^4 &\lesssim \sum_{e\in\mathcal{E}_h^{\mathrm{b}}}\left(\sum_{j=1}^{\bar m} h^{k+j}|u|_{k+1,E_e}\right)|I_{\mathcal{S}}\zeta|_{1,E_e}+\left(\sum_{e\in\mathcal{E}_h^{\mathrm{b}}}\left(\sum_{j=1}^{\bar m}h^{2j}\right)|u-\mathfrak{R}^h u|^2_{1,E_e}\right)^{\frac{1}{2}}|I_{\mathcal{S}}\zeta|_{1,\Omega_h} \\ &\lesssim \left(\sum_{j=1}^{\bar m}h^{k+j}\right)\left(|u|^2_{k+1,\Omega}+\int_0^t |u(\tau)|^2_{k+1,\Omega}\mathrm{d}\tau\right)^{\frac{1}{2}}|I_{\mathcal{S}}\zeta|_{1,\Omega_h} \\ &\lesssim h^{k+1}\left(|u|^2_{k+1,\Omega}+\int_0^t |u(\tau)|^2_{k+1,\Omega}\mathrm{d}\tau\right)^{\frac{1}{2}}\big(|I_{\mathcal{S}}\zeta-\zeta|_{1,\Omega_h}+|\zeta|_{1,\Omega_h}\big) \\ &\lesssim h^{k+1}\left(|u|^2_{k+1,\Omega}+\int_0^t |u(\tau)|^2_{k+1,\Omega}\mathrm{d}\tau\right)^{\frac{1}{2}}\|u-\mathfrak{R}^h u\|_{\Omega_h}. \end{aligned} \tag{3.18}$$

Rewrite the integrand function of R^5 as

$$\mathcal{A}_2^h\big(\mathfrak{R}^h u(\tau), I_{\mathcal{S}}\zeta\big)-\big(a_2\nabla u(\tau),\nabla I_{\mathcal{S}}\zeta\big)_{\Omega_h}=\sum_{E\in\mathcal{T}_h}\big(R_1^5(\tau)+R_2^5(\tau)+R_3^5(\tau)\big),$$

where

$$\begin{aligned} R_1^5(\tau) &= \mathcal{A}_2^E\big(\mathfrak{R}^h u(\tau)-\Pi_0^{k,E}u(\tau), I_{\mathcal{S}}\zeta-\Pi_0^{1,E}\zeta\big) \\ &\quad -\big(a_2\nabla\big(u(\tau)-\Pi_0^{k,E}u(\tau)\big),\nabla\big(I_{\mathcal{S}}\zeta-\Pi_0^{1,E}\zeta\big)\big)_E, \\ R_2^5(\tau) &= \mathcal{A}_2^E\big(\mathfrak{R}^h u(\tau),\Pi_0^{1,E}\zeta\big)-\big(a_2\nabla u(\tau),\nabla\Pi_0^{1,E}\zeta\big)_E, \\ R_3^5(\tau) &= \mathcal{A}_2^E\big(\Pi_0^{k,E}u(\tau), I_{\mathcal{S}}\zeta\big)-\big(a_2\nabla\Pi_0^{k,E}u(\tau),\nabla I_{\mathcal{S}}\zeta\big)_E. \end{aligned}$$

The following estimates for $R_1^5(\tau)$ and $R_3^5(\tau)$ can be obtained by using [39, Lemma 4.2]:

$$\sum_{E\in\mathcal{T}_h}\big(R_1^5(\tau)+R_3^5(\tau)\big)\lesssim h^{k+1}\bigg(|u(\tau)|_{k+1,\Omega}^2+\int_0^\tau|u(\sigma)|_{k+1,\Omega}^2\mathrm{d}\sigma\bigg)^{\frac12}\|u(t)-\mathfrak{R}^hu(t)\|_{\Omega_h}.$$

Rewrite $R_2^5(\tau)$ as

$$\begin{aligned}R_2^5(\tau)=&\big(a_2\big(\Pi_1^{k-1,E}\nabla\mathfrak{R}^hu(\tau)-\nabla\mathfrak{R}^hu(\tau)\big),\nabla\Pi_0^{1,E}\zeta\big)_E\\&+\big(a_2\big(\nabla\mathfrak{R}^hu(\tau)-\nabla u(\tau)\big),\nabla\big(\Pi_0^{1,E}\zeta-\zeta\big)\big)_E\\&+\big(a_2\big(\nabla\mathfrak{R}^hu(\tau)-\nabla u(\tau)\big),\nabla\zeta\big)_E.\end{aligned}$$

Employing [39, Lemma 4.2] again, using (2.15), (3.9), and integrating by parts, we have

$$\begin{aligned}\sum_{E\in\mathcal{T}_h}R_2^5(\tau)\lesssim&\ h^{k+1}\bigg(|u(\tau)|_{k+1,\Omega}^2+\int_0^\tau|u(\sigma)|_{k+1,\Omega}^2\mathrm{d}\sigma\bigg)^{\frac12}\|u(t)-\mathfrak{R}^hu(t)\|_{\Omega_h}\\&+\big(a_2\big(\nabla\mathfrak{R}^hu(\tau)-\nabla u(\tau)\big),\nabla\zeta\big)_{\Omega_h}\\=&\ h^{k+1}\bigg(|u(\tau)|_{k+1,\Omega}^2+\int_0^\tau|u(\sigma)|_{k+1,\Omega}^2\mathrm{d}\sigma\bigg)^{\frac12}\|u(t)-\mathfrak{R}^hu(t)\|_{\Omega_h}\\&-\big(\mathfrak{R}^hu(\tau)-u(\tau),\nabla\cdot(a_2\nabla\zeta)\big)_{\Omega_h}+\sum_{e\in\mathcal{E}_h^{\mathrm{b}}}\int_e a_2\nabla\zeta\cdot\boldsymbol{n}\big(\mathfrak{R}^hu(\tau)-u(\tau)\big)\mathrm{d}s\\\lesssim&\ h^{k+1}\bigg(|u(\tau)|_{k+1,\Omega}^2+\int_0^\tau|u(\sigma)|_{k+1,\Omega}^2\mathrm{d}\sigma\bigg)^{\frac12}\|u(t)-\mathfrak{R}^hu(t)\|_{\Omega_h}\\&+\|u(\tau)-\mathfrak{R}^hu(\tau)\|_{\Omega_h}\|u(t)-\mathfrak{R}^hu(t)\|_{\Omega_h}+\sum_{e\in\mathcal{E}_h^{\mathrm{b}}}\int_e a_2\nabla\zeta\cdot\boldsymbol{n}\big(\mathfrak{R}^hu(\tau)-u(\tau)\big)\mathrm{d}s.\end{aligned}$$

To sum up, we get

$$\begin{aligned}R^5\lesssim&\int_0^t h^{k+1}\bigg(|u(\tau)|_{k+1,\Omega}^2+\int_0^\tau|u(\sigma)|_{k+1,\Omega}^2\mathrm{d}\sigma\bigg)^{\frac12}\|u(t)-\mathfrak{R}^hu(t)\|_{\Omega_h}\mathrm{d}\tau\\&+\int_0^t\|u(\tau)-\mathfrak{R}^hu(\tau)\|_{\Omega_h}\|u(t)-\mathfrak{R}^hu(t)\|_{\Omega_h}\mathrm{d}\tau\\&+\int_0^t\sum_{e\in\mathcal{E}_h^{\mathrm{b}}}\int_e a_2\nabla\zeta\cdot\boldsymbol{n}\big(\mathfrak{R}^hu(\tau)-u(\tau)\big)\mathrm{d}s\mathrm{d}\tau.\end{aligned}\tag{3.19}$$

For R^6, adding and subtracting $a_2\nabla\zeta\cdot\boldsymbol{n}$, and employing a similar analysis for R^3, we obtain

$$\begin{aligned}R^6\lesssim&\ h^{k+1}\int_0^t\bigg(|u(\tau)|_{k+1,\Omega}^2+\int_0^\tau|u(\sigma)|_{k+1,\Omega}^2\mathrm{d}\sigma\bigg)^{\frac12}\|u(t)-\mathfrak{R}^hu(t)\|_{\Omega_h}\mathrm{d}\tau\\&+\int_0^t\sum_{e\in\mathcal{E}_h^{\mathrm{b}}}\int_e a_2\nabla\zeta\cdot\boldsymbol{n}\big(u(\tau)-\mathfrak{R}^hu(\tau)\big)\mathrm{d}s\mathrm{d}\tau.\end{aligned}\tag{3.20}$$

Analogous to R^4, we can estimate R^7 as

$$R^7\lesssim h^{k+1}\int_0^t\bigg(|u(\tau)|_{k+1,\Omega}^2+\int_0^\tau|u(\sigma)|_{k+1,\Omega}^2\mathrm{d}\sigma\bigg)^{\frac12}\|u(t)-\mathfrak{R}^hu(t)\|_{\Omega_h}\mathrm{d}\tau.\tag{3.21}$$

Inserting the estimates (3.15)-(3.21) into (3.14), we have by Young's inequality that

$$\begin{aligned}\|u-\mathfrak{R}^h u\|_{\Omega_h}^2 &\lesssim h^{2k+2}\Big(|u|_{k+1,\Omega}^2+\int_0^t |u(\tau)|_{k+1,\Omega}^2 \mathrm{d}\tau+\int_0^t\int_0^\tau |u(\sigma)|_{k+1,\Omega}^2 \mathrm{d}\sigma\mathrm{d}\tau\Big)\\ &\quad+\int_0^t \|u(\tau)-\mathfrak{R}^h u(\tau)\|_{\Omega_h}^2 \mathrm{d}\tau\\ &\lesssim h^{2k+2}\Big(|u|_{k+1,\Omega}^2+\int_0^t |u(\tau)|_{k+1,\Omega}^2 \mathrm{d}\tau\Big)+\int_0^t \|u(\tau)-\mathfrak{R}^h u(\tau)\|_{\Omega_h}^2 \mathrm{d}\tau,\end{aligned}$$

then utilizing the continuous Grönwall's inequality yields the desired result (3.11). □

In order to establish the error estimates of the fully discrete scheme, it is necessary to estimate $\|u_t-(\mathfrak{R}^h u)_t\|_{\Omega_h}$. To do this, we can utilize the standard duality argument and focus on estimating $\|u_t-(\mathfrak{R}^h u)_t\|_{\mathcal{N}}$ as a starting point.

Lemma 3.5. *Suppose for* (1.1)*, the weak solution u satisfies $u\in L^\infty((0,T);H^{k+1}(\Omega))$ with $u_t\in L^\infty((0,T);H^{k+1}(\Omega))$, then for any $t\in(0,T)$, the following estimates hold:*

$$\big\|u_t-(\mathfrak{R}^h u)_t\big\|_{\mathcal{N}}\lesssim h^k\Big(|u|_{k+1,\Omega}^2+|u_t|_{k+1,\Omega}^2+\int_0^t |u(\tau)|_{k+1,\Omega}^2 \mathrm{d}\tau\Big)^{\frac{1}{2}}. \tag{3.22}$$

Proof. Let $\eta_t^h=I_S u_t-(\mathfrak{R}^h u)_t$, and according to (3.7), we have

$$\mathcal{N}_1^h\big(\eta_t^h,v_h\big)=\mathcal{N}_1^h(I_S u_t,v_h)-\mathcal{N}_1(u_t,v_h)+\mathcal{N}_2^h\big(\mathfrak{R}^h u,v_h\big)-\mathcal{N}_2(u,v_h).$$

In line with the analysis established in Lemma 3.3, we arrive at

$$\big\|\eta_t^h\big\|_{\mathcal{N}}\lesssim h^k\Big(|u|_{k+1,\Omega}^2+|u_t|_{k+1,\Omega}^2+\int_0^t |u(\tau)|_{k+1,\Omega}^2 \mathrm{d}\tau\Big)^{\frac{1}{2}},$$

then employing the triangular inequality, (2.15) and (3.2) leads to (3.22). □

Lemma 3.6. *Assume for* (1.1)*, the weak solution u satisfies $u\in L^\infty((0,T);H^{k+1}(\Omega))$ with $u_t\in L^\infty((0,T);H^{k+1}(\Omega))$, then for any $t\in(0,T)$, the following estimates hold:*

$$\big\|u_t-(\mathfrak{R}^h u)_t\big\|_{\Omega_h}\lesssim h^{k+1}\Big(|u|_{k+1,\Omega}^2+|u_t|_{k+1,\Omega}^2+\int_0^t |u(\tau)|_{k+1,\Omega}^2 \mathrm{d}\tau\Big)^{\frac{1}{2}}. \tag{3.23}$$

Proof. Consider the following dual problem with the solution $\hat{\zeta}\in H^2(\Omega_h)\cap H_0^1(\Omega_h)$:

$$\begin{aligned}-\nabla\cdot\big(a_1(\boldsymbol{x})\nabla\hat{\zeta}\big)&=u_t-(\mathfrak{R}^h u)_t, && \boldsymbol{x}\in\Omega_h,\\ \hat{\zeta}&=0, && \boldsymbol{x}\in\partial\Omega_h.\end{aligned}$$

Carrying out an analysis similar to that of (3.14), we obtain

$$\big\|u_t-(\mathfrak{R}^h u)_t\big\|_{\Omega_h}^2=\hat{R}^1+\hat{R}^2+\hat{R}^3+\hat{R}^4+\hat{R}^5+\hat{R}^6+\hat{R}^7$$

with

$$\begin{aligned}\hat{R}^1&=\big(a_1\nabla\big(u_t-(\mathfrak{R}^h u)_t\big),\nabla\big(\hat{\zeta}-I_S\hat{\zeta}\big)\big)_{\Omega_h},\\ \hat{R}^2&=\mathcal{A}_1^h\big((\mathfrak{R}^h u)_t,I_S\hat{\zeta}\big)-\big(a_1\nabla(\mathfrak{R}^h u)_t,\nabla I_S\hat{\zeta}\big)_{\Omega_h},\end{aligned}$$

$$\hat{R}^3 = \sum_{e\in\mathcal{E}_h^{\mathrm{b}}} \int_e \big(a_1\nabla\big(\Pi_0^{k,E_e} I_S\hat{\zeta}\big)\cdot\boldsymbol{n} - a_1\nabla\hat{\zeta}\cdot\boldsymbol{n}\big)\big(u_t - (\mathfrak{R}^h u)_t\big)\mathrm{d}s,$$

$$\hat{R}^4 = \sum_{e\in\mathcal{E}_h^{\mathrm{b}}} \int_e \left(\sum_{j=1}^{\bar{m}} \frac{\rho^j}{j!}\partial_{\boldsymbol{n}}^j\big(u_t - \Pi_0^{k,E_e}(\mathfrak{R}^h u)_t\big)\right) a_1\nabla\big(\Pi_0^{k,E_e} I_S\hat{\zeta}\big)\cdot\boldsymbol{n}\mathrm{d}s,$$

$$\hat{R}^5 = \mathcal{A}_2^h\big(\mathfrak{R}^h u, I_S\hat{\zeta}\big) - \big(a_2\nabla u, \nabla I_S\hat{\zeta}\big)_{\Omega_h},$$

$$\hat{R}^6 = \sum_{e\in\mathcal{E}_h^{\mathrm{b}}} \int_e a_2\nabla\big(\Pi_0^{k,E_e} I_S\hat{\zeta}\big)\cdot\boldsymbol{n}(u - \mathfrak{R}^h u)\mathrm{d}s,$$

$$\hat{R}^7 = \sum_{e\in\mathcal{E}_h^{\mathrm{b}}} \int_e \left(\sum_{j=1}^{\bar{m}} \frac{\rho^j}{j!}\partial_{\boldsymbol{n}}^j\big(u - \Pi_0^{k,E_e}\mathfrak{R}^h u\big)\right) a_2\nabla\big(\Pi_0^{k,E_e} I_S\hat{\zeta}\big)\cdot\boldsymbol{n}\mathrm{d}s.$$

Then, in a similar vein to the proof of Lemma 3.4 and using Lemmas 3.3 and 3.5, we obtain (3.23). The proof is complete. □

3.2. Error estimates for the fully discrete scheme

In this subsection, we begin by deriving error analysis for the terms that involve the Dirichlet boundary condition g. Subsequently, the error estimates are presented for the fully discrete scheme (2.31) based on the approximation properties of the Ritz-Volterra projection $\mathfrak{R}^h$.

Lemma 3.7 ([19]). *For any $E \in \mathcal{T}_h$ and any $v_h \in V(E)$, we have the following inverse inequality:*

$$|v_h|_{1,E} \lesssim h_E^{-1}\|v_h\|_E. \tag{3.24}$$

Lemma 3.8. *Assume that the weak solution u of* (1.1) *satisfies $u(\cdot,t) \in W^{\bar{m}+1,\infty}(\Omega)$ for $t \in (0,T)$, then for any $t \in (0,T)$ and any $v_h \in V_S$, we have*

$$\begin{aligned}
&\sum_{e\in\mathcal{E}_h^{\mathrm{b}}} \int_e \left(\hat{g}(t) - u - \sum_{j=1}^{\bar{m}} \frac{\rho^j}{j!}\partial_{\boldsymbol{n}}^j u\right)\big(a_1\nabla\big(\Pi_0^{k,E_e} v_h\big)\cdot\boldsymbol{n} - \gamma_1 h_e^{-1} v_h\big)\mathrm{d}s \\
&\lesssim h^{k+1}|u|_{\bar{m}+1,\infty,\Omega}\|v_h\|_{\Omega_h},
\end{aligned} \tag{3.25}$$

$$\begin{aligned}
&\int_0^t \sum_{e\in\mathcal{E}_h^{\mathrm{b}}} \int_e \left(\hat{g}(\tau) - u(\tau) - \sum_{j=1}^{\bar{m}} \frac{\rho^j}{j!}\partial_{\boldsymbol{n}}^j u(\tau)\right)\big(a_2\nabla\big(\Pi_0^{k,E_e} v_h\big)\cdot\boldsymbol{n} - \gamma_2 h_e^{-1} v_h\big)\mathrm{d}s\mathrm{d}\tau \\
&\lesssim h^{k+1}\int_0^t |u(\tau)|_{\bar{m}+1,\infty,\Omega}\mathrm{d}\tau\|v_h\|_{\Omega_h}.
\end{aligned} \tag{3.26}$$

Proof. For $\boldsymbol{x} \in \partial\Omega_h$, we have the following estimates according to Taylor expansion [12] and (2.2):

$$\begin{aligned}
&\left|\hat{g}(t) - u - \sum_{j=1}^{\bar{m}} \frac{\rho^j}{j!}\partial_{\boldsymbol{n}}^j u\right| \\
=& \left|u\big(\boldsymbol{x} + \rho(\boldsymbol{x})\boldsymbol{n}, t\big) - u(\boldsymbol{x},t) - \sum_{j=1}^{\bar{m}} \frac{\rho^j}{j!}\partial_{\boldsymbol{n}}^j u(\boldsymbol{x},t)\right| \\
\lesssim& h^{2\bar{m}+2}|u|_{\bar{m}+1,\infty,\Omega}.
\end{aligned}$$

Since we set $\bar{m} = \lfloor (k+1)/2 \rfloor$, the value of $\bar{m}$ is $(k+1)/2$ when k is odd and $k/2$ when k is even. Then we have

$$h^{2\bar{m}+2} = \begin{cases} h^{k+3}, & \text{if} \quad k \quad \text{is odd}, \\ h^{k+2}, & \text{if} \quad k \quad \text{is even}. \end{cases}$$

Due to the fact that $0 < h \leq 1$, we arrive at

$$\left| \hat{g}(t) - u - \sum_{j=1}^{\bar{m}} \frac{\rho^j}{j!} \partial_{\boldsymbol{n}}^j u \right| \lesssim h^{k+2} |u|_{\bar{m}+1,\infty,\Omega}. \tag{3.27}$$

Utilizing (2.23), (3.2), (3.24) and (3.27), we obtain

$$\begin{aligned}
&\sum_{e\in\mathcal{E}_h^{\mathrm{b}}} \int_e \left(\hat{g}(t) - u - \sum_{j=1}^{\bar{m}} \frac{\rho^j}{j!} \partial_{\boldsymbol{n}}^j u \right) \big(a_1 \nabla \big(\Pi_0^{k,E_e} v_h \big) \cdot \boldsymbol{n} - \gamma_1 h_e^{-1} v_h \big) \mathrm{d}s \\
\lesssim &\sum_{e\in\mathcal{E}_h^{\mathrm{b}}} \left\| \hat{g}(t) - u - \sum_{j=1}^{\bar{m}} \frac{\rho^j}{j!} \partial_{\boldsymbol{n}}^j u \right\|_e \big(\big\| \nabla \Pi_0^{k,E_e} v_h \big\|_e + h_e^{-1} \|v_h\|_e \big) \\
\lesssim &\sum_{e\in\mathcal{E}_h^{\mathrm{b}}} h^{k+2} h_e^{\frac{1}{2}} |u|_{\bar{m}+1,\infty,\Omega} \big(\big\| \nabla \Pi_0^{k,E_e} v_h \big\|_e + h_e^{-1} \|v_h\|_e \big) \\
\lesssim &\sum_{e\in\mathcal{E}_h^{\mathrm{b}}} h^{k+2} |u|_{\bar{m}+1,\infty,\Omega} \big(|v_h|_{1,E_e} + h_{E_e}^{-1} \|v_h\|_{E_e} \big) \lesssim h^{k+1} |u|_{\bar{m}+1,\infty,\Omega} \|v_h\|_{\Omega_h}.
\end{aligned}$$

Therefore, (3.25) is demonstrated. In a similar way, (3.26) can be obtained. □

Theorem 3.1. *Let u be the solution of* (1.1) *and $\{u_h^n\}_{n=1}^{N_T}$ be the solution of* (2.31)*. Assume*

$$\begin{aligned}
&u \in L^\infty\big((0,T); H^{k+1}(\Omega) \cap W^{\bar{m}+1,\infty}(\Omega)\big), && u_t \in L^\infty\big((0,T); H^{k+1}(\Omega)\big), \\
&u_{tt} \in L^\infty\big((0,T); H^{\bar{m}+1}(\Omega)\big), && u_{ttt} \in L^2\big((0,T); L^2(\Omega)\big), \\
&f, b(u) \in L^\infty\big((0,T); H^{k+1}(\Omega)\big), && u_0 \in H^{k+1}(\Omega), \quad \Delta t < 1,
\end{aligned}$$

then for all $n = 1, 2, \ldots, N_T$, we have the following error estimates:

$$\begin{aligned}
\big\| u(t_n) - u_h^n \big\|_{\Omega_h} \lesssim h^{k+1} \Big(&\|u\|_{L^2((0,t_n);H^{k+1}(\Omega))} + \|u_t\|_{L^2((0,t_n);H^{k+1}(\Omega))} + \|f\|_{L^\infty((0,t_n);H^{k+1}(\Omega))} \\
&+ \|b(u)\|_{L^\infty((0,t_n);H^{k+1}(\Omega))} + \|u\|_{L^\infty((0,t_n);H^{k+1}(\Omega))} + |u_0|_{k+1,\Omega} \\
&+ \|u\|_{L^\infty((0,t_n);W^{\bar{m}+1,\infty}(\Omega))} + \|u\|_{L^2((0,t_n);W^{\bar{m}+1,\infty}(\Omega))} \Big) \\
+ (\Delta t)^2 \Big(&\|u_{ttt}\|_{L^2((0,t_n);L^2(\Omega))} + \|u\|_{L^2((0,t_n);H^{\bar{m}+1}(\Omega))} + \|u\|_{L^2((0,t_n);H^1(\Omega_h))} \\
&+ \|u_t\|_{L^2((0,t_n);H^{\bar{m}+1}(\Omega))} + \|u_t\|_{L^2((0,t_n);H^1(\Omega_h))} \\
&+ \|u_{tt}\|_{L^2((0,t_n);H^{\bar{m}+1}(\Omega))} + \|u_{tt}\|_{L^2((0,t_n);H^1(\Omega_h))} \Big),
\end{aligned} \tag{3.28}$$

$$\begin{aligned}
\big\| u(t_n) - u_h^n \big\|_{\mathcal{N}} \lesssim h^{k+1} \Big(&\|u\|_{L^2((0,t_n);H^{k+1}(\Omega))} + \|u_t\|_{L^2((0,t_n);H^{k+1}(\Omega))} + \|f\|_{L^\infty((0,t_n);H^{k+1}(\Omega))} \\
&+ \|b(u)\|_{L^\infty((0,t_n);H^{k+1}(\Omega))} + \|u\|_{L^\infty((0,t_n);H^{k+1}(\Omega))} + |u_0|_{k+1,\Omega} \\
&+ \|u\|_{L^\infty((0,t_n);W^{\bar{m}+1,\infty}(\Omega))} + \|u\|_{L^2((0,t_n);W^{\bar{m}+1,\infty}(\Omega))} \Big) \\
+ h^k \Big(&\|u\|_{L^\infty((0,t_n);H^{k+1}(\Omega))} + \|u\|_{L^2((0,t_n);H^{k+1}(\Omega))} + |u_0|_{k+1,\Omega} \Big)
\end{aligned}$$

$$+ (\Delta t)^2 \Big(\|u_{ttt}\|_{L^2((0,t_n);L^2(\Omega))} + \|u\|_{L^2((0,t_n);H^{\bar{m}+1}(\Omega))} + \|u\|_{L^2((0,t_n);H^1(\Omega_h))} + \|u_t\|_{L^2((0,t_n);H^{\bar{m}+1}(\Omega))} + \|u_t\|_{L^2((0,t_n);H^1(\Omega_h))} + \|u_{tt}\|_{L^2((0,t_n);H^{\bar{m}+1}(\Omega))} + \|u_{tt}\|_{L^2((0,t_n);H^1(\Omega_h))} \Big), \tag{3.29}$$

where

$$\|w\|_{L^2((0,t);H^1(\Omega_h))} = \left(\int_0^t \|w(\tau)\|^2_{\mathcal{N}} \mathrm{d}\tau \right)^{\frac{1}{2}}, \quad w \in \{u, u_t, u_{tt}\}.$$

Proof. Through the Ritz-Volterra projection $\mathfrak{R}^h$, we can decompose the error $u(t_n) - u_h^n$ as

$$u(t_n) - u_h^n = \big(u(t_n) - \mathfrak{R}^h u(t_n)\big) + \big(\mathfrak{R}^h u(t_n) - u_h^n\big) = \Theta_1^n + \Theta_2^n,$$

and Lemmas 3.3 and 3.4 have provided the following established estimates for Θ_1^n:

$$\big\|\Theta_1^n\big\|_{\mathcal{N}} \lesssim h^k \big(\|u\|_{L^\infty((0,t_n);H^{k+1}(\Omega))} + \|u\|_{L^2((0,t_n);H^{k+1}(\Omega))}\big), \tag{3.30}$$
$$\big\|\Theta_1^n\big\|_{\Omega_h} \lesssim h^{k+1} \big(\|u\|_{L^\infty((0,t_n);H^{k+1}(\Omega))} + \|u\|_{L^2((0,t_n);H^{k+1}(\Omega))}\big). \tag{3.31}$$

Introduce the following notations:

$$\Xi^n = \Xi(t_n), \quad \bar{\delta}\Xi^n = \frac{\Xi^n - \Xi^{n-1}}{\Delta t}, \quad \overline{\Xi^n} = \frac{\Xi^n + \Xi^{n-1}}{2}, \quad \Xi \in \{u, u_t, f, \hat{g}, \Theta_2, u_h\}.$$

For model problem (1.1), it is easy to deduce that for any $v_h \in V_{\mathcal{S}}$,

$$(f, v_h)_{\Omega_h} = (a_0 u_t, v_h)_{\Omega_h} + (a_1 \nabla u, \nabla v_h)_{\Omega_h} - \sum_{e \in \mathcal{E}_h^{\mathrm{b}}} \int_e a_1 \nabla u \cdot \boldsymbol{n} v_h \mathrm{d}s + \big(b(u), v_h\big)_{\Omega_h} + \int_0^t \big(a_2 \nabla u(\tau), \nabla v_h\big)_{\Omega_h} \mathrm{d}\tau - \int_0^t \sum_{e \in \mathcal{E}_h^{\mathrm{b}}} \int_e a_2 \nabla u(\tau) \cdot \boldsymbol{n} v_h \mathrm{d}s \mathrm{d}\tau, \tag{3.32}$$

then it follows from (2.31), (3.1) and (3.32) that

$$\begin{aligned}
&\mathcal{A}_0^h\big(\bar{\delta}\Theta_2^n, v_h\big) + \mathcal{N}_1^h\big(\overline{\Theta_2^n}, v_h\big) \\
&= \frac{1}{\Delta t}\mathcal{A}_0^h\big(\mathfrak{R}^h u(t_n) - \mathfrak{R}^h u(t_{n-1}), v_h\big) + \frac{1}{2}\mathcal{N}_1^h\big(\mathfrak{R}^h u(t_n) + \mathfrak{R}^h u(t_{n-1}), v_h\big) \\
&\quad + \mathcal{N}_2^h\big(\mathbb{Q}_n^h, v_h\big) + \frac{1}{2}\mathcal{B}_0^h\big(I_{\mathcal{S}} b(u_h^n) + I_{\mathcal{S}} b(u_h^{n-1}), v_h\big) - \mathcal{L}_n^h(t_n; v_h) \\
&= \frac{1}{\Delta t}\mathcal{A}_0^h\big(\mathfrak{R}^h u(t_n) - \mathfrak{R}^h u(t_{n-1}), v_h\big) + \mathcal{N}_2^h\big(\mathbb{Q}_n^h, v_h\big) - \mathcal{L}_n^h(t_n; v_h) \\
&\quad + \frac{1}{2}\mathcal{B}_0^h\big(I_{\mathcal{S}} b(u_h^n) + I_{\mathcal{S}} b(u_h^{n-1}), v_h\big) + \mathcal{N}_1\big(\overline{u^n}, v_h\big) + \frac{1}{2}\int_0^{t_n} \mathcal{N}_2\big(u(\tau), v_h\big)\mathrm{d}\tau \\
&\quad + \frac{1}{2}\int_0^{t_{n-1}} \mathcal{N}_2\big(u(\tau), v_h\big)\mathrm{d}\tau - \frac{1}{2}\int_0^{t_n} \mathcal{N}_2^h\big(\mathfrak{R}^h u(\tau), v_h\big)\mathrm{d}\tau \\
&\quad - \frac{1}{2}\int_0^{t_{n-1}} \mathcal{N}_2^h\big(\mathfrak{R}^h u(\tau), v_h\big)\mathrm{d}\tau \\
&= \mathtt{Q}^1 + \mathtt{Q}^2 + \mathtt{Q}^3 + \mathtt{Q}^4 + \mathtt{Q}^5 + \mathtt{Q}^6 + \mathtt{Q}^7
\end{aligned} \tag{3.33}$$

with

$$\mathtt{Q}^1 = \frac{1}{\Delta t}\mathcal{A}_0^h\big(\mathfrak{R}^h u(t_n) - \mathfrak{R}^h u(t_{n-1}), v_h\big) - \big(a_0 \overline{u_t^n}, v_h\big)_{\Omega_h},$$

$$\mathtt{Q}^2 = \big(\overline{f^n}, v_h\big)_{\Omega_h} - \frac{1}{2}\big(f^h(t_n; v_h) + f^h(t_{n-1}; v_h)\big),$$

$$\mathtt{Q}^3 = \frac{1}{2}\mathcal{B}_0^h\big(I_{\mathcal{S}}b\big(u_h^n\big) + I_{\mathcal{S}}b\big(u_h^{n-1}\big), v_h\big) - \frac{1}{2}\big(b(u^n) + b(u^{n-1}), v_h\big)_{\Omega_h},$$

$$\mathtt{Q}^4 = \sum_{e\in\mathcal{E}_h^{\mathrm{b}}}\int_e\left(\overline{\hat{g}^n} - \overline{u^n} - \sum_{j=1}^{\bar{m}}\frac{\rho^j}{j!}\partial_{\boldsymbol{n}}^j\overline{u^n}\right)\big(a_1\nabla\big(\Pi_0^{k,E_e}v_h\big)\cdot\boldsymbol{n} - \gamma_1 h_e^{-1}v_h\big)\mathrm{d}s,$$

$$\mathtt{Q}^5 = \frac{1}{2}\int_0^{t_n}\sum_{e\in\mathcal{E}_h^{\mathrm{b}}}\int_e\left(\hat{g}(\tau) - u(\tau) - \sum_{j=1}^{\bar{m}}\frac{\rho^j}{j!}\partial_{\boldsymbol{n}}^j u(\tau)\right)(a_2\nabla(\Pi_0^{k,E_e}v_h)\cdot\boldsymbol{n} - \gamma_2 h_e^{-1}v_h)\mathrm{d}s\mathrm{d}\tau,$$

$$\mathtt{Q}^6 = \frac{1}{2}\int_0^{t_{n-1}}\sum_{e\in\mathcal{E}_h^{\mathrm{b}}}\int_e\left(\hat{g}(\tau) - u(\tau) - \sum_{j=1}^{\bar{m}}\frac{\rho^j}{j!}\partial_{\boldsymbol{n}}^j u(\tau)\right)\big(a_2\nabla\big(\Pi_0^{k,E_e}v_h\big)\cdot\boldsymbol{n} - \gamma_2 h_e^{-1}v_h\big)\mathrm{d}s\mathrm{d}\tau,$$

$$\mathtt{Q}^7 = \mathcal{N}_2^h\big(\mathbb{Q}_n^h, v_h\big) - \frac{1}{2}\int_0^{t_n}\mathcal{N}_2^h\big(\mathfrak{R}^h u(\tau), v_h\big)\mathrm{d}\tau - \frac{1}{2}\int_0^{t_{n-1}}\mathcal{N}_2^h\big(\mathfrak{R}^h u(\tau), v_h\big)\mathrm{d}\tau.$$

By replacing v_h with $\overline{\Theta_2^n}$ in (3.33), we have

$$\mathcal{A}_0^h\big(\bar{\delta}\Theta_2^n, \overline{\Theta_2^n}\big) + \mathcal{N}_1^h\big(\overline{\Theta_2^n}, \overline{\Theta_2^n}\big) = \mathtt{Q}^1 + \mathtt{Q}^2 + \mathtt{Q}^3 + \mathtt{Q}^4 + \mathtt{Q}^5 + \mathtt{Q}^6 + \mathtt{Q}^7. \tag{3.34}$$

In view of the symmetry of $\mathcal{A}_0^h(\cdot\,,\cdot)$, its left-hand side can be rewritten as

$$\begin{aligned}
&\mathcal{A}_0^h\big(\bar{\delta}\Theta_2^n, \overline{\Theta_2^n}\big) + \mathcal{N}_1^h\big(\overline{\Theta_2^n}, \overline{\Theta_2^n}\big)\\
&= \frac{1}{2\Delta t}\mathcal{A}_0^h\big(\Theta_2^n - \Theta_2^{n-1}, \Theta_2^n + \Theta_2^{n-1}\big) + \mathcal{N}_1^h\big(\overline{\Theta_2^n}, \overline{\Theta_2^n}\big)\\
&= \frac{1}{2\Delta t}\big(\mathcal{A}_0^h\big(\Theta_2^n, \Theta_2^n\big) - \mathcal{A}_0^h\big(\Theta_2^{n-1}, \Theta_2^{n-1}\big)\big) + \mathcal{N}_1^h\big(\overline{\Theta_2^n}, \overline{\Theta_2^n}\big).
\end{aligned}$$

Then, multiplying both sides of (3.34) by $2\Delta t$, we derive

$$\begin{aligned}
&\mathcal{A}_0^h\big(\Theta_2^n, \Theta_2^n\big) - \mathcal{A}_0^h\big(\Theta_2^{n-1}, \Theta_2^{n-1}\big) + 2\Delta t\mathcal{N}_1^h\big(\overline{\Theta_2^n}, \overline{\Theta_2^n}\big)\\
&= 2\Delta t(\mathtt{Q}^1 + \mathtt{Q}^2 + \mathtt{Q}^3 + \mathtt{Q}^4 + \mathtt{Q}^5 + \mathtt{Q}^6 + \mathtt{Q}^7).
\end{aligned} \tag{3.35}$$

Similarly, replacing v_h with $\bar{\delta}\Theta_2^n$ in (3.33), we obtain

$$\mathcal{A}_0^h\big(\bar{\delta}\Theta_2^n, \bar{\delta}\Theta_2^n\big) + \mathcal{N}_1^h\big(\overline{\Theta_2^n}, \bar{\delta}\Theta_2^n\big) = \mathtt{Q}^1 + \mathtt{Q}^2 + \mathtt{Q}^3 + \mathtt{Q}^4 + \mathtt{Q}^5 + \mathtt{Q}^6 + \mathtt{Q}^7, \tag{3.36}$$

whose left-hand side can be rewritten as

$$\begin{aligned}
&\mathcal{A}_0^h\big(\bar{\delta}\Theta_2^n, \bar{\delta}\Theta_2^n\big) + \mathcal{N}_1^h\big(\overline{\Theta_2^n}, \bar{\delta}\Theta_2^n\big)\\
&= \mathcal{A}_0^h\big(\bar{\delta}\Theta_2^n, \bar{\delta}\Theta_2^n\big) + \frac{1}{2\Delta t}\mathcal{N}_1^h\big(\Theta_2^n + \Theta_2^{n-1}, \Theta_2^n - \Theta_2^{n-1}\big)\\
&= \mathcal{A}_0^h\big(\bar{\delta}\Theta_2^n, \bar{\delta}\Theta_2^n\big) + \frac{1}{2\Delta t}\Big(\mathcal{N}_1^h\big(\Theta_2^n, \Theta_2^n\big) - \mathcal{N}_1^h\big(\Theta_2^n, \Theta_2^{n-1}\big)\\
&\qquad + \mathcal{N}_1^h\big(\Theta_2^{n-1}, \Theta_2^n\big) - \mathcal{N}_1^h\big(\Theta_2^{n-1}, \Theta_2^{n-1}\big)\Big).
\end{aligned}$$

Then, multiplying both sides of (3.36) by $2\Delta t$, we have

$$\begin{aligned}
&\mathcal{N}_1^h\big(\Theta_2^n, \Theta_2^n\big) - \mathcal{N}_1^h\big(\Theta_2^{n-1}, \Theta_2^{n-1}\big) + 2\Delta t\mathcal{A}_0^h\big(\bar{\delta}\Theta_2^n, \bar{\delta}\Theta_2^n\big)\\
&= 2\Delta t(\mathtt{Q}^1 + \mathtt{Q}^2 + \mathtt{Q}^3 + \mathtt{Q}^4 + \mathtt{Q}^5 + \mathtt{Q}^6 + \mathtt{Q}^7)\\
&\quad + \mathcal{N}_1^h\big(\Theta_2^n, \Theta_2^{n-1}\big) - \mathcal{N}_1^h\big(\Theta_2^{n-1}, \Theta_2^n\big).
\end{aligned} \tag{3.37}$$

To estimate $\mathtt{Q}^1$, we first rewrite it as

$$\begin{aligned}\mathtt{Q}^1 &= \frac{1}{\Delta t}\mathcal{A}_0^h\big(\mathfrak{R}^h u(t_n) - u^n + u^n - u^{n-1} + u^{n-1} - \mathfrak{R}^h u(t_{n-1}), v_h\big) - \big(a_0\overline{u_t^n}, v_h\big)_{\Omega_h}\\ &= \mathtt{Q}_1^1 + \mathtt{Q}_2^1\end{aligned}$$

with

$$\begin{aligned}\mathtt{Q}_1^1 &= \frac{1}{\Delta t}\mathcal{A}_0^h\big(\mathfrak{R}^h u(t_n) - u^n + u^{n-1} - \mathfrak{R}^h u(t_{n-1}), v_h\big)\\ \mathtt{Q}_2^1 &= \mathcal{A}_0^h\big(\overline{\delta} u^n, v_h\big) - \big(a_0\overline{u_t^n}, v_h\big)_{\Omega_h}.\end{aligned}$$

By (3.23), $\mathtt{Q}_1^1$ can be estimated as

$$\begin{aligned}\mathtt{Q}_1^1 &= \frac{1}{\Delta t}\int_{t_{n-1}}^{t_n}\mathcal{A}_0^h\big((\mathfrak{R}^h u)_t - u_t, v_h\big)\mathrm{d}\tau\\ &\lesssim \frac{h^{k+1}}{\Delta t}\left(\int_{t_{n-1}}^{t_n}|u(\tau)|_{k+1,\Omega} + |u_t(\tau)|_{k+1,\Omega}\mathrm{d}\tau + \Delta t\left(\int_0^{t_n}|u(\tau)|_{k+1,\Omega}^2\mathrm{d}\tau\right)^{\frac{1}{2}}\right)\|v_h\|_{\Omega_h}.\end{aligned}$$

From (3.35) and (3.37), it can be found that the coefficient $h^{k+1}/\Delta t$ in the estimate for $\mathtt{Q}_1^1$ becomes h^{k+1} for $\Delta t\mathtt{Q}^1$. Thus, no restrictions on Δt are required.

With the L^2-projection operator $\Pi_0^{k,E}$, we can rewrite $\mathtt{Q}_2^1$ as

$$\begin{aligned}\mathtt{Q}_2^1 &= \sum_{E\in\mathcal{T}_h}\mathcal{A}_0^E\big(\overline{\delta}u^n - \Pi_0^{k,E}\overline{\delta}u^n, v_h\big) + \big(a_0\Pi_0^{k,E}\overline{\delta}u^n, \Pi_0^{k,E}v_h\big)_E - \big(a_0\overline{u_t^n}, v_h\big)_E\\ &= \sum_{E\in\mathcal{T}_h}\mathcal{A}_0^E\big(\overline{\delta}u^n - \Pi_0^{k,E}\overline{\delta}u^n, v_h\big) + \big(\Pi_0^{k,E}\big(a_0\Pi_0^{k,E}\overline{\delta}u^n\big) - a_0\Pi_0^{k,E}\overline{\delta}u^n, v_h\big)_E\\ &\qquad + \big(a_0\Pi_0^{k,E}\overline{\delta}u^n - a_0\overline{u_t^n}, v_h\big)_E,\end{aligned}$$

then employing (2.13) yields

$$\mathtt{Q}_2^1 \lesssim h^{k+1}|\overline{\delta}u^n|_{k+1,\Omega}\|v_h\|_{\Omega_h} + \big\|\overline{\delta}u^n - \overline{u_t^n}\big\|_\Omega\|v_h\|_{\Omega_h}.$$

It is easy to derive that

$$\begin{aligned}|\overline{\delta}u^n|_{k+1,\Omega} &= \left|\frac{u^n - u^{n-1}}{\Delta t}\right|_{k+1,\Omega} = \frac{1}{\Delta t}\left|\int_{t_{n-1}}^{t_n}u_t(\tau)\mathrm{d}\tau\right|_{k+1,\Omega} \lesssim \frac{1}{\Delta t}\int_{t_{n-1}}^{t_n}|u_t(\tau)|_{k+1,\Omega}\mathrm{d}\tau,\\ \big\|\overline{\delta}u^n - \overline{u_t^n}\big\|_\Omega &= \frac{1}{2\Delta t}\big\|2u^n - 2u^{n-1} - \Delta t u_t^n - \Delta t u_t^{n-1}\big\|_\Omega\\ &\lesssim \frac{1}{2\Delta t}\left\|2u^n - 2u^{n-1} - 2\Delta t u_t\left(\frac{t_{n-1}+t_n}{2}\right)\right\|_\Omega\\ &\quad + \frac{1}{2}\left\|2u_t\left(\frac{t_{n-1}+t_n}{2}\right) - u_t^n - u_t^{n-1}\right\|_\Omega\\ &= \frac{1}{2\Delta t}\left\|\int_{t_{n-1}}^{(t_n+t_{n-1})/2}(\tau - t_{n-1})^2 u_{ttt}(\tau)\mathrm{d}\tau + \int_{(t_n+t_{n-1})/2}^{t_n}(\tau - t_n)^2 u_{ttt}(\tau)\mathrm{d}\tau\right\|_\Omega\\ &\quad + \frac{1}{2}\left\|\int_{(t_n+t_{n-1})/2}^{t_n}(\tau - t_n)u_{ttt}(\tau)\mathrm{d}\tau - \int_{t_{n-1}}^{(t_n+t_{n-1})/2}(\tau - t_{n-1})u_{ttt}(\tau)\mathrm{d}\tau\right\|_\Omega\\ &\lesssim \Delta t\int_{t_{n-1}}^{t_n}\|u_{ttt}(\tau)\|_\Omega\mathrm{d}\tau.\end{aligned}$$

Hence, we arrive at

$$\mathtt{Q}^1 \lesssim \frac{h^{k+1}}{\Delta t}\bigg(\int_{t_{n-1}}^{t_n} |u(\tau)|_{k+1,\Omega} + |u_t(\tau)|_{k+1,\Omega}\mathrm{d}\tau + \Delta t\bigg(\int_0^{t_n} |u(\tau)|_{k+1,\Omega}^2\mathrm{d}\tau\bigg)^{\frac{1}{2}}\bigg)\|v_h\|_{\Omega_h} + \Delta t\int_{t_{n-1}}^{t_n} \|u_{ttt}(\tau)\|_{\Omega}\mathrm{d}\tau\|v_h\|_{\Omega_h}.$$

By [22, Theorem 1] and (2.13), we can derive the following estimates for $\mathtt{Q}^2$ and $\mathtt{Q}^3$:

$$\begin{aligned}
\mathtt{Q}^2 &\lesssim h^{k+1}\big(|f^n|_{k+1,\Omega} + |f^{n-1}|_{k+1,\Omega}\big)\|v_h\|_{\Omega_h},\\
\mathtt{Q}^3 &\lesssim h^{k+1}\big(|b(u^n)|_{k+1,\Omega} + |b(u^{n-1})|_{k+1,\Omega} + |u^n|_{k+1,\Omega} + |u^{n-1}|_{k+1,\Omega}\big)\|v_h\|_{\Omega_h}\\
&\quad + \Big(\big\|u^n - u_h^n\big\|_{\Omega_h} + \big\|u^{n-1} - u_h^{n-1}\big\|_{\Omega_h}\Big)\|v_h\|_{\Omega_h}.
\end{aligned}$$

The following estimates for $\mathtt{Q}^4, \mathtt{Q}^5$ and $\mathtt{Q}^6$ can be obtained immediately from Lemma 3.8:

$$\begin{aligned}
\mathtt{Q}^4 &\lesssim h^{k+1}\big(|u^n|_{\bar{m}+1,\infty,\Omega} + |u^{n-1}|_{\bar{m}+1,\infty,\Omega}\big)\|v_h\|_{\Omega_h},\\
\mathtt{Q}^5 + \mathtt{Q}^6 &\lesssim h^{k+1}\int_0^{t_n} |u(\tau)|_{\bar{m}+1,\infty,\Omega}\mathrm{d}\tau\|v_h\|_{\Omega_h} + h^{k+1}\int_0^{t_{n-1}} |u(\tau)|_{\bar{m}+1,\infty,\Omega}\mathrm{d}\tau\|v_h\|_{\Omega_h}.
\end{aligned}$$

We now begin to establish the estimates of $\|\Theta_2^n\|_{\Omega_h}$ for $n = 1, 2, \ldots, N_T$. It is easy to derive the following error formula for the trapezoidal quadrature rule:

$$\frac{t_b - t_a}{2}\big(r(t_a) + r(t_b)\big) - \int_{t_a}^{t_b} r(\tau)\mathrm{d}\tau = -\frac{1}{2}\int_{t_a}^{t_b} (\tau - t_a)(\tau - t_b)r_{tt}(\tau)\mathrm{d}\tau. \tag{3.38}$$

In the case of $n = 1$, we see that

$$\begin{aligned}
\mathtt{Q}^7 &= -\frac{\Delta t}{2}\mathcal{N}_2^h\big(\overline{\Theta_2^1}, v_h\big) + \frac{\Delta t}{2}\mathcal{N}_2^h\bigg(\frac{\mathfrak{R}^h u(t_0) + \mathfrak{R}^h u(t_1)}{2}, v_h\bigg) - \frac{1}{2}\int_0^{t_1} \mathcal{N}_2^h\big(\mathfrak{R}^h u(\tau), v_h\big)\mathrm{d}\tau,\\
&= -\frac{\Delta t}{2}\mathcal{N}_2^h\big(\overline{\Theta_2^1}, v_h\big) - \frac{1}{4}\int_0^{t_1} \tau(\tau - t_1)\mathcal{N}_2^h\big((\mathfrak{R}^h u)_{tt}(\tau), v_h\big)\mathrm{d}\tau.
\end{aligned} \tag{3.39}$$

Taking $n = 1$ and replacing v_h with $\overline{\Theta_2^1}$ in (3.33), and also noticing the above estimates for $\mathtt{Q}^1$ to $\mathtt{Q}^7$, we have

$$\begin{aligned}
&\big\|\Theta_2^1\big\|_{\Omega_h}^2 + \Delta t\big\|\overline{\Theta_2^1}\big\|_{\mathcal{N}}^2 + (\Delta t)^2\big\|\overline{\Theta_2^1}\big\|_{\mathcal{N}}^2\\
&\lesssim h^{2k+2}\Big(\|u\|_{L^2((0,t_1);H^{k+1}(\Omega))}^2 + \|u_t\|_{L^2((0,t_1);H^{k+1}(\Omega))}^2 + \|f\|_{L^\infty((0,t_1);H^{k+1}(\Omega))}^2\\
&\qquad + \|b(u)\|_{L^\infty((0,t_1);H^{k+1}(\Omega))}^2 + \|u\|_{L^\infty((0,t_1);H^{k+1}(\Omega))}^2\Big)\\
&\quad + \Delta t\sum_{q=0}^{1} \|\Theta_2^q\|_{\Omega_h}^2 + (\Delta t)^4\|u_{ttt}\|_{L^2((0,t_1);L^2(\Omega))}^2\\
&\quad + h^{2k+2}\Big(|u_0|_{k+1,\Omega}^2 + \|u\|_{L^\infty((0,t_1);W^{\bar{m}+1,\infty}(\Omega))}^2 + \|u\|_{L^2((0,t_1);W^{\bar{m}+1,\infty}(\Omega))}^2\Big)\\
&\quad + (\Delta t)^4\Big(\|u\|_{L^2((0,t_1);H^{\bar{m}+1}(\Omega))}^2 + \|u\|_{L^2((0,t_1);H^1(\Omega_h))}^2 + \|u_t\|_{L^2((0,t_1);H^{\bar{m}+1}(\Omega))}^2\\
&\qquad + \|u_t\|_{L^2((0,t_1);H^1(\Omega_h))}^2 + \|u_{tt}\|_{L^2((0,t_1);H^{\bar{m}+1}(\Omega))}^2 + \|u_{tt}\|_{L^2((0,t_1);H^1(\Omega_h))}^2\Big),
\end{aligned}$$

where we have made use of the continuity and coercivity of $\mathcal{A}_0^h(\cdot,\cdot)$, $\mathcal{N}_1^h(\cdot,\cdot)$ and $\mathcal{N}_2^h(\cdot,\cdot)$, Young's inequality, (3.31) and the stability (3.6) of $(\mathfrak{R}^h u)_{tt}$. Further using the discrete Grönwall's inequality [33], we obtain

$$\begin{aligned}\big\|\Theta_2^1\big\|_{\Omega_h} \lesssim h^{k+1}\Big(&\|u\|_{L^2((0,t_1);H^{k+1}(\Omega))} + \|u_t\|_{L^2((0,t_1);H^{k+1}(\Omega))} + \|f\|_{L^\infty((0,t_1);H^{k+1}(\Omega))}\\ &+ \|b(u)\|_{L^\infty((0,t_1);H^{k+1}(\Omega))} + \|u\|_{L^\infty((0,t_1);H^{k+1}(\Omega))}\\ &+ \|u\|_{L^\infty((0,t_1);W^{\bar m+1,\infty}(\Omega))} + \|u\|_{L^2((0,t_1);W^{\bar m+1,\infty}(\Omega))} + |u_0|_{k+1,\Omega}\Big)\\ + (\Delta t)^2\Big(&\|u_{ttt}\|_{L^2((0,t_1);L^2(\Omega))} + \|u\|_{L^2((0,t_1);H^{\bar m+1}(\Omega))} + \|u\|_{L^2((0,t_1);H^1(\Omega_h))}\\ &+ \|u_t\|_{L^2((0,t_1);H^{\bar m+1}(\Omega))} + \|u_t\|_{L^2((0,t_1);H^1(\Omega_h))}\\ &+ \|u_{tt}\|_{L^2((0,t_1);H^{\bar m+1}(\Omega))} + \|u_{tt}\|_{L^2((0,t_1);H^1(\Omega_h))}\Big). \end{aligned} \tag{3.40}$$

In the case of $n = 2, 3, \ldots, N_T$, it follows from (3.38) that

$$\begin{aligned}\mathtt{Q}^7 &= \frac{1}{2}\sum_{q=0}^{n-1}\frac{\Delta t}{2}\mathcal{N}_2^h\big(u_h^q + u_h^{q+1}, v_h\big) - \frac{1}{2}\int_0^{t_n}\mathcal{N}_2^h\big(\mathfrak{R}^h u(\tau), v_h\big)\mathrm{d}\tau\\ &\quad + \frac{1}{2}\sum_{q=0}^{n-2}\frac{\Delta t}{2}\mathcal{N}_2^h\big(u_h^q + u_h^{q+1}, v_h\big) - \frac{1}{2}\int_0^{t_{n-1}}\mathcal{N}_2^h\big(\mathfrak{R}^h u(\tau), v_h\big)\mathrm{d}\tau\\ &= -\Delta t\sum_{q=1}^{n-1}\mathcal{N}_2^h\big(\overline{\Theta_2^q}, v_h\big) - \frac{\Delta t}{2}\mathcal{N}_2^h\big(\overline{\Theta_2^n}, v_h\big)\\ &\quad - \frac{1}{4}\sum_{q=0}^{n-1}\int_{t_q}^{t_{q+1}}(\tau - t_q)(\tau - t_{q+1})\mathcal{N}_2^h\big((\mathfrak{R}^h u)_{tt}(\tau), v_h\big)\mathrm{d}\tau\\ &\quad - \frac{1}{4}\sum_{q=0}^{n-2}\int_{t_q}^{t_{q+1}}(\tau - t_q)(\tau - t_{q+1})\mathcal{N}_2^h\big((\mathfrak{R}^h u)_{tt}(\tau), v_h\big)\mathrm{d}\tau.\end{aligned}$$

Substituting $\overline{\Theta_2^n}$ for v_h in (3.33), employing Young's inequality, the inequality (3.6), and the above estimates for $\mathtt{Q}^1$ to $\mathtt{Q}^7$, we have

$$\begin{aligned}&\mathcal{A}_0^h\big(\Theta_2^n, \Theta_2^n\big) - \mathcal{A}_0^h\big(\Theta_2^{n-1}, \Theta_2^{n-1}\big) + \Delta t\big\|\overline{\Theta_2^n}\big\|_{\mathcal{N}}^2\\ &\lesssim h^{2k+2}\Big(\|u\|^2_{L^2((t_{n-1},t_n);H^{k+1}(\Omega))} + \|u_t\|^2_{L^2((t_{n-1},t_n);H^{k+1}(\Omega))}\Big)\\ &\quad + \Delta t h^{2k+2}\Big(\|u\|^2_{L^2((0,t_n);H^{k+1}(\Omega))} + \|u\|^2_{L^\infty((0,t_n);H^{k+1}(\Omega))} + \|f\|^2_{L^\infty((t_{n-1},t_n);H^{k+1}(\Omega))}\\ &\qquad + \|b(u)\|^2_{L^\infty((t_{n-1},t_n);H^{k+1}(\Omega))} + \|u\|^2_{L^\infty((t_{n-1},t_n);H^{k+1}(\Omega))}\Big)\\ &\quad + \Delta t h^{2k+2}\Big(\|u\|^2_{L^\infty((t_{n-1},t_n);W^{\bar m+1,\infty}(\Omega))} + \|u\|^2_{L^2((0,t_n);W^{\bar m+1,\infty}(\Omega))}\Big)\\ &\quad + \Delta t\Big(\big\|\Theta_2^n\big\|^2_{\Omega_h} + \big\|\Theta_2^{n-1}\big\|^2_{\Omega_h}\Big) + (\Delta t)^4\|u_{ttt}\|^2_{L^2((t_{n-1},t_n);L^2(\Omega))} + (\Delta t)^2\sum_{q=0}^{n}\big\|\overline{\Theta_2^q}\big\|^2_{\mathcal{N}}\\ &\quad + (\Delta t)^5\Big(\|u\|^2_{L^2((0,t_n);H^{\bar m+1}(\Omega))} + \|u\|^2_{L^2((0,t_n);H^1(\Omega_h))} + \|u_t\|^2_{L^2((0,t_n);H^{\bar m+1}(\Omega))}\\ &\qquad + \|u_t\|^2_{L^2((0,t_n);H^1(\Omega_h))} + \|u_{tt}\|^2_{L^2((0,t_n);H^{\bar m+1}(\Omega))} + \|u_{tt}\|^2_{L^2((0,t_n);H^1(\Omega_h))}\Big).\end{aligned}$$

By adding the above inequality for n from 1 to r, where r is an integer satisfying $2 \leq r \leq N_T$, and using the discrete Grönwall's inequality, we obtain

$$\begin{aligned}\|\Theta_2^r\|_{\Omega_h} \lesssim h^{k+1}\Big(&\|u\|_{L^2((0,t_r);H^{k+1}(\Omega))} + \|u_t\|_{L^2((0,t_r);H^{k+1}(\Omega))} + \|f\|_{L^\infty((0,t_r);H^{k+1}(\Omega))}\\ &+ \|b(u)\|_{L^\infty((0,t_r);H^{k+1}(\Omega))} + \|u\|_{L^\infty((0,t_r);H^{k+1}(\Omega))}\\ &+ \|u\|_{L^\infty((0,t_r);W^{\bar{m}+1,\infty}(\Omega))} + \|u\|_{L^2((0,t_r);W^{\bar{m}+1,\infty}(\Omega))} + |u_0|_{k+1,\Omega}\Big)\\ + (\Delta t)^2\Big(&\|u_{ttt}\|_{L^2((0,t_r);L^2(\Omega))} + \|u\|_{L^2((0,t_r);H^{\bar{m}+1}(\Omega))} + \|u\|_{L^2((0,t_r);H^1(\Omega_h))}\\ &+ \|u_t\|_{L^2((0,t_r);H^{\bar{m}+1}(\Omega))} + \|u_t\|_{L^2((0,t_r);H^1(\Omega_h))} + \|u_{tt}\|_{L^2((0,t_r);H^{\bar{m}+1}(\Omega))}\\ &+ \|u_{tt}\|_{L^2((0,t_r);H^1(\Omega_h))}\Big),\end{aligned}$$

then employing (3.31) and (3.40) leads to (3.28).

We now proceed to give the estimates of $\|\Theta_2^n\|_{\mathcal{N}}$ for $n = 1, 2, \ldots, N_T$. In the case of $n = 1$, replacing v_h with $\overline{\delta}\Theta_2^1$ in (3.39), we have by Young's inequality that

$$\mathtt{Q}^7 \lesssim \sum_{q=0}^{1} \big\|\Theta_2^q\big\|_{\mathcal{N}}^2 + (\Delta t)^3 \int_0^{t_1} \big\|(\mathfrak{R}^h u)_{tt}(\tau)\big\|_{\mathcal{N}}^2 \mathrm{d}\tau.$$

Taking $n = 1$ and replacing v_h with $\overline{\delta}\Theta_2^1$ in (3.33), and employing the estimates for $\mathtt{Q}^1$ to $\mathtt{Q}^7$, (3.40) and Young's inequality, we arrive at

$$\begin{aligned}&\Delta t\big\|\overline{\delta}\Theta_2^1\big\|_{\Omega_h}^2 + \big\|\Theta_2^1\big\|_{\mathcal{N}}^2\\ &\lesssim h^{2k+2}\Big(\|u\|^2_{L^2((0,t_1);H^{k+1}(\Omega))} + \|u_t\|^2_{L^2((0,t_1);H^{k+1}(\Omega))} + \|f\|^2_{L^\infty((0,t_1);H^{k+1}(\Omega))}\\ &\qquad + \|b(u)\|^2_{L^\infty((0,t_1);H^{k+1}(\Omega))} + \|u\|^2_{L^\infty((0,t_1);H^{k+1}(\Omega))}\Big)\\ &\quad + \Delta t \sum_{q=0}^{1} \|\Theta_2^q\|_{\mathcal{N}}^2 + (\Delta t)^4 \|u_{ttt}\|^2_{L^2((0,t_1);L^2(\Omega))} + \|\Theta_2^0\|_{\mathcal{N}}^2\\ &\quad + h^{2k+2}\Big(|u_0|^2_{k+1,\Omega} + \|u\|^2_{L^\infty((0,t_1);W^{\bar{m}+1,\infty}(\Omega))} + \|u\|^2_{L^2((0,t_1);W^{\bar{m}+1,\infty}(\Omega))}\Big)\\ &\quad + (\Delta t)^4\Big(\|u\|^2_{L^2((0,t_1);H^{\bar{m}+1}(\Omega))} + \|u\|^2_{L^2((0,t_1);H^1(\Omega_h))} + \|u_t\|^2_{L^2((0,t_1);H^{\bar{m}+1}(\Omega))}\\ &\qquad + \|u_t\|^2_{L^2((0,t_1);H^1(\Omega_h))} + \|u_{tt}\|^2_{L^2((0,t_1);H^{\bar{m}+1}(\Omega))} + \|u_{tt}\|^2_{L^2((0,t_1);H^1(\Omega_h))}\Big).\end{aligned}$$

Utilizing (3.9), (3.10) and discrete Grönwall's inequality, we deduce that

$$\begin{aligned}\big\|\Theta_2^1\big\|_{\mathcal{N}} \lesssim h^{k+1}\Big(&\|u\|_{L^2((0,t_1);H^{k+1}(\Omega))} + \|u_t\|_{L^2((0,t_1);H^{k+1}(\Omega))} + \|f\|_{L^\infty((0,t_1);H^{k+1}(\Omega))}\\ &+ \|b(u)\|_{L^\infty((0,t_1);H^{k+1}(\Omega))} + \|u\|_{L^\infty((0,t_1);H^{k+1}(\Omega))} + |u_0|_{k+1,\Omega}\\ &+ \|u\|_{L^\infty((0,t_1);W^{\bar{m}+1,\infty}(\Omega))} + \|u\|_{L^2((0,t_1);W^{\bar{m}+1,\infty}(\Omega))}\Big) + h^k|u_0|_{k+1,\Omega}\\ + (\Delta t)^2\Big(&\|u_{ttt}\|_{L^2((0,t_1);L^2(\Omega))} + \|u\|_{L^2((0,t_1);H^{\bar{m}+1}(\Omega))} + \|u\|_{L^2((0,t_1);H^1(\Omega_h))}\\ &+ \|u_t\|_{L^2((0,t_1);H^{\bar{m}+1}(\Omega))} + \|u_t\|_{L^2((0,t_1);H^1(\Omega_h))}\\ &+ \|u_{tt}\|_{L^2((0,t_1);H^{\bar{m}+1}(\Omega))} + \|u_{tt}\|_{L^2((0,t_1);H^1(\Omega_h))}\Big). \qquad (3.41)\end{aligned}$$

In the case of $n=2$, based on the process of analysing $\|\Theta_2^1\|_{\mathcal{N}}$, we can similarly get

$$\begin{aligned}\|\Theta_2^2\|_{\mathcal{N}} \lesssim h^{k+1}\Big(&\|u\|_{L^2((0,t_2);H^{k+1}(\Omega))} + \|u_t\|_{L^2((0,t_2);H^{k+1}(\Omega))} + \|f\|_{L^\infty((0,t_2);H^{k+1}(\Omega))}\\ &+ \|b(u)\|_{L^\infty((0,t_2);H^{k+1}(\Omega))} + \|u\|_{L^\infty((0,t_2);H^{k+1}(\Omega))} + |u_0|_{k+1,\Omega}\\ &+ \|u\|_{L^\infty((0,t_2);W^{\bar m+1,\infty}(\Omega))} + \|u\|_{L^2((0,t_2);W^{\bar m+1,\infty}(\Omega))}\Big) + h^k|u_0|_{k+1,\Omega}\\ + (\Delta t)^2\Big(&\|u_{ttt}\|_{L^2((0,t_2);L^2(\Omega))} + \|u\|_{L^2((0,t_2);H^{\bar m+1}(\Omega))} + \|u\|_{L^2((0,t_2);H^1(\Omega_h))}\\ &+ \|u_t\|_{L^2((0,t_2);H^{\bar m+1}(\Omega))} + \|u_t\|_{L^2((0,t_2);H^1(\Omega_h))}\\ &+ \|u_{tt}\|_{L^2((0,t_2);H^{\bar m+1}(\Omega))} + \|u_{tt}\|_{L^2((0,t_2);H^1(\Omega_h))}\Big). \qquad (3.42)\end{aligned}$$

In the case of $n=3,4,\ldots,N_T$, by substituting $\overline{\delta}\Theta_2^n$ for v_h in $\mathtt{Q}^7$ and performing straightforward calculation, we arrive at

$$\begin{aligned}\widehat{\mathtt{Q}^7} &= \mathcal{N}_2^h\big(\mathbb{Q}_n^h,\overline{\delta}\Theta_2^n\big) - \frac{1}{2}\int_0^{t_n}\mathcal{N}_2^h\big(\mathfrak{R}^h u(\tau),\overline{\delta}\Theta_2^n\big)\mathrm{d}\tau - \frac{1}{2}\int_0^{t_{n-1}}\mathcal{N}_2^h\big(\mathfrak{R}^h u(\tau),\overline{\delta}\Theta_2^n\big)\mathrm{d}\tau\\ &= \frac{\Delta t}{2}\sum_{q=1}^{n}\mathcal{N}_2^h\big(\overline{u_h^q},\overline{\delta}\Theta_2^n\big) - \frac{1}{2}\int_0^{t_n}\mathcal{N}_2^h\big(\mathfrak{R}^h u(\tau),\overline{\delta}\Theta_2^n\big)\mathrm{d}\tau\\ &\quad + \frac{\Delta t}{2}\sum_{q=1}^{n-1}\mathcal{N}_2^h\big(\overline{u_h^q},\overline{\delta}\Theta_2^n\big) - \frac{1}{2}\int_0^{t_{n-1}}\mathcal{N}_2^h\big(\mathfrak{R}^h u(\tau),\overline{\delta}\Theta_2^n\big)\mathrm{d}\tau\\ &= \frac{1}{2}\left(\sum_{q=1}^{n}\mathcal{N}_2^h\big(\overline{u_h^q},\Theta_2^n\big) - \sum_{q=1}^{n-1}\mathcal{N}_2^h\big(\overline{u_h^q},\Theta_2^{n-1}\big)\right)\\ &\quad - \frac{1}{2\Delta t}\left(\int_0^{t_n}\mathcal{N}_2^h\big(\mathfrak{R}^h u(\tau),\Theta_2^n\big)\mathrm{d}\tau - \int_0^{t_{n-1}}\mathcal{N}_2^h\big(\mathfrak{R}^h u(\tau),\Theta_2^{n-1}\big)\mathrm{d}\tau\right)\\ &\quad + \frac{1}{2}\left(\sum_{q=1}^{n-1}\mathcal{N}_2^h\big(\overline{u_h^q},\Theta_2^n\big) - \sum_{q=1}^{n-2}\mathcal{N}_2^h\big(\overline{u_h^q},\Theta_2^{n-1}\big)\right)\\ &\quad - \frac{1}{2\Delta t}\left(\int_0^{t_{n-1}}\mathcal{N}_2^h\big(\mathfrak{R}^h u(\tau),\Theta_2^n\big)\mathrm{d}\tau - \int_0^{t_{n-2}}\mathcal{N}_2^h\big(\mathfrak{R}^h u(\tau),\Theta_2^{n-1}\big)\mathrm{d}\tau\right)\\ &\quad + \frac{1}{2\Delta t}\int_{t_{n-1}}^{t_n}\mathcal{N}_2^h\big(\mathfrak{R}^h u(\tau),\Theta_2^{n-1}\big)\mathrm{d}\tau - \frac{1}{2}\mathcal{N}_2^h\big(\overline{u_h^n},\Theta_2^{n-1}\big)\\ &\quad + \frac{1}{2\Delta t}\int_{t_{n-2}}^{t_{n-1}}\mathcal{N}_2^h\big(\mathfrak{R}^h u(\tau),\Theta_2^{n-1}\big)\mathrm{d}\tau - \frac{1}{2}\mathcal{N}_2^h\big(\overline{u_h^{n-1}},\Theta_2^{n-1}\big).\end{aligned}$$

Replacing v_h with $\overline{\delta}\Theta_2^n$ in (3.33), employing Young's inequality, the inequality (3.6), and the above estimates for $\mathtt{Q}^1$-$\mathtt{Q}^7$, we have

$$\begin{aligned}&\mathcal{N}_1^h\big(\Theta_2^n,\Theta_2^n\big) - \mathcal{N}_1^h\big(\Theta_2^{n-1},\Theta_2^{n-1}\big) + \Delta t\big\|\overline{\delta}\Theta_2^n\big\|_{\Omega_h}^2\\ &\lesssim h^{2k+2}\Big(\|u\|^2_{L^2((t_{n-1},t_n);H^{k+1}(\Omega))} + \|u_t\|^2_{L^2((t_{n-1},t_n);H^{k+1}(\Omega))}\Big) + \Delta t\widehat{\mathtt{Q}^7}\\ &\quad + \Delta t h^{2k+2}\Big(\|u\|^2_{L^2((0,t_n);H^{k+1}(\Omega))} + \|f\|^2_{L^\infty((t_{n-1},t_n);H^{k+1}(\Omega))}\Big) + \big\|\Theta_2^n\big\|_{\mathcal{N}}\big\|\Theta_2^{n-1}\big\|_{\mathcal{N}}\\ &\quad + \Delta t h^{2k+2}\Big(\|b(u)\|^2_{L^\infty((t_{n-1},t_n);H^{k+1}(\Omega))} + \|u\|^2_{L^\infty((t_{n-1},t_n);H^{k+1}(\Omega))}\Big)\\ &\quad + \Delta t h^{2k+2}\Big(\|u\|^2_{L^\infty((t_{n-1},t_n);W^{\bar m+1,\infty}(\Omega))} + \|u\|^2_{L^2((0,t_n);W^{\bar m+1,\infty}(\Omega))}\Big)\end{aligned}$$

$$+ \Delta t\Big(\big\|u^n - u_h^n\big\|_{\Omega_h}^2 + \big\|u^{n-1} - u_h^{n-1}\big\|_{\Omega_h}^2\Big) + (\Delta t)^4 \|u_{ttt}\|^2_{L^2((t_{n-1},t_n);L^2(\Omega))}.$$

Adding the above inequality for n from 3 to r $(3 \le r \le N_T)$, it follows from Young's inequality that

$$\begin{aligned}
\big\|\Theta_2^r\big\|_{\mathcal{N}}^2 \lesssim{}& (\Delta t)^4 \|u_{ttt}\|^2_{L^2((0,t_r);L^2(\Omega))} + h^{2k+2}\Big(\|u\|^2_{L^2((0,t_r);H^{k+1}(\Omega))} + \|u_t\|^2_{L^2((0,t_r);H^{k+1}(\Omega))}\Big) \\
&+ h^{2k+2}\Big(\|u\|^2_{L^2((0,t_r);H^{k+1}(\Omega))} + \|f\|^2_{L^\infty((0,t_r);H^{k+1}(\Omega))} + \|b(u)\|^2_{L^\infty((0,t_r);H^{k+1}(\Omega))} \\
&\qquad + \|u\|^2_{L^\infty((0,t_r);H^{k+1}(\Omega))} + \|u\|^2_{L^\infty((0,t_r);W^{\bar{m}+1,\infty}(\Omega))} + \|u\|^2_{L^2((0,t_r);W^{\bar{m}+1,\infty}(\Omega))}\Big) \\
&+ \Delta t \sum_{n=3}^{r}\Big(\big\|u^n - u_h^n\big\|_{\Omega_h}^2 + \big\|u^{n-1} - u_h^{n-1}\big\|_{\Omega_h}^2\Big) + \sum_{n=0}^{r-1}\big\|\Theta_2^n\big\|_{\mathcal{N}}^2 \\
&+ \frac{\Delta t}{2}\Bigg(\sum_{q=1}^{r}\mathcal{N}_2^h\big(\overline{u_h^q}, \Theta_2^r\big) - \sum_{q=1}^{2}\mathcal{N}_2^h\big(\overline{u_h^q}, \Theta_2^2\big)\Bigg) \\
&- \frac{1}{2}\Big(\int_0^{t_r}\mathcal{N}_2^h\big(\mathfrak{R}^h u(\tau), \Theta_2^r\big)\mathrm{d}\tau - \int_0^{t_2}\mathcal{N}_2^h\big(\mathfrak{R}^h u(\tau), \Theta_2^2\big)\mathrm{d}\tau\Big) \\
&+ \frac{\Delta t}{2}\Bigg(\sum_{q=1}^{r-1}\mathcal{N}_2^h\big(\overline{u_h^q}, \Theta_2^r\big) - \sum_{q=1}^{1}\mathcal{N}_2^h\big(\overline{u_h^q}, \Theta_2^2\big)\Bigg) \\
&- \frac{1}{2}\Big(\int_0^{t_{r-1}}\mathcal{N}_2^h\big(\mathfrak{R}^h u(\tau), \Theta_2^r\big)\mathrm{d}\tau - \int_0^{t_1}\mathcal{N}_2^h\big(\mathfrak{R}^h u(\tau), \Theta_2^2\big)\mathrm{d}\tau\Big) \\
&+ \sum_{n=3}^{r}\frac{1}{2}\int_{t_{n-1}}^{t_n}\mathcal{N}_2^h\big(\mathfrak{R}^h u(\tau), \Theta_2^{n-1}\big)\mathrm{d}\tau - \frac{\Delta t}{2}\mathcal{N}_2^h\big(\overline{u_h^n}, \Theta_2^{n-1}\big) \\
&+ \sum_{n=3}^{r}\frac{1}{2}\int_{t_{n-2}}^{t_{n-1}}\mathcal{N}_2^h\big(\mathfrak{R}^h u(\tau), \Theta_2^{n-1}\big)\mathrm{d}\tau - \frac{\Delta t}{2}\mathcal{N}_2^h\big(\overline{u_h^{n-1}}, \Theta_2^{n-1}\big).
\end{aligned}$$

Applying (3.6), (3.38), and Young's inequality, we further have

$$\begin{aligned}
\big\|\Theta_2^r\big\|_{\mathcal{N}}^2 \lesssim{}& (\Delta t)^4 \|u_{ttt}\|^2_{L^2((0,t_r);L^2(\Omega))} + h^{2k+2}\Big(\|u\|^2_{L^2((0,t_r);H^{k+1}(\Omega))} + \|u_t\|^2_{L^2((0,t_r);H^{k+1}(\Omega))}\Big) \\
&+ h^{2k+2}\Big(\|u\|^2_{L^2((0,t_r);H^{k+1}(\Omega))} + \|f\|^2_{L^\infty((0,t_r);H^{k+1}(\Omega))} \\
&\qquad + \|b(u)\|^2_{L^\infty((0,t_r);H^{k+1}(\Omega))} + \|u\|^2_{L^\infty((0,t_r);H^{k+1}(\Omega))} \\
&\qquad + \|u\|^2_{L^\infty((0,t_r);W^{\bar{m}+1,\infty}(\Omega))} + \|u\|^2_{L^2((0,t_r);W^{\bar{m}+1,\infty}(\Omega))}\Big) \\
&+ \Delta t \sum_{n=3}^{r}\Big(\big\|u^n - u_h^n\big\|_{\Omega_h}^2 + \big\|u^{n-1} - u_h^{n-1}\big\|_{\Omega_h}^2\Big) + \Delta t\sum_{n=0}^{r}\big\|\Theta_2^n\big\|_{\mathcal{N}}^2 + \sum_{n=0}^{r-1}\big\|\Theta_2^n\big\|_{\mathcal{N}}^2 \\
&+ (\Delta t)^4\Big(\|u\|^2_{L^2((0,t_r);H^{\bar{m}+1}(\Omega))} + \|u\|^2_{L^2((0,t_r);H^1(\Omega_h))} + \|u_t\|^2_{L^2((0,t_r);H^{\bar{m}+1}(\Omega))} \\
&\qquad + \|u_t\|^2_{L^2((0,t_r);H^1(\Omega_h))} + \|u_{tt}\|^2_{L^2((0,t_r);H^{\bar{m}+1}(\Omega))} + \|u_{tt}\|^2_{L^2((0,t_r);H^1(\Omega_h))}\Big).
\end{aligned}$$

Using (3.28), (3.30), (3.41), (3.42), and the discrete Grönwall's inequality, we obtain (3.29). The proof is complete. □

4. Extension to 3D Case

In this section, the numerical solutions of the semilinear PIDEs (1.1) on 3D curved domains are addressed using the Nitsche-based projection method and the serendipity virtual element method.

4.1. Serendipity virtual element space

Similar to 2D case, a sequence of polyhedral domains $\{\overline{\Omega}_h\}_h$ are employed to approximate the curved domain Ω. Following [12], we assume that $\overline{\Omega}_h \subset \Omega$. A polyhedral mesh $\overline{\mathcal{T}}_{h^*}$ is utilized to decompose each polyhedral domain $\overline{\Omega}_h$. The subscript h^* corresponds to the size of the polyhedral mesh, which is defined as $h^* := \max_{P\in\overline{\mathcal{T}}_{h^*}} h_P$, where h_P represents the diameter of the polyhedron P. For simplicity, we set $h = h^*$. The polyhedral mesh $\overline{\mathcal{T}}_h$ is assumed to satisfy the shape regularity described in [7, 12, 24]. For any point $\boldsymbol{x}$ on $\partial\overline{\Omega}_h$ which is the boundary of $\overline{\Omega}_h$, it is assumed that there is a nonnegative function $\overline{\rho}(\boldsymbol{x})$ which depends on $\boldsymbol{x}$ such that $\boldsymbol{x} + \overline{\rho}(\boldsymbol{x})\boldsymbol{\sigma} \in \partial\Omega$, where $\boldsymbol{\sigma}$ represents an unit outward vector on $\partial\overline{\Omega}_h$.

The set of mesh faces in $\overline{\mathcal{T}}_h$ is denoted as $\mathcal{F}_h$ and gather the faces lying on $\partial\overline{\Omega}_h$ into the set $\mathcal{F}_h^{\mathtt{b}}$. We introduce the notation $\mathcal{N}_{\mathtt{lines}}(\partial\mathcal{F})$ to represent the minimum number of straight lines needed to completely enclose $\partial\mathcal{F}$ (the boundary of $\mathcal{F}$) for every face $\mathcal{F} \in \mathcal{F}_h$. We then define $\overline{\mathcal{N}}^h_{\mathtt{lines}} := \min_{\mathcal{F}\in\mathcal{F}_h} \mathcal{N}_{\mathtt{lines}}(\partial\mathcal{F})$. We denote the minimum number of distinct planes needed to completely enclose ∂P (the boundary of P) for each mesh element $P \in \overline{\mathcal{T}}_h$ as $\mathcal{N}_{\mathtt{planes}}(\partial P)$. Then we define $\mathcal{N}^h_{\mathtt{planes}} := \min_{P\in\overline{\mathcal{T}}_h} \mathcal{N}_{\mathtt{planes}}(\partial P)$. It can be observed that $\overline{\mathcal{N}}^h_{\mathtt{lines}} < \mathcal{N}^h_{\mathtt{planes}}$.

We assume that k is a positive integer representing the order of SVEM, and require that $1 \leq k < \overline{\mathcal{N}}^h_{\mathtt{lines}}$. Obviously, $k < \mathcal{N}^h_{\mathtt{planes}}$. For any $P \in \overline{\mathcal{T}}_h$, an auxiliary space $\widetilde{V}(P)$ is defined as follows:

$$\widetilde{V}(P) := \big\{v_h \in H^1(P) : \Delta v_h \in \mathbb{P}_k(P),\ v_h|_{\partial P} \in C^0(\partial P),\ v_h|_{\mathcal{F}} \in V(\mathcal{F}),\ \forall\, \mathcal{F} \subset \partial P\big\},$$

where $C^0(\partial P)$ refers to the space of continuous functions on the boundary ∂P, while $V(\mathcal{F})$ is defined in (2.5). By [7], for any $v_h \in \widetilde{V}(P)$, given the following information about v_h:

(D1) The function values of v_h at the vertices of P,

(D2) The function values of v_h at $k-1$ different internal points in each edge e of P,

the boundary projection $\Pi^{k,P}_{\mathcal{S}} v_h \in \mathbb{P}_k(P)$, whose definition is similar to (2.4), can be uniquely determined by (D1) and (D2). Then we define the k-th order local space $V(P)$ using the operator $\Pi^{k,P}_{\mathcal{S}}$ as

$$V(P) := \big\{v_h \in \widetilde{V}(P) : (v_h, p)_P = \big(\Pi^{k,P}_{\mathcal{S}} v_h, p\big)_P,\ \forall\, p \in \mathbb{P}_k(P)\big\}.$$

The unisolvency of the degrees of freedom (D1)-(D2) for $V(P)$ can be found in [7].

On each element $P \in \overline{\mathcal{T}}_h$, for any $v_h \in V(P)$ and its gradient ∇v_h, the computation of $\Pi^{k,P}_0 v_h$ and $\Pi^{k-1,P}_1 \nabla v_h$ can be achieved by utilizing $\Pi^{k,P}_{\mathcal{S}} v_h$. In addition, for any $\mathcal{F} \in \mathcal{F}_h$, using (D1)-(D2), we can also compute L^2-projection $\Pi^{k,\mathcal{F}}_0 v_h$ according to Section 2.

Based on the local space $V(P)$, we define the global space $\overline{V}_{\mathcal{S}}$ as

$$\overline{V}_{\mathcal{S}} := \big\{v_h \in H^1(\overline{\Omega}_h) : v_h|_P \in V(P),\ \forall\, P \in \overline{\mathcal{T}}_h\big\},$$

and the interpolation operator $\overline{I}_{\mathcal{S}} : H^1(\Omega) \to \overline{V}_{\mathcal{S}}$ can be constructed in a manner analogous to (2.14).

4.2. Discrete bilinear form

Following the approaches outlined in [6,17] and Section 2, we can construct discrete bilinear forms $\overline{\mathcal{A}}_0^h(\cdot,\cdot), \overline{\mathcal{A}}_1^h(\cdot,\cdot)$ and $\overline{\mathcal{A}}_2^h(\cdot,\cdot)$ to approximate $(a_0\cdot,\cdot)_{\overline{\Omega}_h}$, $(a_1\nabla\cdot,\nabla\cdot)_{\overline{\Omega}_h}$ and $(a_2\nabla\cdot,\nabla\cdot)_{\overline{\Omega}_h}$, respectively. By replacing a_0 with 1 in $\overline{\mathcal{A}}_0^h(\cdot,\cdot)$, we can derive a discrete bilinear form $\overline{\mathcal{B}}_0^h(\cdot,\cdot)$ for the inner product $(\cdot,\cdot)_{\overline{\Omega}_h}$. Similar to 2D case, utilizing the continuity and coercivity of the stabilization terms with respect to the energy norm established in [9] and the norm equivalence of the stabilization terms in [24], the continuity and coercivity of $\overline{\mathcal{A}}_0^h(\cdot,\cdot), \overline{\mathcal{A}}_1^h(\cdot,\cdot)$ and $\overline{\mathcal{A}}_2^h(\cdot,\cdot)$ can be obtained (see also [17]).

For any $v_h, w_h \in \overline{V}_{\mathcal{S}}$, we now shift to the construction of bilinear form $\overline{\mathcal{N}}_1^h(v_h,w_h)$ and $\overline{\mathcal{N}}_2^h(v_h,w_h)$ on the basis of the Nitsche-based projection method [12], which are defined as

$$\begin{aligned}\overline{\mathcal{N}}_1^h(v_h,w_h) &\coloneqq \overline{\mathcal{A}}_1^h(v_h,w_h) - \sum_{\mathcal{F}\in\mathcal{F}_h^{\mathrm{b}}}\int_{\mathcal{F}} a_1\nabla\big(\Pi_0^{k,P_{\mathcal{F}}}v_h\big)\cdot\overline{\boldsymbol{n}}\Pi_0^{k,\mathcal{F}}w_h\,\mathrm{d}s\\ &\quad-\sum_{\mathcal{F}\in\mathcal{F}_h^{\mathrm{b}}}\int_{\mathcal{F}}\left(\Pi_0^{k,\mathcal{F}}v_h+\sum_{j=1}^{\bar{m}^\star}\frac{\overline{\rho}^j}{j!}\partial_{\boldsymbol{\sigma}}^j\big(\Pi_0^{k,P_{\mathcal{F}}}v_h\big)\right)\\ &\qquad\times\left(a_1\nabla\big(\Pi_0^{k,P_{\mathcal{F}}}w_h\big)\cdot\overline{\boldsymbol{n}}-\frac{\overline{\gamma}_1}{h_{\mathcal{F}}}\Pi_0^{k,\mathcal{F}}w_h\right)\mathrm{d}s,\\ \overline{\mathcal{N}}_2^h(v_h,w_h) &\coloneqq \overline{\mathcal{A}}_2^h(v_h,w_h) - \sum_{\mathcal{F}\in\mathcal{F}_h^{\mathrm{b}}}\int_{\mathcal{F}} a_2\nabla\big(\Pi_0^{k,P_{\mathcal{F}}}v_h\big)\cdot\overline{\boldsymbol{n}}\Pi_0^{k,\mathcal{F}}w_h\,\mathrm{d}s\\ &\quad-\sum_{\mathcal{F}\in\mathcal{F}_h^{\mathrm{b}}}\int_{\mathcal{F}}\left(\Pi_0^{k,\mathcal{F}}v_h+\sum_{j=1}^{\bar{m}^\star}\frac{\overline{\rho}^j}{j!}\partial_{\boldsymbol{\sigma}}^j\big(\Pi_0^{k,P_{\mathcal{F}}}v_h\big)\right)\\ &\qquad\times\left(a_2\nabla\big(\Pi_0^{k,P_{\mathcal{F}}}w_h\big)\cdot\overline{\boldsymbol{n}}-\frac{\overline{\gamma}_2}{h_{\mathcal{F}}}\Pi_0^{k,\mathcal{F}}w_h\right)\mathrm{d}s,\end{aligned}$$

where the nonnegative integer $\bar{m}^\star \le k, \overline{\boldsymbol{n}}$ typifies the outward unit normal on $\partial\overline{\Omega}_h, \partial_{\boldsymbol{\sigma}}^j$ denotes the j-th order directional derivative in the direction of $\boldsymbol{\sigma}, P_{\mathcal{F}} \in \overline{\mathcal{T}}_h$ represents the unique element satisfying $\mathcal{F}\subset\partial P_{\mathcal{F}}, h_{\mathcal{F}}$ denotes the diameter of $\mathcal{F}$, and $\overline{\gamma}_1$ and $\overline{\gamma}_2$ are the penalty parameters in the Nitsche-based projection method.

Introduce an energy norm $\|\cdot\|_{\overline{\mathcal{N}}}$ for $\overline{V}_{\mathcal{S}}$ with the form

$$\|v_h\|_{\overline{\mathcal{N}}}^2 \coloneqq |v_h|_{1,\overline{\Omega}_h}^2 + |v_h|_{\partial\overline{\Omega}_h}^2, \quad \forall\, v_h \in \overline{V}_{\mathcal{S}},$$

where

$$|v_h|_{\partial\overline{\Omega}_h}^2 \coloneqq \sum_{\mathcal{F}\in\mathcal{F}_h^{\mathrm{b}}} h_{\mathcal{F}}^{-1}\big\|\Pi_0^{k,\mathcal{F}}v_h\big\|_{\mathcal{F}}^2.$$

According to [12] and Section 2, we know that $\|\cdot\|_{\overline{\mathcal{N}}}$ defines a norm on both $\overline{V}_{\mathcal{S}}$ and $H^1(\overline{\Omega}_h)$. Similar to the proof of Theorem 2.1, we can obtain the following coercivity and continuity of $\overline{\mathcal{N}}_1^h(\cdot,\cdot)$ and $\overline{\mathcal{N}}_2^h(\cdot,\cdot)$.

Theorem 4.1. *There exist $\overline{\gamma}_1^0, \overline{\gamma}_2^0 > 0$ and $h_0 > 0$ such that if $\overline{\gamma}_1 > \overline{\gamma}_1^0$, $\overline{\gamma}_2 > \overline{\gamma}_2^0$ and $h < h_0$, then $\overline{\mathcal{N}}_1^h(\cdot,\cdot)$ and $\overline{\mathcal{N}}_2^h(\cdot,\cdot)$ are coercive and bounded.*

4.3. Fully discrete scheme

The fully discrete scheme based on the Nitsche-based projection method for the semilinear PIDEs (1.1) on 3D curved domains is defined as finding a sequence $\{u_h^n\}_{n=1}^{N_T}$ of functions in $\overline{V}_{\mathcal{S}}$ such that

$$\begin{cases} \overline{\mathcal{A}}_0^h\Big(\dfrac{u_h^n - u_h^{n-1}}{\Delta t}, v_h\Big) + \overline{\mathcal{N}}_1^h\Big(\dfrac{u_h^n + u_h^{n-1}}{2}, v_h\Big) + \overline{\mathcal{N}}_2^h(\mathbb{Q}_n^h, v_h) \\ \quad + \overline{\mathcal{B}}_0^h\Big(\dfrac{\overline{I}_{\mathcal{S}} b(u_h^n) + \overline{I}_{\mathcal{S}} b(u_h^{n-1})}{2}, v_h\Big) = \overline{\mathcal{L}}_n^h(t_n; v_h), \quad \forall\, v_h \in \overline{V}_{\mathcal{S}}, \\ u_h^0 = \overline{I}_{\mathcal{S}} u_0, \end{cases} \tag{4.1}$$

where the trapezoidal quadrature rule $\mathbb{Q}_n^h$ is defined in (2.32) and the linear form $\overline{\mathcal{L}}_n^h(t_n; v_h)$ is defined as

$$\begin{aligned} \overline{\mathcal{L}}_n^h(t_n; v_h) :=& \frac{1}{2} \sum_{P \in \overline{\mathcal{T}}_h} \int_P \big(\Pi_0^{k,P}\big(f(t_n) + f(t_{n-1})\big)\big) v_h \mathrm{d}\boldsymbol{x} \\ & - \sum_{\mathcal{F} \in \mathcal{F}_h^{\mathrm{b}}} \int_{\mathcal{F}} \frac{1}{2}\big(\hat{g}(t_n) + \hat{g}(t_{n-1})\big)\big(a_1 \nabla\big(\Pi_0^{k,P_{\mathcal{F}}} v_h\big) \cdot \overline{\boldsymbol{n}} - \overline{\gamma}_1 h_{\mathcal{F}}^{-1} \Pi_0^{k,\mathcal{F}} v_h\big)\mathrm{d}s \\ & - \frac{1}{2} \int_0^{t_n} \sum_{\mathcal{F} \in \mathcal{F}_h^{\mathrm{b}}} \int_{\mathcal{F}} \hat{g}(\tau)\big(a_2 \nabla\big(\Pi_0^{k,P_{\mathcal{F}}} v_h\big) \cdot \overline{\boldsymbol{n}} - \overline{\gamma}_2 h_{\mathcal{F}}^{-1} \Pi_0^{k,\mathcal{F}} v_h\big)\mathrm{d}s\mathrm{d}\tau \\ & - \frac{1}{2} \int_0^{t_{n-1}} \sum_{\mathcal{F} \in \mathcal{F}_h^{\mathrm{b}}} \int_{\mathcal{F}} \hat{g}(\tau)\big(a_2 \nabla\big(\Pi_0^{k,P_{\mathcal{F}}} v_h\big) \cdot \overline{\boldsymbol{n}} - \overline{\gamma}_2 h_{\mathcal{F}}^{-1} \Pi_0^{k,\mathcal{F}} v_h\big)\mathrm{d}s\mathrm{d}\tau, \end{aligned}$$

in which $\hat{g}(\tau) = g(\boldsymbol{x} + \overline{\rho}(\boldsymbol{x})\boldsymbol{\sigma}, \tau), \tau \in [0, t_n]$. Analogous to (2.34), the Newton's iteration algorithm for (4.1) can be constructed.

Furthermore, for the strategy of imposing Dirichlet boundary conditions strongly, we can also construct corresponding fully discrete scheme and Newton's iteration algorithm based on Section 2.4. It should be noted that for the r-th iteration at the n-th time step, to impose the Dirichlet boundary conditions, we assign the value to the j-th global degree of freedom $\mathtt{DOF}_j(u_h^{n,r})$ in the following approximate way:

$$\mathtt{DOF}_j\big(u_h^{n,r}\big) \approx g\big(\boldsymbol{M}_h(\boldsymbol{x}_j), t_n\big), \quad \forall\, j \in \overline{\mathfrak{B}},$$

where $\overline{\mathfrak{B}}$ denotes the set of indices for degrees of freedom associated with the points on the boundary $\partial\overline{\Omega}_h$, $\boldsymbol{x}_j = (x_j, y_j, z_j)$ represents the corresponding boundary point for $j \in \overline{\mathfrak{B}}$ and the mapping $\boldsymbol{M}_h : \partial\overline{\Omega}_h \to \partial\Omega$ is defined in [3, Section 2.1].

Remark 4.1. Unless a_1 and a_2 are assumed to be constants, the error analysis process established in Section 3 cannot be trivially generalised to 3D case. The reason for this lies in the fact that if Ritz-Volterra projection $\overline{\mathfrak{R}}^h u$ is defined in the manner of (3.1), then when analyzing the L^2-error estimates for $\overline{\mathfrak{R}}^h u$ following Lemma 3.4, we encounter the following two terms:

$$\begin{aligned} \overline{R}^3 &= \sum_{\mathcal{F} \in \mathcal{F}_h^{\mathrm{b}}} \int_{\mathcal{F}} a_1 \nabla\big(\Pi_0^{k,P_{\mathcal{F}}} \overline{I}_{\mathcal{S}} \zeta\big) \cdot \overline{\boldsymbol{n}}\big(u - \Pi_0^{k,\mathcal{F}} \overline{\mathfrak{R}}^h u\big)\mathrm{d}s - \sum_{\mathcal{F} \in \mathcal{F}_h^{\mathrm{b}}} \int_{\mathcal{F}} a_1 \nabla \zeta \cdot \overline{\boldsymbol{n}}\big(u - \overline{\mathfrak{R}}^h u\big)\mathrm{d}s, \\ \overline{R}^6 &= \int_0^t \sum_{\mathcal{F} \in \mathcal{F}_h^{\mathrm{b}}} \int_{\mathcal{F}} a_2 \nabla\big(\Pi_0^{k,P_{\mathcal{F}}} \overline{I}_{\mathcal{S}} \zeta\big) \cdot \overline{\boldsymbol{n}}\big(u(\tau) - \Pi_0^{k,\mathcal{F}} \overline{\mathfrak{R}}^h u(\tau)\big)\mathrm{d}s\mathrm{d}\tau, \end{aligned}$$

for which we have not found a correct estimation method to yield the desired results. Nevertheless, if a_1 and a_2 are both constants, then by the fact that

$$a_1\nabla\big(\Pi_0^{k,P_{\mathcal{F}}}\overline{I}_{\mathcal{S}}\zeta\big)\cdot\overline{\boldsymbol{n}}\in\mathbb{P}_{k-1}(\mathcal{F}),$$
$$a_2\nabla\big(\Pi_0^{k,P_{\mathcal{F}}}\overline{I}_{\mathcal{S}}\zeta\big)\cdot\overline{\boldsymbol{n}}\in\mathbb{P}_{k-1}(\mathcal{F}),$$

and the definition of the L^2-projection operator $\Pi_0^{k,\mathcal{F}}$, $\overline{R}^3$ and $\overline{R}^6$ can be rewritten as

$$\overline{R}^3=\sum_{\mathcal{F}\in\mathcal{F}_h^{\mathrm{b}}}\int_{\mathcal{F}}\big(a_1\nabla\big(\Pi_0^{k,P_{\mathcal{F}}}\overline{I}_{\mathcal{S}}\zeta\big)\cdot\overline{\boldsymbol{n}}-a_1\nabla\zeta\cdot\overline{\boldsymbol{n}}\big)\big(u-\overline{\mathfrak{R}}^h u\big)\mathrm{d}s,$$
$$\overline{R}^6=\int_0^t\sum_{\mathcal{F}\in\mathcal{F}_h^{\mathrm{b}}}\int_{\mathcal{F}}a_2\nabla\big(\Pi_0^{k,P_{\mathcal{F}}}\overline{I}_{\mathcal{S}}\zeta\big)\cdot\overline{\boldsymbol{n}}\big(u(\tau)-\overline{\mathfrak{R}}^h u(\tau)\big)\mathrm{d}s\mathrm{d}\tau,$$

then following Section 3, the subsequent error analysis become feasible.

5. Numerical Experiments

In this section, we will investigate the convergence orders of the errors (abbreviated as ECO) for the fully discrete schemes (2.31) and (4.1) regarding h and Δt. Additionally, we will compare the spatial convergence orders among (2.31), (4.1) and the fully discrete scheme based on imposing Dirichlet boundary conditions strongly. In both experiments, the final time T is set to be 1, and regarding the stopping criterion for the Newton's iteration algorithms used to solve the fully discrete schemes, we will set the tolerance uniformly to be 10^{-8}.

Since the closed forms for functions in the virtual element spaces $V_{\mathcal{S}}$ and $\overline{V}_{\mathcal{S}}$ are not explicitly obtainable, we approximate the errors $\|u(T)-u_h^{N_T}\|_{\mathcal{N}}$, $\|u(T)-u_h^{N_T}\|_{\Omega_h}$, $\|u(T)-u_h^{N_T}\|_{\overline{\mathcal{N}}}$ and $\|u(T)-u_h^{N_T}\|_{\overline{\Omega}_h}$ at the final time T with the approximation errors $\mathtt{E}_{\mathcal{N}}$, $\mathtt{E}_{\Omega_h}$, $\mathtt{E}_{\overline{\mathcal{N}}}$ and $\mathtt{E}_{\overline{\Omega}_h}$, respectively, which are defined by

$$\mathtt{E}_{\mathcal{N}}:=\left(\sum_{E\in\mathcal{T}_h}\big|u(T)-\Pi_0^{k,E}u_h^{N_T}\big|_{1,E}^2+\sum_{e\in\mathcal{E}_h^{\mathrm{b}}}h_e^{-1}\big\|u(T)-u_h^{N_T}\big\|_e^2\right)^{\frac{1}{2}},$$
$$\mathtt{E}_{\Omega_h}:=\left(\sum_{E\in\mathcal{T}_h}\big\|u(T)-\Pi_0^{k,E}u_h^{N_T}\big\|_E^2\right)^{\frac{1}{2}},$$
$$\mathtt{E}_{\overline{\mathcal{N}}}:=\left(\sum_{P\in\overline{\mathcal{T}}_h}\big|u(T)-\Pi_0^{k,P}u_h^{N_T}\big|_{1,P}^2+\sum_{\mathcal{F}\in\mathcal{F}_h^{\mathrm{b}}}h_{\mathcal{F}}^{-1}\big\|u(T)-\Pi_0^{k,\mathcal{F}}u_h^{N_T}\big\|_{\mathcal{F}}^2\right)^{\frac{1}{2}},$$
$$\mathtt{E}_{\overline{\Omega}_h}:=\left(\sum_{P\in\overline{\mathcal{T}}_h}\big\|u(T)-\Pi_0^{k,P}u_h^{N_T}\big\|_P^2\right)^{\frac{1}{2}}.$$

Example 5.1. Let $a_0(\boldsymbol{x})=1, a_1(\boldsymbol{x})=2$ and $a_2(\boldsymbol{x})=3$. Consider the following initial-boundary value problem of PIDEs (1.1):

$$\begin{aligned}&a_0u_t-\nabla\cdot(a_1\nabla u)-\int_0^t\nabla\cdot\big(a_2\nabla u(\tau)\big)\mathrm{d}\tau+\sqrt{u^2+1}=f && \text{in }\ \Omega\times(0,T),\\&u=g && \text{on }\ \partial\Omega\times(0,T),\\&u(\cdot,0)=u_0 && \text{in }\ \Omega,\end{aligned}$$

where

$$\Omega = \{(x,y) \in \mathbb{R}^2 |\ x^2+y^2 \leq 1\},$$

and f, g and u_0 are derived from the exact solution

$$u = \exp(-t)\left(x^2+y^2+\sin\left(\frac{\pi x}{2}\right)\cos(\pi y)\right).$$

It is easy to derive that for $b(u)=\sqrt{u^2+1}$, the derivative satisfies

$$|b^{'}(u)| = \left|\frac{u}{\sqrt{u^2+1}}\right| \leq 1.$$

By the Lagrange's mean value theorem, we have for any $u_1, u_2 \in \mathbb{R}$,

$$|b(u_1)-b(u_2)| \leq |u_1-u_2|,$$

which implies that $b(u)$ is globally Lipschitz continuous.

Two types of polygonal meshes, which are denoted as $\mathtt{MESH}_1$ and $\mathtt{MESH}_2$, are employed for the purpose of decomposing the computational domain Ω in this example, and they are shown schematically in Fig. 5.1. Considering the shapes of $\mathtt{MESH}_1$ and $\mathtt{MESH}_2$, we choose the order k of SVEM to range from 1 to 3. For the selection of penalty parameters γ_1 and γ_2 in the bilinear forms $\mathcal{N}_1^h(\cdot\,,\cdot)$ and $\mathcal{N}_2^h(\cdot\,,\cdot)$, we set $\gamma_1=2000$ and $\gamma_2=4000$.

It is apparent that for $u \in L^\infty((0,T);H^{k+1}(\Omega))$, and under the assumptions of Theorem 3.1, we have

$$\mathtt{E}_{\mathcal{N}} \lesssim \left(\sum_{E\in\mathcal{T}_h}\left|u(T)-\Pi_0^{k,E}u(T)\right|_{1,E}^2\right)^{\frac{1}{2}} + \left\|u(T)-u_h^{N_T}\right\|_{\mathcal{N}} \lesssim h^k + (\Delta t)^2, \tag{5.1}$$

$$\mathtt{E}_{\Omega_h} \lesssim \left(\sum_{E\in\mathcal{T}_h}\left\|u(T)-\Pi_0^{k,E}u(T)\right\|_{E}^2\right)^{\frac{1}{2}} + \left\|u(T)-u_h^{N_T}\right\|_{\Omega_h} \lesssim h^{k+1} + (\Delta t)^2. \tag{5.2}$$

Hence, it follows that $\mathtt{E}_{\mathcal{N}}$ and $\mathtt{E}_{\Omega_h}$ converge with the same orders as $\|u(T)-u_h^{N_T}\|_{\mathcal{N}}$ and $\|u(T)-u_h^{N_T}\|_{\Omega_h}$, respectively.

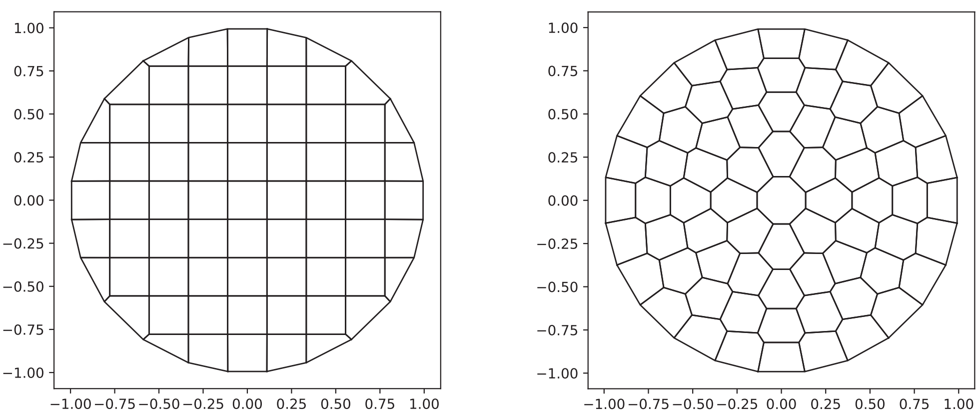

Fig. 5.1. $\mathtt{MESH}_1$ (left) and $\mathtt{MESH}_2$ (right) used in Example 5.1.

We begin by examining the convergence orders of the approximation errors $\mathtt{E}_{\mathcal{N}}$ and $\mathtt{E}_{\Omega_h}$ with respect to the spatial mesh size h. To ensure that the spatial errors dominate, we set Δt to be 1/1000. In Table 5.1, we provide the calculated results of errors $\mathtt{E}_{\mathcal{N}}$, $\mathtt{E}_{\Omega_h}$, as well as the corresponding convergence orders, for Example 5.1 with $\mathtt{MESH}_1$. From Table 5.1, we can observe that for the fully discrete scheme (2.31), $\mathtt{E}_{\mathcal{N}} = \mathcal{O}(h^k)$ and $\mathtt{E}_{\Omega_h} = \mathcal{O}(h^{k+1})$. For Example 5.1 with $\mathtt{MESH}_2$, we can obtain a similar conclusion from Table 5.2. Therefore, the predicted convergence orders with respect to h in (5.1) and (5.2) hold true, further confirming the established spatial convergence of Theorem 3.1. Furthermore, from Tables 5.1 and 5.2, we can observe that, for

Table 5.1: Approximation errors $\mathtt{E}_{\mathcal{N}}, \mathtt{E}_{\Omega_h}$ and ECO for Example 5.1 using $\mathtt{MESH}_1$.

	h	Scheme (2.31)				Scheme based on strong imposition strategy			
		$\mathtt{E}_{\mathcal{N}}$	ECO	$\mathtt{E}_{\Omega_h}$	ECO	$\mathtt{E}_{\mathcal{N}}$	ECO	$\mathtt{E}_{\Omega_h}$	ECO
$k=1$	2.3134E-01	1.9534E-01		1.0566E-02		1.9535E-01		1.0566E-02	
	1.4565E-01	1.1972E-01	1.0582	4.1108E-03	2.0402	1.1972E-01	1.0582	4.1110E-03	2.0402
	1.1253E-01	8.9712E-02	1.1186	2.3659E-03	2.1416	8.9713E-02	1.1186	2.3661E-03	2.1416
	8.3326E-02	6.7205E-02	0.9613	1.2833E-03	2.0360	6.7206E-02	0.9614	1.2833E-03	2.0361
$k=2$	4.4223E-01	6.2057E-02		3.4718E-03		1.1642E-01		2.2957E-02	
	2.7591E-01	2.3194E-02	2.0861	7.3314E-04	3.2963	4.7233E-02	1.9122	7.3534E-03	2.4132
	2.3134E-01	1.6229E-02	2.0267	4.1798E-04	3.1892	3.2572E-02	2.1094	4.6961E-03	2.5453
	1.4565E-01	6.3288E-03	2.0353	1.0253E-04	3.0372	1.6762E-02	1.4359	1.8804E-03	1.9782
$k=3$	5.7957E-01	1.7292E-02		9.6756E-04		1.3374E-01		3.8491E-02	
	3.6714E-01	4.2580E-03	3.0698	1.3545E-04	4.3067	6.3839E-02	1.6199	1.3973E-02	2.2196
	2.7591E-01	1.6391E-03	3.3417	3.8018E-05	4.4474	3.8861E-02	1.7375	7.1081E-03	2.3659
	2.2015E-01	7.8856E-04	3.2407	1.4365E-05	4.3108	2.6912E-02	1.6273	4.2869E-03	2.2396

Table 5.2: Approximation errors $\mathtt{E}_{\mathcal{N}}, \mathtt{E}_{\Omega_h}$ and ECO for Example 5.1 using $\mathtt{MESH}_2$.

	h	Scheme (2.31)				Scheme based on strong imposition strategy			
		$\mathtt{E}_{\mathcal{N}}$	ECO	$\mathtt{E}_{\Omega_h}$	ECO	$\mathtt{E}_{\mathcal{N}}$	ECO	$\mathtt{E}_{\Omega_h}$	ECO
$k=1$	2.0381E-01	1.7732E-01		9.4446E-03		1.7733E-01		9.4457E-03	
	1.7646E-01	1.5365E-01	0.9942	6.7639E-03	2.3166	1.5366E-01	0.9942	6.7647E-03	2.3166
	1.5914E-01	1.3836E-01	1.0151	5.6221E-03	1.7899	1.3836E-01	1.0151	5.6227E-03	1.7900
	1.2829E-01	1.1214E-01	0.9751	3.6796E-03	1.9673	1.1214E-01	0.9751	3.6799E-03	1.9673
$k=2$	2.8966E-01	2.5242E-02		8.4770E-04		4.9826E-02		6.8742E-03	
	2.4424E-01	1.7969E-02	1.9922	5.0344E-04	3.0546	4.0136E-02	1.2678	5.2680E-03	1.5601
	2.0381E-01	1.2333E-02	2.0803	2.8174E-04	3.2084	3.3146E-02	1.0576	4.1117E-03	1.3697
	1.5914E-01	7.5565E-03	1.9800	1.3442E-04	2.9910	2.0858E-02	1.8721	2.2660E-03	2.4083
$k=3$	7.6537E-01	4.2343E-02		4.1636E-03		2.0670E-01		7.4509E-02	
	3.0101E-01	2.4629E-03	3.0481	6.8137E-05	4.4070	4.5865E-02	1.6133	8.8620E-03	2.2816
	2.5655E-01	1.4516E-03	3.3081	3.3602E-05	4.4233	3.6334E-02	1.4576	6.4906E-03	1.9486
	2.1113E-01	8.1469E-04	2.9643	1.5282E-05	4.0435	2.6088E-02	1.7001	3.9628E-03	2.5322

Table 5.3: Approximation errors $\mathtt{E}_{\mathcal{N}}, \mathtt{E}_{\Omega_h}$ and ECO for Example 5.1 when $k = 3$.

Δt	$\mathtt{MESH}_1$ (973 elements)				$\mathtt{MESH}_2$ (973 elements)			
	$\mathtt{E}_{\mathcal{N}}$	ECO	$\mathtt{E}_{\Omega_h}$	ECO	$\mathtt{E}_{\mathcal{N}}$	ECO	$\mathtt{E}_{\Omega_h}$	ECO
1/5	1.8957E-02		1.8666E-03		1.8878E-02		1.8713E-03	
1/10	4.7057E-03	2.0102	4.6550E-04	2.0035	4.6862E-03	2.0102	4.6668E-04	2.0036
1/15	2.0940E-03	1.9970	2.0652E-04	2.0044	2.0859E-03	1.9963	2.0705E-04	2.0043
1/20	1.1793E-03	1.9959	1.1622E-04	1.9986	1.1741E-03	1.9978	1.1652E-04	1.9986

the fully discrete scheme based on imposing Dirichlet boundary conditions strongly, except for the case of $k = 1$, there is a obvious presence of suboptimal convergence orders in other cases, which validates the assertion provided in Remark 2.1.

Next, we focus on the convergence orders of the approximation errors $\mathtt{E}_{\mathcal{N}}$ and $\mathtt{E}_{\Omega_h}$ with respect to the time step size Δt. To make sure the dominance of the temporal errors, we set $k = 3$ and use a small h. For different values of Δt, we present the computational results for Example 5.1 in Table 5.3 for both $\mathtt{MESH}_1$ and $\mathtt{MESH}_2$. From these results, we can observe the second-order convergence in the temporal direction, thus validating the predicted convergence orders with respect to Δt in (5.1) and (5.2). This further confirms the established temporal convergence in Theorem 3.1.

Example 5.2. Let

$$a_0(\boldsymbol{x}) = x^2 + y^2 + z^2 + 1, \quad a_1(\boldsymbol{x}) = x^2 + y^2 + z^2 + 2, \quad a_2(\boldsymbol{x}) = x^2 + y^2 + z^2 + 3.$$

Consider the following initial-boundary value problem of PIDEs (1.1):

$$\begin{aligned} & a_0 u_t - \nabla \cdot (a_1 \nabla u) - \int_0^t \nabla \cdot \big(a_2 \nabla u(\tau)\big) \mathrm{d}\tau + \sin(u) = f && \text{in } \Omega \times (0, T), \\ & u = g && \text{on } \partial\Omega \times (0, T), \\ & u(\cdot, 0) = u_0 && \text{in } \Omega, \end{aligned}$$

where the curved domain Ω considered is a torus (see Fig. 5.2) which is represented as

$$\Omega = \big\{(x, y, z) \in \mathbb{R}^3 \mid x = \big(R + r\cos(\theta_1)\big)\cos(\theta_2),\ y = \big(R + r\cos(\theta_1)\big)\sin(\theta_2),\ z = r\sin(\theta_1)\big\},$$

in which $R = 1, r = 0.3$ and $\theta_1, \theta_2 \in [0, 2\pi]$. The data f, g and u_0 are derived from the exact solution

$$u = \exp(-t)\sin(2xy)\cos(z).$$

The polyhedral meshes considered in Example 5.2 are $\mathtt{MESH}_3$ and $\mathtt{MESH}_4$, and their schematic diagrams are shown in Fig. 5.2. $\mathtt{MESH}_3$ and $\mathtt{MESH}_4$ are generated in the following way. Firstly, polygonal meshes $\mathtt{MESH}_3^{'}$ and $\mathtt{MESH}_4^{'}$ (see Fig. 5.2) with boundary vertices all lying on $\partial\Omega^{'}$ are generated in the plane $y = 0$ for the circle domain

$$\Omega^{'} = \{(x, z) \in \mathbb{R}^2 \mid (x - 1)^2 + z^2 \le 0.09\},$$

and then they are rotated around the z-axis stepwise to obtain $\mathtt{MESH}_3$ and $\mathtt{MESH}_4$. It is easy to verify that $\overline{\rho} \lesssim h^2$, then according to [12] and to be consistent with the fully discrete scheme in

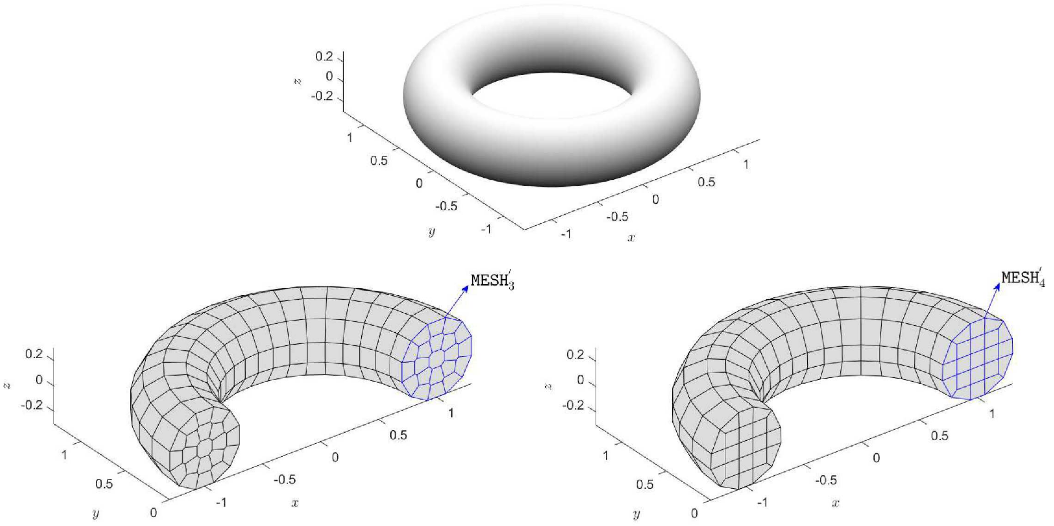

Fig. 5.2. The torus Ω (top), $\mathtt{MESH}_3$ (bottom left), and $\mathtt{MESH}_4$ (bottom right) considered in Example 5.2.

2D case, we choose $\bar{m}^\star = \lfloor (k+1)/2 \rfloor$. For the selection of penalty parameters $\overline{\gamma}_1, \overline{\gamma}_2$ and the outward vector $\boldsymbol{\sigma}$ in $\overline{\mathcal{N}}_1^h(\cdot\,,\cdot), \overline{\mathcal{N}}_2^h(\cdot\,,\cdot)$ and $\overline{\mathcal{L}}_n^h(t_n;\cdot)$, we set $\overline{\gamma}_1 = 2000, \overline{\gamma}_2 = 4000$ and $\boldsymbol{\sigma} = \overline{\boldsymbol{n}}$. We select the order k of SVEM to vary from 1 to 3, taking into account the shapes of $\mathtt{MESH}_3$ and $\mathtt{MESH}_4$.

To demonstrate spatial convergence, we employ the same setting of Δt as in Example 5.1. Tables 5.4 and 5.5 provide the computed results of the approximation errors $\mathtt{E}_{\overline{\mathcal{N}}}$ and $\mathtt{E}_{\overline{\Omega}_h}$ for Example 5.2 with $\mathtt{MESH}_3$ and $\mathtt{MESH}_4$, respectively, alongside their corresponding convergence orders. It can be seen that $\mathtt{E}_{\overline{\mathcal{N}}} = \mathcal{O}(h^k)$ and $\mathtt{E}_{\overline{\Omega}_h} = \mathcal{O}(h^{k+1})$, thus optimal convergence for

Table 5.4: Approximation errors $\mathtt{E}_{\overline{\mathcal{N}}}, \mathtt{E}_{\overline{\Omega}_h}$ and ECO for Example 5.2 using $\mathtt{MESH}_3$.

	h	Scheme (4.1)				Scheme based on strong imposition strategy			
		$\mathtt{E}_{\overline{\mathcal{N}}}$	ECO	$\mathtt{E}_{\overline{\Omega}_h}$	ECO	$\mathtt{E}_{\overline{\mathcal{N}}}$	ECO	$\mathtt{E}_{\overline{\Omega}_h}$	ECO
$k=1$	3.7004E-01	9.8787E-02		3.6860E-03		1.0636E-01		8.5768E-03	
	2.8061E-01	7.5891E-02	0.9530	2.0744E-03	2.0779	8.0567E-02	1.0038	5.0988E-03	1.8798
	2.3430E-01	6.3229E-02	1.0122	1.4322E-03	2.0543	6.6481E-02	1.0656	3.6013E-03	1.9281
	1.8674E-01	4.9814E-02	1.0509	8.7288E-04	2.1820	5.1828E-02	1.0972	2.2274E-03	2.1173
$k=2$	4.5106E-01	2.5823E-02		8.7577E-04		3.6916E-02		1.6286E-03	
	3.7004E-01	1.7086E-02	2.0859	4.5658E-04	3.2899	2.7197E-02	1.5433	1.0352E-03	2.2887
	2.8061E-01	9.6553E-03	2.0631	2.0819E-04	2.8385	1.5660E-02	1.9952	5.8180E-04	2.0828
	2.3430E-01	6.4217E-03	2.2614	1.1914E-04	3.0949	1.1731E-02	1.6017	4.0940E-04	1.9486
$k=3$	6.5289E-01	9.0206E-03		3.9130E-04		4.3069E-02		3.0841E-03	
	4.5106E-01	3.2145E-03	2.7902	8.5099E-05	4.1256	2.6344E-02	1.3292	1.5636E-03	1.8369
	3.7004E-01	1.7881E-03	2.9626	3.6224E-05	4.3140	1.9149E-02	1.6111	1.0333E-03	2.0921
	2.3430E-01	3.7619E-04	3.4109	5.0826E-06	4.2973	9.0690E-03	1.6354	4.1654E-04	1.9880

Table 5.5: Approximation errors $\mathtt{E}_{\overline{\mathcal{N}}}, \mathtt{E}_{\overline{\Omega}_h}$ and ECO for Example 5.2 using $\mathtt{MESH}_4$.

	h	Scheme (4.1)				Scheme based on strong imposition strategy			
		$\mathtt{E}_{\overline{\mathcal{N}}}$	ECO	$\mathtt{E}_{\overline{\Omega}_h}$	ECO	$\mathtt{E}_{\overline{\mathcal{N}}}$	ECO	$\mathtt{E}_{\overline{\Omega}_h}$	ECO
$k=1$	3.6997E-01	9.8861E-02		3.7215E-03		1.0613E-01		8.6136E-03	
	2.5799E-01	6.9507E-02	0.9772	1.7454E-03	2.1002	7.3212E-02	1.0299	4.3118E-03	1.9195
	2.2885E-01	6.1712E-02	0.9926	1.3638E-03	2.0590	6.4732E-02	1.0273	3.4308E-03	1.9074
	1.9063E-01	5.0903E-02	1.0535	9.1792E-04	2.1661	5.2944E-02	1.0998	2.3364E-03	2.1020
$k=2$	4.6844E-01	2.6409E-02		9.2930E-04		3.3528E-02		1.7493E-03	
	3.6997E-01	1.5573E-02	2.2381	4.3175E-04	3.2483	2.3201E-02	1.5602	1.0468E-03	2.1759
	2.5799E-01	7.4885E-03	2.0309	1.5760E-04	2.7955	1.1754E-02	1.8862	5.0300E-04	2.0329
	2.2885E-01	5.8599E-03	2.0464	1.1047E-04	2.9652	9.9501E-03	1.3905	3.9671E-04	1.9810
$k=3$	6.4360E-01	8.3047E-03		3.6032E-04		4.0268E-02		2.9894E-03	
	3.6997E-01	1.3784E-03	3.2436	3.1439E-05	4.4051	1.7173E-02	1.5393	1.0486E-03	1.8921
	2.5799E-01	4.5532E-04	3.0727	7.4657E-06	3.9881	9.4702E-03	1.6510	5.1338E-04	1.9812
	2.2885E-01	3.1367E-04	3.1099	4.5053E-06	4.2148	7.8228E-03	1.5947	4.0262E-04	2.0281

Table 5.6: Approximation errors $\mathtt{E}_{\overline{\mathcal{N}}}, \mathtt{E}_{\overline{\Omega}_h}$ and ECO for Example 5.2 when $k=3$.

Δt	$\mathtt{MESH}_3$ (3492 elements)				$\mathtt{MESH}_4$ (3589 elements)			
	$\mathtt{E}_{\overline{\mathcal{N}}}$	ECO	$\mathtt{E}_{\overline{\Omega}_h}$	ECO	$\mathtt{E}_{\overline{\mathcal{N}}}$	ECO	$\mathtt{E}_{\overline{\Omega}_h}$	ECO
1/4	3.7270E-02		1.4667E-03		5.9567E-02		1.2118E-03	
1/6	1.6440E-02	2.0186	6.5034E-04	2.0057	2.6104E-02	2.0347	5.3886E-04	1.9986
1/8	9.2370E-03	2.0040	3.6570E-04	2.0011	1.4622E-02	2.0146	3.0323E-04	1.9985
1/10	5.9230E-03	1.9914	2.3414E-04	1.9982	9.3497E-03	2.0040	1.9416E-04	1.9978

the fully discrete scheme (4.1) is observed. Moreover, by examining Tables 5.4 and 5.5, it is evident that, except for the case of $k=1$, the fully discrete scheme based on imposing Dirichlet boundary conditions strongly exhibits noticeable suboptimal convergence orders in other cases.

To showcase temporal convergence, we set $k=3$ and choose a small h. The relationships $\mathtt{E}_{\overline{\mathcal{N}}} = \mathcal{O}((\Delta t)^2)$ and $\mathtt{E}_{\overline{\Omega}_h} = \mathcal{O}((\Delta t)^2)$ can be seen from Table 5.6, thus the second-order convergence in the time direction for the fully discrete scheme (4.1) is observed.

6. Conclusions

The classical Nitsche-based projection method is incorporated into the framework of a special class of serendipity virtual element methods to solve semilinear parabolic integro-differential equations on 2D curved domains. A Ritz-Volterra projection is constructed based on the Nitsche-based projection method, and error estimates for the fully discrete scheme with respect to L^2-norm and an energy norm are derived on the basis of the approximation properties of the Ritz-Volterra projection. The extension of the fully discrete scheme to 3D case is addressed as well. Compared with the strategy of imposing Dirichlet boundary conditions strongly, the proposed scheme in this paper can maintain optimal convergence.

Acknowledgements. The authors are grateful to the reviewers for their insightful comments. This work is supported by the National Natural Science Foundation of China (Project Nos. 12471373, 12071100).

References

[1] D. Adak, E. Natarajan, and S. Kumar, Convergence analysis of virtual element methods for semilinear parabolic problems on polygonal meshes, *Numer. Methods Partial Differential Equations*, **35**:1 (2019), 222–245.

[2] D. Adak and S. Natarajan, Virtual element method for semilinear sine-Gordon equation over polygonal mesh using product approximation technique, *Math. Comput. Simul.*, **172** (2020), 224–243.

[3] N.M. Atallah, C. Canuto, and G. Scovazzi, Analysis of the shifted boundary method for the Poisson problem in domains with corners, *Math. Comp.*, **90**:331 (2021), 2041–2069.

[4] L. Beirão da Veiga, F. Brezzi, A. Cangiani, G. Manzini, L.D. Marini, and A. Russo, Basic principles of virtual element methods, *Math. Models Methods Appl. Sci.*, **23**:1 (2013), 199–214.

[5] L. Beirão da Veiga, F. Brezzi, F. Dassi, L.D. Marini, and A. Russo, Lowest order virtual element approximation of magnetostatic problems, *Comput. Methods Appl. Mech. Engrg.*, **332** (2018), 343–362.

[6] L. Beirão da Veiga, F. Brezzi, F. Dassi, L.D. Marini, and A. Russo, Serendipity virtual elements for general elliptic equations in three dimensions, *Chinese Ann. Math. Ser. B*, **39**:2 (2018), 315–334.

[7] L. Beirão da Veiga, F. Brezzi, L.D. Marini, and A. Russo, Serendipity nodal VEM spaces, *Comput. Fluids*, **141** (2016), 2–12.

[8] L. Beirão da Veiga, F. Brezzi, L.D. Marini, and A. Russo, The virtual element method, *Acta Numer.*, **32** (2023), 123–202.

[9] L. Beirão da Veiga and L. Mascotto, Stability and interpolation properties of serendipity nodal virtual elements, *Appl. Math. Lett.*, **142** (2023), 108639.

[10] L. Beirão da Veiga, A. Russo, and G. Vacca, The virtual element method with curved edges, *ESAIM Math. Model. Numer. Anal.*, **53**:2 (2019), 375–404.

[11] S. Bertoluzza, M. Pennacchio, and D. Prada, High order VEM on curved domains, *Rend. Lincei-Mat. Appl.*, **30**:2 (2019), 391–412.

[12] S. Bertoluzza, M. Pennacchio, and D. Prada, Weakly imposed Dirichlet boundary conditions for 2D and 3D virtual elements, *Comput. Methods Appl. Mech. Engrg.*, **400** (2022), 115454.

[13] J.H. Bramble, T. Dupont, and V. Thomée, Projection methods for Dirichlet's problem in approximating polygonal domains with boundary-value corrections, *Math. Comp.*, **26** (1972), 869–879.

[14] S.C. Brenner, Q. Guan, and L.Y. Sung, Some estimates for virtual element methods, *Comput. Methods Appl. Math.*, **17**:4 (2017), 553–574.

[15] S.C. Brenner and L.R. Scott, *The Mathematical Theory of Finite Element Methods*, Springer, 2008.

[16] A. Cangiani, Z. Dong, E.H. Georgoulis, and P. Houston, *hp-Version Discontinuous Galerkin Methods on Polygonal and Polyhedral Meshes*, Springer, 2017.

[17] A. Cangiani, G. Manzini, and O.J. Sutton, Conforming and nonconforming virtual element methods for elliptic problems, *IMA J. Numer. Anal.*, **37**:3 (2017), 1317–1354.

[18] V. Capasso, Asymptotic stability for an integro-differential reaction-diffusion system, *J. Math. Anal. Appl.*, **103**:2 (1984), 575–588.

[19] L. Chen and J. Huang, Some error analysis on virtual element methods, *Calcolo*, **55**:1 (2018), 5.

[20] G. Dagan, The significance of heterogeneity of evolving scales to transport in porous formations, *Water Resour. Res.*, **30**:12 (1994), 3327–3336.

[21] R. Dautray and J.L. Lions, *Mathematical Analysis and Numerical Methods for Science and Technology. Vol. 5: Evolution Problems I*, Springer-Verlag, 1992.

[22] S.A. Gómez, High-order interpolatory serendipity virtual element method for semilinear parabolic problems, *Calcolo*, **59**:3 (2022), 25.
[23] M.L. Heard and S.M. Rankin, Weak solutions for a class of parabolic Volterra integrodifferential equations, *J. Math. Anal. Appl.*, **139**:1 (1989), 78–109.
[24] J. Huang and Y. Yu, Some estimates for virtual element methods in three dimensions, *Comput. Methods Appl. Math.*, **23**:1 (2023), 177–187.
[25] Y.Q. Huang, Time discretization schemes for an integro-differential equation of parabolic type, *J. Comput. Math.*, **12**:3 (1994), 259–264.
[26] R. Jain, A.K. Pani, and S. Yadav, HDG method for linear parabolic integro-differential equations, *Appl. Math. Comput.*, **450** (2023), 127987.
[27] M. Li, Cut-off error splitting technique for conservative nonconforming VEM for N-coupled nonlinear Schrödinger-Boussinesq equations, *J. Sci. Comput.*, **93**:3 (2022), 86.
[28] W. McLean, I.H. Sloan, and V. Thomée, Time discretization via Laplace transformation of an integro-differential equation of parabolic type, *Numer. Math.*, **102**:3 (2006), 497–522.
[29] R.K. Miller, An integrodifferential equation for rigid heat conductors with memory, *J. Math. Anal. Appl.*, **66**:2 (1978), 313–332.
[30] K. Mustapha, H. Brunner, H. Mustapha, and D. Schötzau, An *hp*-version discontinuous Galerkin method for integro-differential equations of parabolic type, *SIAM J. Numer. Anal.*, **49**:4 (2011), 1369–1396.
[31] K. Mustapha and H. Mustapha, A second-order accurate numerical method for a semilinear integro-differential equation with a weakly singular kernel, *IMA J. Numer. Anal.*, **30**:2 (2010), 555–578.
[32] C. Pao, Solution of a nonlinear integrodifferential system arising in nuclear reactor dynamics, *J. Math. Anal. Appl.*, **48**:2 (1974), 470–492.
[33] B. Rivière, *Discontinuous Galerkin Methods for Solving Elliptic and Parabolic Equations*, SIAM, 2008.
[34] R.K. Sinha, R.E. Ewing, and R.D. Lazarov, Mixed finite element approximations of parabolic integro-differential equations with nonsmooth initial data, *SIAM J. Numer. Anal.*, **47**:5 (2009), 3269–3292.
[35] I.H. Sloan and V. Thomée, Time discretization of an integro-differential equation of parabolic type, *SIAM J. Numer. Anal.*, **23**:5 (1986), 1052–1061.
[36] V. Thomée and N.Y. Zhang, Error estimates for semidiscrete finite element methods for parabolic integro-differential equations, *Math. Comp.*, **53**:187 (1989), 121–139.
[37] G. Vacca and L. Beirão da Veiga, Virtual element methods for parabolic problems on polygonal meshes, *Numer. Methods Partial Differential Equations*, **31**:6 (2015), 2110–2134.
[38] P. Wriggers, B. Hudobivnik, and F. Aldakheel, NURBS-based geometries: A mapping approach for virtual serendipity elements, *Comput. Methods Appl. Mech. Engrg.*, **378** (2021), 113732.
[39] Y. Xu, Z. Zhou, and J. Zhao, Error analysis of serendipity virtual element methods for semilinear parabolic integro-differential equations, *J. Sci. Comput.*, **100** (2024), 55.
[40] H.M. Yin, On parabolic Volterra equations in several space dimensions, *SIAM J. Math. Anal.*, **22**:6 (1991), 1723–1737.
[41] A. Zhu, T. Xu, and Q. Xu, Weak Galerkin finite element methods for linear parabolic integro-differential equations, *Numer. Methods Partial Differential Equations*, **32**:5 (2016), 1357–1377.
[42] G. Zou, X. Wang, and J. Li, An extrapolated Crank-Nicolson virtual element scheme for the nematic liquid crystal flows, *Adv. Comput. Math.*, **49**:3 (2023), 30.